HYBRID DECONTAMINATION METHOD FOR FACIAL RESPIRATORS USING ULTRAVIOLET GERMICIDAL IRRADIATION AND MICROWAVE GENERATED STEAM

THIRUMAARAN A/L GOPALAN

FACULTY OF ENGINEERING
UNIVERSITI MALAYA
KUALA LUMPUR

2024

HYBRID DECONTAMINATION METHOD FOR FACIAL RESPIRATORS USING ULTRAVIOLET GERMICIDAL IRRADIATION AND MICROWAVE GENERATED STEAM

THIRUMAARAN A/L GOPALAN

DISSERTATION SUBMITTED IN FULFILMENT OF THE REQUIREMENTS FOR THE DEGREE OF MASTER OF ENGINEERING SCIENCE

FACULTY OF ENGINEERING
UNIVERSITI MALAYA
KUALA LUMPUR

2024

UNIVERSITI MALAYA

ORIGINAL LITERARY WORK DECLARATION

Name of Candidate: Thirumaaran A/L Gopalan

Matric No: 17065296

Name of Degree: Master of Engineering Science

Title of Project Paper/Research Report/Dissertation/Thesis ("this Work"):

Hybrid Decontamination Method for Facial Respirator Using Ultraviolet Germicidal Irradiation and Microwave Generated Steam

Field of Study: Engineering Design (NEC 521: Mechanics and Metal Works)

I do solemnly and sincerely declare that:

(1) I am the sole author/writer of this Work;
(2) This Work is original;
(3) Any use of any work in which copyright exists was done by way of fair dealing and for permitted purposes and any excerpt or extract from, or reference to or reproduction of any copyright work has been disclosed expressly and sufficiently and the title of the Work and its authorship have been acknowledged in this Work;
(4) I do not have any actual knowledge nor do I ought reasonably to know that the making of this work constitutes an infringement of any copyright work;
(5) I hereby assign all and every rights in the copyright to this Work to the Universiti Malaya ("UM"), who henceforth shall be owner of the copyright in this Work and that any reproduction or use in any form or by any means whatsoever is prohibited without the written consent of UM having been first had and obtained;
(6) I am fully aware that if in the course of making this Work I have infringed any copyright whether intentionally or otherwise, I may be subject to legal action or any other action as may be determined by UM.

Candidate's Signature Date: 27.2.2024

Subscribed and solemnly declared before,

Witness's Signature Date: 28.2.2024

Name:

Designation:

HYBRID DECONTAMINATION METHOD FOR FACIAL RESPIRATORS USING ULTRAVIOLET GERMICIDAL IRRADIATION AND MICROWAVE GENERATED STEAM

ABSTRACT

The unprecedented Covid-19 pandemic caused by SARS-CoV-2 has caused a significant escalation in global demand for Personal Protective Equipment (PPE). PPE especially face masks acts as primary respiratory protection against this lethal virus. The worldwide shortage of masks issues due to ever-expanding demand poses a serious threat to health workers worldwide who battling this pandemic on the frontlines. Decontaminating face masks for reuse purposes could be a rewarding solution to mitigate the issue. Ultraviolet Germicidal Irradiation (UVGI), Aerosolized Hydrogen Peroxide (aHP), and Microwave-Generated Steam (MGS) are among the investigated decontamination methods that exhibit astounding virucidal results while preserving the integrity and performance of the treated mask. This research aims to investigate the decontamination efficiency of the hybrid decontamination system (UVGI + aHP) and (UVGI + MGS) on an N95 respirator contaminated with Feline Coronavirus (FCoV). A mask sterilizing machine prototype equipped with UVGI and aHP decontamination system was designed and developed. Virus viability tests were conducted to measure the efficiency of the selected decontamination treatments. In these tests, N95 respirators inoculated with viable FCoV were treated with selected three decontamination systems in a single and hybrid treatment design by applying varying exposure times. UVGI achieved a log reduction of at least 3 at a lower treatment time compared to MGS and aHP. MGS exhibits higher efficiency in achieving 4 log reduction compared to the other two single treatments. Results exhibit that the tested rapid treatment time of aHP was not effective against the virus. In addition, hybrid decontamination of (UVGI + MGS) achieved at least 4 log reduction in microbial load faster than single treatments of MGS

and UVGI. The results indicated that the hybrid decontamination procedure is effective in achieving higher log reduction values.

Keywords: hybrid decontamination; N95 respirators; FCoV; UVGI; aHP; MGS

KAEDAH PENYAHCEMARAN HIBRID RESPIRATOR MUKA MENGGUNAKAN SINARAN KUMAN ULTRAVIOLET DAN WAP GELOMBANG MIKRO

ABSTRAK

Pandemik Covid-19 yang disebabkan oleh Sars-CoV-2 telah menyebabkan peningkatan yang ketara dalam permintaan global bagi Peralatan Pelindung Diri (PPE). PPE terutamanya topeng muka bertindak sebagai perlindungan pernafasan utama terhadap virus yang berbahaya ini. Isu kekurangan topeng muka di seluruh dunia adalah disebabkan oleh permintaan yang semakin meningkat secara mendadak. Keadaan ini menimbulkan ancaman serius kepada pekerja kesihatan di seluruh dunia yang sedang memerangi wabak ini di barisan hadapan. Menyahkontaminasi topeng muka untuk tujuan penggunaan semula boleh menjadi satu penyelesaian yang dapat menangani isu ini. Penyinaran Kuman Ultraviolet (UVGI), Hidrogen Peroksida Diaerosol (aHP) dan Wap Dijana Gelombang Mikro (MGS) adalah antara kaedah penyahcemaran yang menonjolkan hasil penyahakifan virus yang berkesan serta mengekalkan integriti dan prestasi topeng yang dirawat. Penyelidikan ini bertujuan untuk mengkaji keberkesanan kaedah penyahcemaran hibrid (UVGI + aHP) dan (UVGI + MGS) pada alat pernafasan N95 yang tercemar dengan Koronavirus Feline (FCoV). Sebuah prototaip mesin pensterilan topeng yang dilengkapi dengan sistem penyahcemaran UVGI dan aHP telah direka dan dibangunkan. Bagi mengukur kecekapan rawatan penyahcemaran yang dipilih, ujian viability virus telah dijalankan. Alat pernafasan N95 yang disuntik dengan FcoV, dirawat menggunakan ketiga - tiga sistem penyahcemaran secara rawatan tunggal dan hibrid dengan masa pendedahan yang berbeza dalam ujian ini. UVGI mencapai pengurangan log sekurang-kurangnya 3 pada masa rawatan yang lebih rendah berbanding dengan MGS dan aHP. MGS mempamerkan kecekapan yang lebih tinggi dalam mencapai 4 pengurangan log berbanding dua rawatan tunggal yang lain. Keputusan menunjukkan

bahawa masa rawatan pantas aHP yang diuji tidak berkesan terhadap virus. Tambahan pula, penyahcemaran hibrid (UVGI + MGS) mencapai 4 pengurangan log dalam beban mikrob lebih cepat daripada rawatan tunggal MGS dan UVGI. Ringkasnya, keputusan menunjukkan bahawa prosedur dekontaminasi hibrid adalah berkesan dalam mencapai nilai pengurangan log yang lebih tinggi.

Keywords: penyahcemaran hibrid; alat pernafasan N95; FCoV; UVGI; aHP; MGS

ACKNOWLEDGEMENTS

First and foremost, I would like to express my sincerest appreciation to my supervisor Dr. Mohd Ridha bin Muhamad for his immense support and guidance throughout this research journey. I would like to thank Prof Dr. Victor Hoe Chee Wai bin Abdullah, my co-supervisor for his guidance and expertise. Special gratitude to Dr. Pouya Hassandarvish and Mr. Mohd Fauzi Bakri for their invaluable support in conducting tests for this research.

Finally, I would like to thank my parents and family. Their support throughout this journey was crucial and invaluable.

TABLE OF CONTENTS

LIST OF FIGURES

LIST OF TABLES

LIST OF SYMBOLS AND ABBREVIATIONS

WHO	:	World Health Organization
PPE	:	Personal Protective Equipment
UVGI	:	Ultraviolet Germicidal Irradiation
HP	:	Hydrogen Peroxide
HPV	:	Hydrogen Peroxide Vapor
aHP	:	Aerosolized Hydrogen Peroxide
MGS	:	Microwave Generated Steam
FFR	:	Filtering Facepiece Respirator
CDC	:	Centers for Disease Control and Prevention
NIOSH	:	National Institute of Occupational Safety and Health
AOP	:	Advanced Oxidation Process

LIST OF APPENDICES

CHAPTER 1: INTRODUCTION

World Health Organization (WHO) reports that early Covid 19 human cases were triggered by a novel coronavirus named SARS-CoV-2 found to be spreading in Wuhan City, China, in December 2019 (World Health Organization [WHO], 2020a). Demand for Personal Protective Equipment (PPE) especially face masks escalated rapidly due to this sudden need for respiratory protection. Healthcare workers who are dealing with Covid-related cases on a daily basis depend solely on PPE specifically N95 respirators to protect against this fatal disease. N95-type respirators are the type of respirators specifically designed and applicable the most for health care applications (3M, 2018). As a precautionary measure for this unprecedented scenario, the Centers for Disease Control and Prevention (CDC) recommends health workers that the usage of an N95 must be limited to 1 per patient visit which should be discarded safely after usage. Nonetheless, prolonged use of N95 equipment (using the same N95 for many patient interactions) with limited reuse (keeping an N95 during interactions for usage across several patient visits) is recommended under shortage of PPE supply situations (Centers for Disease Control and Prevention [CDC], 2020a). Besides, research was conducted on how often duckbill N95s and dome-shaped N95s masks failed by using fit-tests when they were reused. It was recommended that closely monitoring N95 fit in the event of prolonged use and duckbill type respirator should be avoided if better alternatives are available (Degesys et al., 2020).

Hence, a mask decontamination procedure could be a potential solution to alleviate the issues arising from the pandemic. A safe mask decontamination process could assist in reducing the pathogen burden of a contaminated mask which promotes higher reusability of used face masks. The National Institute of Occupational Safety and Health (NIOSH) concludes that Ultraviolet Germicidal Irradiation (UVGI), Hydrogen Peroxide Vapor

(HPV), and moist heat decontamination have proven to be viable options for Filtering Facepiece Respirator (FFR) decontamination (Centers for Disease Control and Prevention [CDC], 2020a).

UVGI treatment has been applied and practiced in sterilization applications worldwide since the late 19th century (Reed, 2010). This type of decontamination procedure offers high virucidal activity while preserving the integrity of the treated specimen (He et al., 2020; Lindsley et al., 2015; Ludwig-Begall et al., 2021; Ozog et al., 2020; Rathnasinghe et al., 2020; Simmons et al., 2021). Multiple reports of research prove the efficiency of the UVGI decontamination system against coronaviruses such as SARS-CoV-2 and MERS-CoV (Bedell et al., 2016; Duan et al., 2003).

In addition, hydrogen peroxide is a chemical that is known for its sterilization abilities and wide application. Vaporized and aerosolized forms of hydrogen peroxide offer the same crucial properties necessary for microbial ability. Studies have shown credible evidence that HPV works well against multiple pathogens such as Transmissible gastroenteritis virus (TGEV - SARS-CoV surrogate), Feline calicivirus, Adenovirus, and Avian virus (Goyal et al., 2014). Specifically, investigations regarding the virucidal efficiency of HPV on face mask surfaces have been remarkable (Fischer et al., 2020; Jatta et al., 2021; Ludwig-Begall et al., 2021).

Microwave-generated steam (MGS) is one of the decontamination techniques that exhibit great potential. Rapid disinfection and affordability are among the advantages this treatment holds over other investigated treatments. Initial investigations clearly indicate that at a relatively short treatment time, MGS was able to produce excellent microbial results while preserving the integrity of the treated masks (Fisher et al., 2011; Lore et al., 2012; Pascoe et al., 2020; Zulauf et al., 2020).

1.1 Problem Statement

The current COVID-19 pandemic era has induced a face mask shortage crisis all around the world. The major cause of this issue is concluded to be a rapid surge in FFR demand which could not be compensated by the current supply market. Approximately, half of the world's face mask production is manufactured by China. Nevertheless, even at full capacity, China will not be able to meet its population demand as shown in Figure 1.1. WHO predicts that face mask production should be increased by 40% to cope with the ever-increasing demand worldwide (World Health Organization [WHO], 2020b).

Developing countries where typically the majority of the population comprises people living in poverty are greatly affected in this pandemic era. The crippled economy coupled with the escalating price of FFRs is proving to accumulate difficulties for people to acquire FFRs as basic protection against the virus (Gray, 2020). As an implication, rationing FFRs among health workers and hospital settings has become a common practice. On the other note, restrictions have been induced on non-Covid-related medical care in healthcare facilities due to FFR scarcity (Parshley, 2020).

Existing and ongoing research on the decontamination of FFR proves the need for more studies. Several issues were reported in the face mask decontamination investigations such as failed fit testing, decontamination efficiency affected by mask models, impairment of mask integrity, and the complexity of decontamination system application (Bopp et al., 2020; Liao et al., 2020; Lieu et al., 2020; Smith et al., 2020).

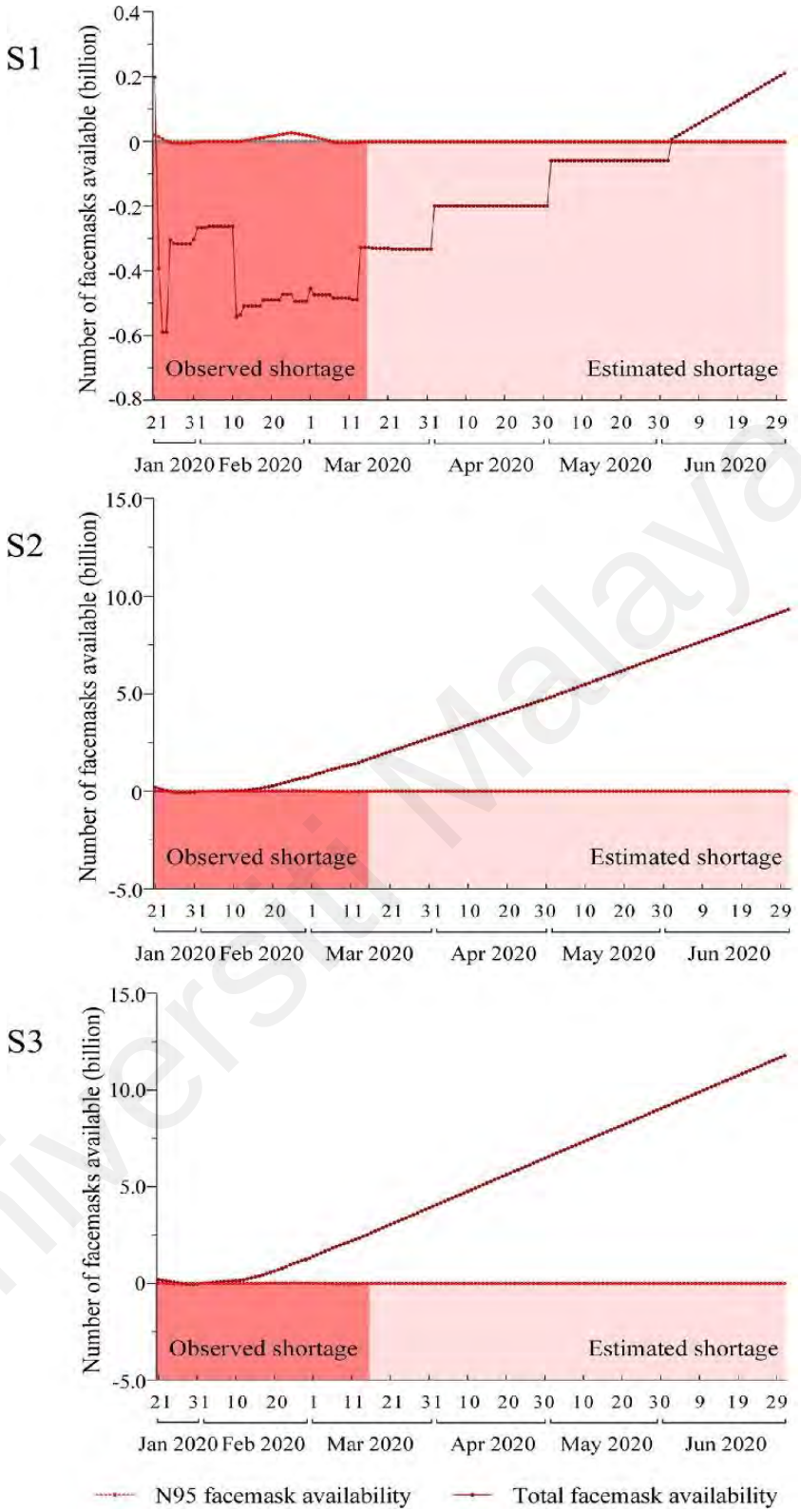

Figure 1.1: Face mask availability during the novel coronavirus disease (COVID-19) in China (S1:assuming a universal face mask wearing policy implementation in all regions of mainland China; S2:assuming a universal face mask wearing policy implementation only in the epicenter (Hubei province, China); S3:Assuming no implementation of a universal face mask wearing policy) (Wu et al., 2020)

1.2 Research Objectives

1) To design and develop a mask sterilizing machine prototype equipped with a novel hybrid decontamination method by applying ultraviolet germicidal irradiation (UVGI) coupled with aerosolized hydrogen peroxide (aHP).
2) To investigate the viability of the SARS-CoV-2 surrogate virus under ultraviolet germicidal irradiation (UVGI), aerosolized hydrogen peroxide (aHP), and microwave-generated steam (MGS) exposure.

1.3 Significance of Study

This current study is crucial in this Covid pandemic era. Decontamination of N95 respirators eases the world shortage of masks issues. Particularly as intended, the success of this research allows health workers to stay protected by crucial personal protective equipment such as N95 respirators. The decontamination method of UVGI based hybrid (UVGI + aHP and UVGI + MGS) decontamination method as proposed in this study could offer safe and rapid decontamination of face masks which could revolutionize the production of single-use face masks and the usage longevity of the FFRs.

1.4 Thesis Structure

The thesis has been segregated into five chapters which are Chapter 1 (Introduction), Chapter 2 (Literature Review), Chapter 3 (Methodology), Chapter 4 (Results and Discussion), and Chapter 5 (Conclusion).

Chapter 1 presents a brief introduction to the main idea of this research. In addition, the problem statement, research objectives, and significance of this study were discussed.

Chapter 2 comprises a discussion of literature covering coronaviruses and the decontamination of face masks. Moreover, a comparison study was conducted on

multiple N95 decontamination treatments such as UVGI, HPV, aHP, MGS, heat, and ethanol.

Chapter 3 depicts the experimental methods conducted in this research which include the design and development of a mask sterilizer machine equipped with two decontamination systems and testing the viability of the virus under various selected - decontamination treatments.

Chapter 4 describes the results obtained from the designing process, fabrication results, and experimental results. In addition, a detailed analysis of the obtained results was presented which was discussed further on the effectiveness and safety of using this decontamination method for face mask sterilization.

Chapter 5 presents the conclusion from the experiment data and recommendations on the adaptability of this decontamination procedure for the intended healthcare application. Limitations present in the current study and recommendations for the future scope of this research were described in this section.

CHAPTER 2: LITERATURE REVIEW

In this chapter, existing research that is notable and related to this study will be reviewed. A literature review is essential to have an in-depth understanding of the specified study of research. A variety of sources were accessed in order to obtain research papers that were apt to the current study such as journals, e-books, policy documents, and product catalogs.

2.1 SARS-CoV-2

On 11th February 2020, WHO named the newly spreading coronavirus as SARS-CoV-2. This virus is a single-stranded positive-sense RNA (+ssRNA) virus (Y. Chen et al., 2020). In addition, in terms of the virus genome, SARS-CoV-2 was known to exhibit 80% similarity with other known coronaviruses (Shereen et al., 2020). Figure 2.1 illustrates the schematic structure of the SARS-CoV-2 virus which is an RNA-enveloped virus.

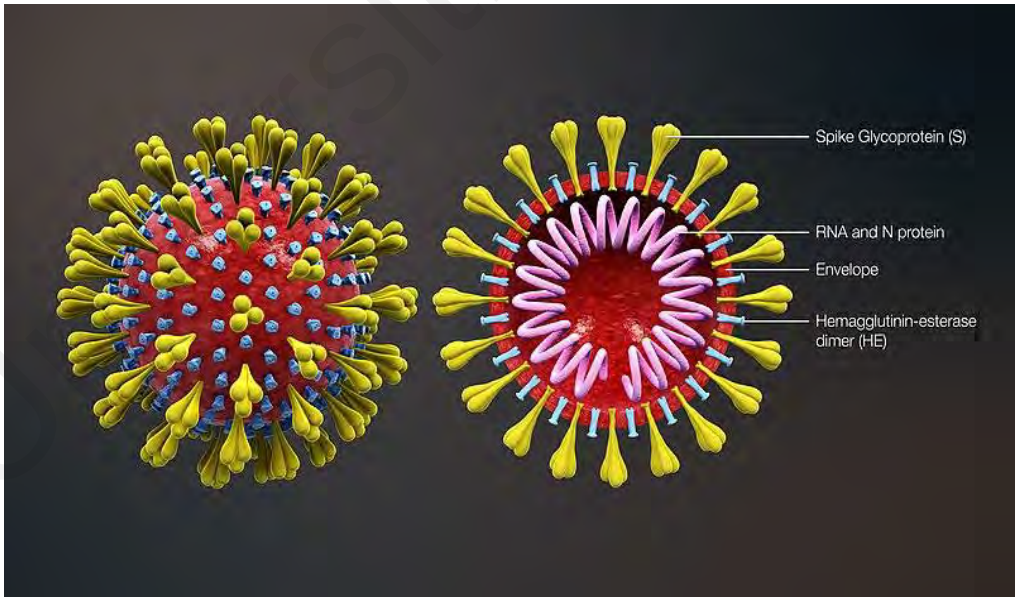

Figure 2.1: Schematic structure of SARS-CoV-2 (Scientific Animations Inc, 2020)

Investigations on the origins of the virus have been directing to bats as the key host and transmitting medium (Shereen et al., 2020). It is concluded that SARS-CoV-2 is transmitted mainly via respiratory droplets and direct contact. In addition, contaminated

enclosed spaces pose a greater risk of spreading. This scenario is due to the concentration of viruses contained in a closed space and increased exposure (Zhang et al., 2020).

2.1.1 Surrogate Virus

A surrogate virus is a term used for a virus that has been used as an alternative virus in specific testing. Chemical inactivation is practically not possible for all viruses. This is due to the risk certain viruses carry in a testing procedure. In addition, the cultivation process cannot be conducted for some viruses related to human medicine. Hence, surrogate viruses are often used to conduct a testing process without handling tremendous risk. Nevertheless, the selection of a surrogate virus is a very distinct criterion. The selection will be often based on morphological similarity with the intended virus (Science Centre, n.d).

2.1.1.1 Feline Coronavirus (FCoV)

Feline coronaviruses (FCoV) is a virus from the coronaviridae taxonomic family which is similar to SARS-CoV-2. This virus belongs to the Alphacoronavirus genus and reports have stated that this virus causes mild diarrhea in cats. At a nucleotide level, both these viruses share a similarity of 44.0 - 44.5 % (Sharun et al., 2020). Table 2.1 shows the characteristics of the two discussed viruses and Figure 2.2 depicts the classification of the coronavirus family.

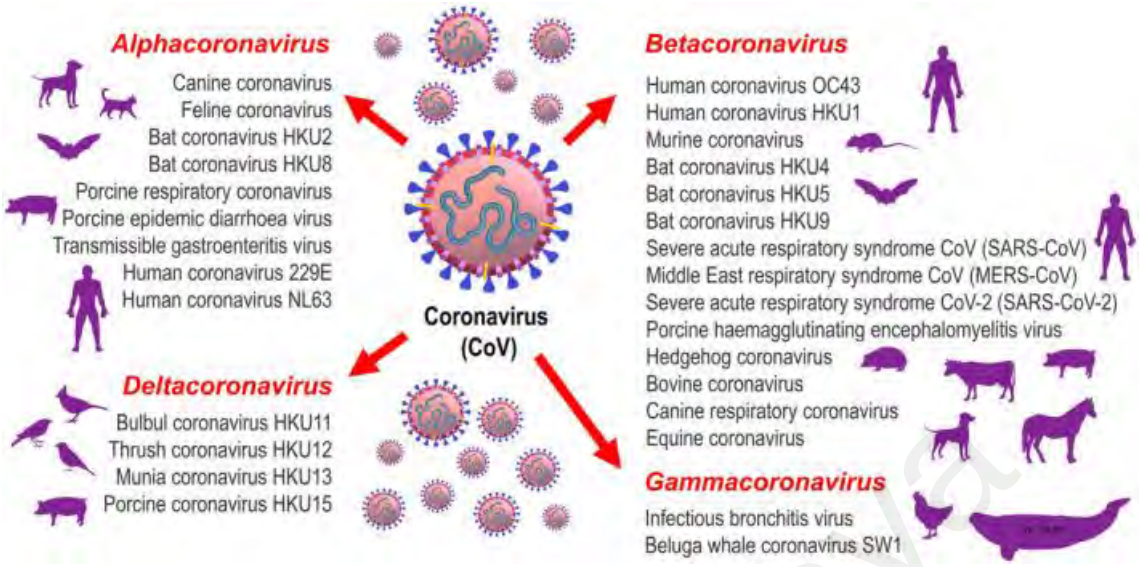

Figure 2.2: Classification of the coronavirus family (Sharun et al., 2020)

Table 2.1: Characteristics of SARS-CoV-2 and FCoV (Derr et al., 2020; Jaimes & Whittaker, 2018; Nie et al., 2021)

Virus species	Diameter	Capdis/ virion shape	Genome type, ~size	Taxonomic family	Biosafety Level (BSL)
Severe acute respiratory syndrome coronavirus 2 (SARS-CoV-2)	120 nm	Enveloped, no icosahedral capsid	linear (+) ssRNA genome, ~30 kbp	Coronaviridae	BSL3
Feline coronavirus (FCoV)	Between 80 and 120 nm	Enveloped and nucleocapsid	Poly-A-tailed single-stranded positive-sense RNA (ssRNA+), ~29 kbp	Coronaviridae	BSL 2

2.2 Filtering Facepiece Respirator (FFR)

Respirators are designed to provide respiratory protection for the user by filtering contaminants from the air from entering the respiratory track of the user (National Institute for Occupational Safety and Health [NIOSH], 2021b). There are several types of respirators available in the market, specifically customized according to the user

preference and environmental hazard encountered as shown in Figure 2.3. Approved models of respirators include N95, surgical N95, N99, N100, R95, P95, P99, and P100 (National Institute for Occupational Safety and Health [NIOSH], 2021a).

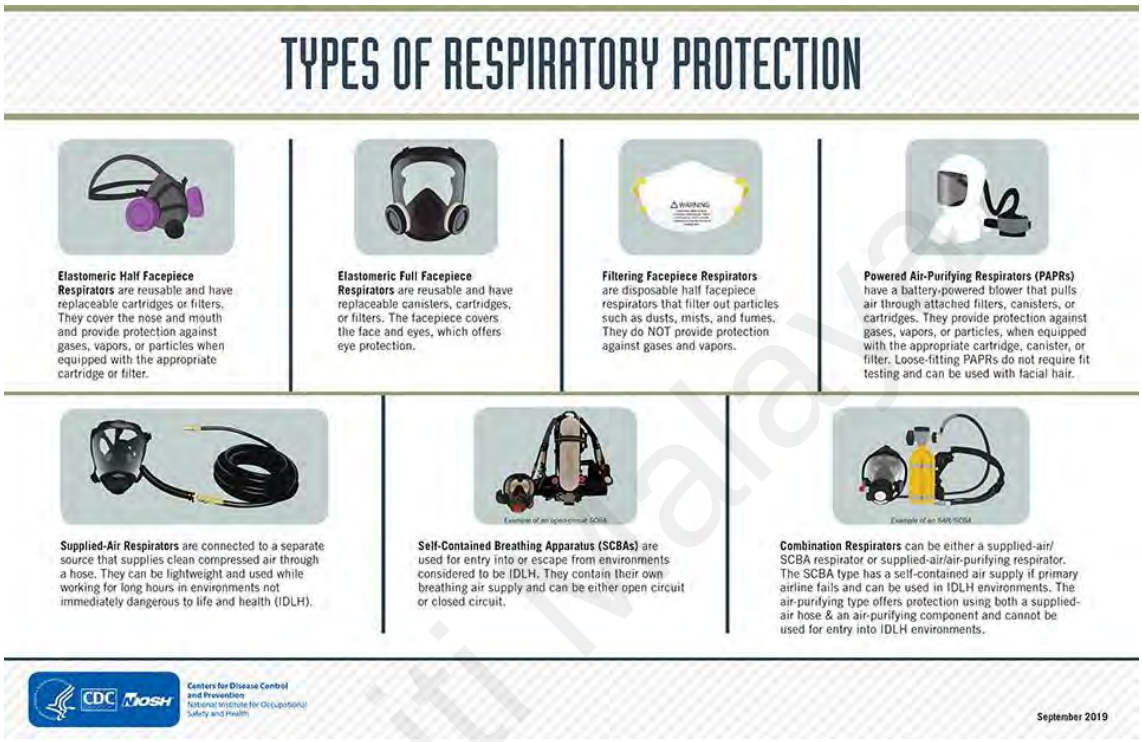

Figure 2.3: Types of Respiratory Protection

2.2.1 N95 Respirator

The design of the N95 respirator is capable of achieving a close tight fitting to the user's face. In addition, a filtration efficiency of at least 95% against airborne particles is offered by an N95-type respirator and it is not resistant to oil (Ji et al., 2020). N95 is able to filter 95% of airborne particles which includes a wide range of sizes. This range includes transmitted SARS-CoV-2 which is 5000nm in size and individual Brownian motion SARS-CoV-2 which are 300nm in size (Rashid et al., 2022). The superior protection offered by N95 respirators is proved by quantitative fit testing investigations (O'Kelly et al., 2021). Surgical N95 Respirators commonly known as N95s are widely used in healthcare applications (U.S. Food and Drug Administration [FDA], 2021a). One investigation on the stability of SARS-CoV-2 revealed that a detectable level of the virus recovered on the outer layer of the surgical mask after 7 days (Chin et al., 2020).

An N95 respirator is made up of four layers as illustrated in Figure 2.4, namely coverweb, shell, filter 1, and filter 2. Coverweb and shell layer is made up of polyester meanwhile, filter layers are made from polypropylene (3M, 2018). The internal filtration layer is made up of high-efficiency melt-blown nonwoven material functions to determine the filtration efficiency of a respirator (Henneberry, n.d).

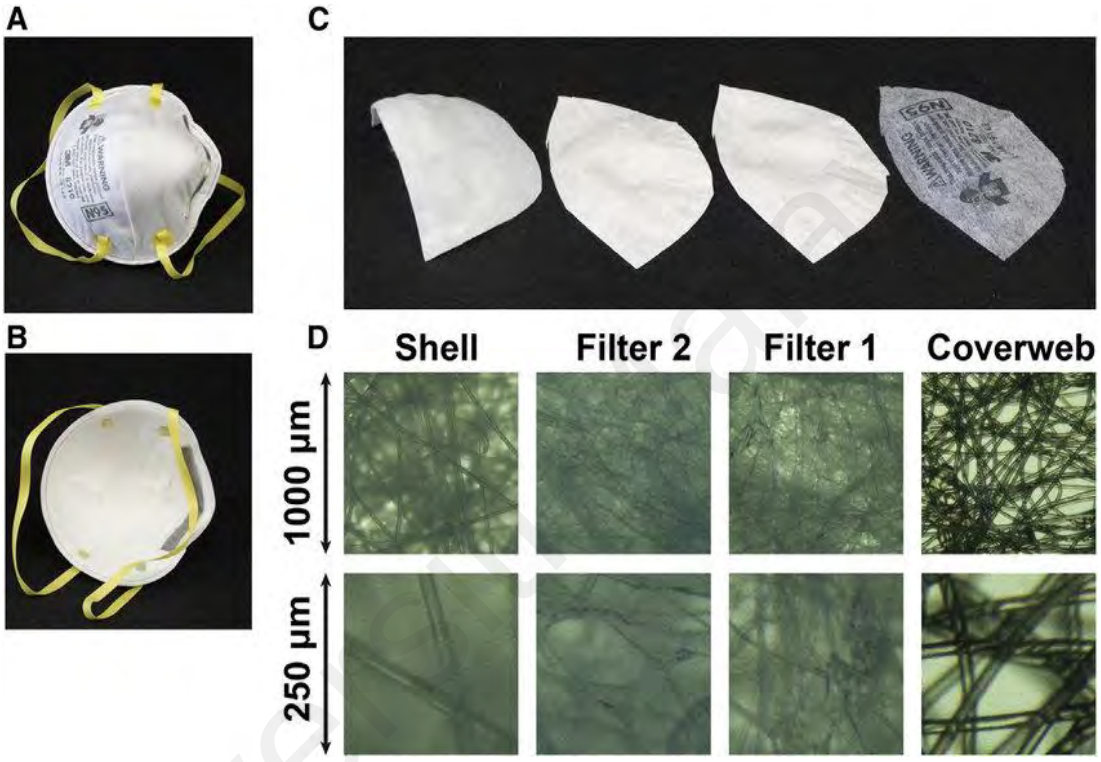

Figure 2.4: Multilayer sandwich anatomy of N95 mask (a) Environmental interface; (b) User interface; (c) From left to right; inner layer (Shell), middle layers (Filter 2 and Filter 1), and outer layer (Coverweb); (d) Light microscope images of the four layers, with a lower row at four-fold higher magnification (3M Model 8210)
(Huber et al., 2020)

2.3 FFR Decontamination Policy

This unprecedented Covid 19 pandemic has led to the need for the introduction of several emergency and mandatory policies that are crucial to navigate the issues encountered in this pandemic. As the shortage of mask supply was experienced worldwide, regulations such as rationing of mask supply, reuse guidelines, and mask decontamination procedures were emphasized in these policies.

According to the Centers for Disease Control and Prevention (CDC), several guidelines were laid down for health workers in the event of a mask crisis scenario. These guidelines include (Centers for Disease Control and Prevention [CDC], 2020b):

- At the end of each workday, the mask needs to be discarded as soon as removed
- In the event that the mask is soiled, damaged, or hard to breathe through, the mask should be discarded
- Health workers must not touch the facemask and hand hygiene needs to be performed if touched.
- Health workers should leave the patient care area in case they need to remove the facemask.
- Prioritize supply of facemasks for essential surgeries and procedures

In addition, the CDC outlines the following policies concerning reusing or usage of a single-use mask for a prolonged period (Centers for Disease Control and Prevention [CDC], 2020a):

- A number of five N95 FFRs are assigned to each healthcare worker which are stored in a breathable bag at the end of the shift. Rotating the assigned N95 between each day allows pathogens to "die off".
- Hand hygiene should be performed in the event of adjusting, donning, and touching the reused FFR.
- The donning process is limited to 5 per device.

An extreme shortage of mask supply calls for the decontamination procedure performed on FFR, in order to safely decontaminate for reuse. The decontamination

procedure on the contaminated mask should satisfy several conditions to be regarded as safe for decontamination purposes as outlined:

- Inactivation of viruses and bacteria is ensured
- No effect on the filtration efficiency of the mask after treatment
- No effect on the fit performance of the mask after treatment
- Off-gassing of decontamination chemicals falls below the permissible range.

In the aspect of the inactivation of pathogens inactivation, the U.S. Food and Drug Administration (FDA) recommended a policy where at least 3 log reductions are achieved in the pathogen burden for sterilization of devices intended for skin contact which includes FFRs (Turtil, 2016).

2.4 FFR Decontamination Methods

Numerous studies and research are being conducted worldwide to explore the possibilities of decontaminating single-use FFR for reuse purposes. The primary concern of utilizing this approach is to reduce the pathogen burden of a contaminated FFR where the integrity and performance are sustained. FFR decontamination procedures studied for this literature comparison include UVGI, HPV, aHP, heat, MGS, and ethanol decontamination.

2.4.1 Ultraviolet Germicidal Irradiation (UVGI)

UVGI is a process that utilizes ultraviolet (UV) rays to sterilize pathogens which include viral, bacterial, and fungal organisms. Set up and design that follows UVGI technology produces UV-C rays for intended purposes. UV-C rays are superior in safety compared to UV-A and UV-B rays due to their shorter wavelength as illustrated in Figure 2.5 and lesser penetrating power (Centers for Disease Control and Prevention [CDC],

2021). In addition, UV-C rays are more efficient in inactivating viruses compared to UV-A and UV-B (U.S. Food and Drug Administration [FDA], 2021b).

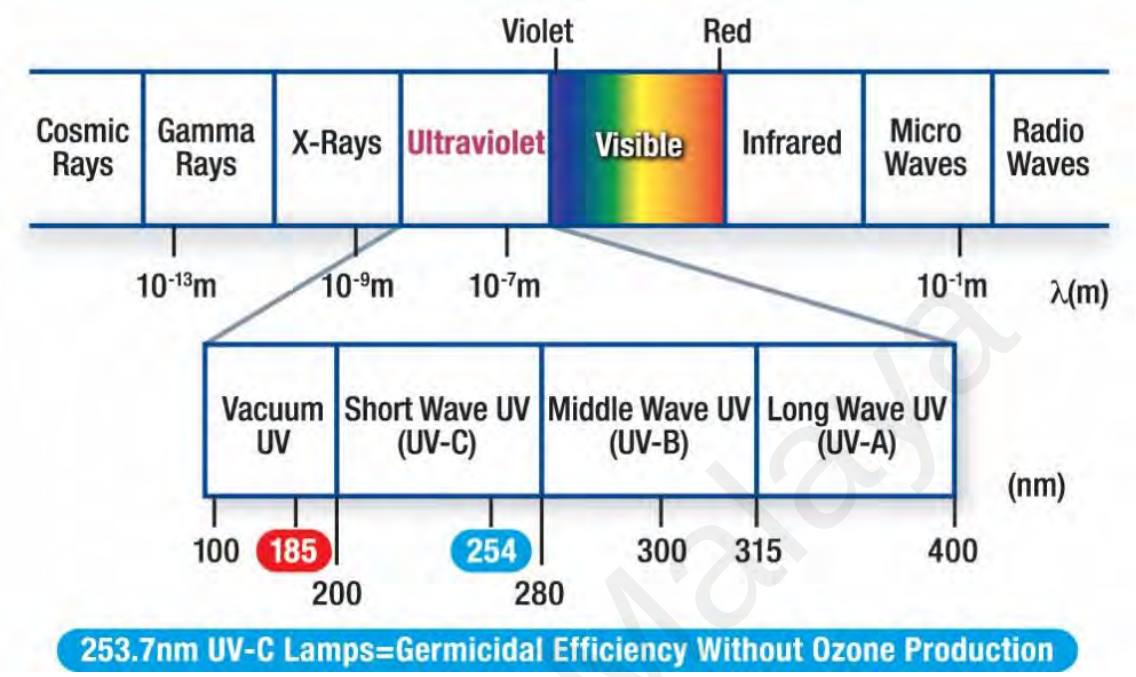

Figure 2.5: Electromagnetic spectrum

There are numerous UV-C sources available in the market, which differ by the range of wavelength produced and the purpose of the product aligned or intended. Types of UV-C lamps include low-pressure mercury lamps, excimer lamps or far-UVC lamps, pulsed xenon lamps, and light-emitting diodes (LEDs) (U.S. Food and Drug Administration [FDA], 2021b).

The design of a UVGI-based decontamination system depends on several controlling variables such as the wavelength of the ultraviolet rays, irradiance, and exposure time. The dosage of UVC delivered from the source to the specimen is directly proportional to the decontamination efficiency of the contaminated specimen. The range of dosage which is required for the decontamination treatment must be calculated beforehand in order to maximize decontamination efficiency. Exceeding the range of dosage can lead to impairment and disintegration of FFR's performance. Meanwhile, the insufficient dosage can result in partial inactivation of the virus which is not optimum for reuse. Equation 2.1

states the UV dose calculation for UVC-based decontamination system design (Mills et al., 2018).

$$\text{UV dose } \left(\frac{\text{J}}{\text{cm}^2}\right) = \text{Irradiance } \left(\frac{\text{W}}{\text{cm}^2}\right) \text{ x Time (s)} \qquad \text{(Equation 2.1)}$$

Table 2.2: UVGI-based FFR decontamination system designs and outcomes

Study	Irradiance (W/m^2)	Exposure Time (s)	Dosage (J/cm^2)	Distance (cm)	Outcomes
Pathogen Inactivation / Load Reduction					
(Ozog et al., 2020)	165	60 - 70	1.5	11.5	- > 3 log reduction in viable SARS-CoV-2 virus - Mask model: 3M 1860
(Simmons et al., 2021)	NA	0 - 300	NA	100	- > 4.79 log reduction in viable SARS-CoV-2 virus - Mask model: 3M 1860
(Rathnasinghe et al., 2020)	54.3	2 - 420	0.01086 - 2.2806	10	- up to 3.5 log reduction in viable SARS-CoV-2 virus - Mask model: 3M 8211
(Golovkine et al., 2021)	10	300	0.3	NA	- Average 3.74 log reduction in viable SARS-CoV-2 virus at 0.6 J/cm^2 dosage (3M 1860) - Average 1.68 log reduction in viable SARS-CoV-2 virus at 0.6 J/cm^2 dosage (3M 8210) - Mask model: 3M 1860 and 3M 8210
		600	0.6		
(Fischer et al., 2020)	5.5	600 - 3600	0.33 - 1.98	50	- ≥ 3 log reduction in viable SARS-CoV-2 virus - Mask model: AOSafety N9504C
(Geldert et al., 2021)	64	NA	0.05 - 1.5	3.4	- >3 log reduction in viable SARS-CoV-2 virus at 0.05 -0.5 J/cm^2 dosage - >5 log reduction in viable SARS-CoV-2 virus at 0.5 -1.5 J/cm^2 dosage - Mask model: 3M 1860
(Kayani et al., 2021)	≥ 300	60	≥ 2	NA	- ≥ 3 log reduction in viable MS2 - Mask model: 3M 1860
(Fisher & Shaffer, 2011)	25	120 - 15960	0.1	NA	- 3 log reduction in viable MS2 - Mask model: 3M 1860
(Vo et al., 2009)	4	3600 - 18 000	1.44 - 7.2	42	- ≥ 3 log reduction in viable MS2 at 4.32 J/cm^2 - No virus detection at ≥7.20 J/cm^2 - Mask model: Honeywell N1105
(Mills et al., 2018)	3900	60	1	100	- 3 log reduction in viable H1N1 influenza virus - Mask model: 3M 1860

Table 2.2, Continued

Study	Irradiance (W/m^2)	Exposure Time (s)	Dosage (J/cm^2)	Distance (cm)	Outcomes
Pathogen Inactivation / Load Reduction					
(Lore et al., 2012)	16 - 22	900	1.8	25	- ≥ 4.65 log reduction in viable H5N1 influenza virus - Mask model: 3M 1860
(Weaver et al., 2021)	2.32	0 - 3600	0 - 0.8352	60.96	- >3 log reduction (5 min of exposure) and complete decontamination (15 min of expo-sure) in viable NL63 coronavirus - Mask model: 3M 1860
(Lin et al., 2018)	189 (UVC)	60 - 1200	1.134 - 22.68	10	- UVA could not decontaminate as effectively as UVC. - No bacteria recovered after 5min UVC exposure. - Mask model: 3M 8210
	312 (UVA)		1.872 - 37.44		
Performance / Structural Integrity					
(Smith et al., 2020)	3.18	57600 (Exterior)	18.4	NA	- Mask integrity was significantly impaired - Average fit score: ≥ 100 - Mask model: 3M 1860
		14400 (Interior)	4.6		
(Lore et al., 2012)	16 - 22	900	1.8	25	- Mean penetration: 0.37%, 0.99% - Mask model: 3M 1860
(Lindsley et al., 2015)	NA	NA	0 - 950	6.2	- Filtration performance slightly affected - No effect on flow resistance - Mask model: 3M 1860
(P. Z. Chen et al., 2020)	≥24.31	NA	≥1	30.48	- Expected penetration: 1.121 % (0.3µm, 5 cycles, 3M 1860) and 0.258 % (0.3µm, 5 cycles, 3M 8210) - Mask model: 3M 1860 and 3M 8210

Table 2.2, Continued

Study	Irradiance (W/m^2)	Exposure Time (s)	Dosage (J/cm^2)	Distance (cm)	Outcomes
Performance / Structural Integrity					
(Liao et al., 2020)	NA	1800	NA	NA	- Efficiency of melt-blown layer: (≥96% at 10 cycles) (≥93% at 20 cycles) - Mask model: 3M 8210
(Ou et al., 2020)	NA	300	>1	100	- Filtration performance preserved for up to 10 cycles - Mask model: 3M 8210
(Ontiveros et al., 2021)	55.56	180	1	36.8	- No visual abnormalities on mask integrity - Mean breaking force of 34.8 ± 5.23 N - Average filtration efficiency = >95% - Fit Factor = >100% - Mask model: 3M 8110S
(Ludwig-Begall et al., 2021)	NA	NA	120	2.6	- Remained physically unaffected for up to 5 cycles - Filtration efficiency of >95% up to five cycles - Breathability well within allowed range after 5 cycles - Mask model: KN95 FFR(Guangzhou Sunjoy Auto Supplies)
(He et al., 2020)	NA	300	0.126	NA	- Filtration performance preserved up to a dosage of 0.378 J/cm2 - Mask model: UVEX FFP2
		600	0.256		
		900	0.378		

In general, the UVGI-based decontamination system portrays excellent virucidal activity against coronaviruses such as SARS-CoV-2. A research reported successful decontamination of viable SARS-CoV-2 with UVC radiation of 1.5 J/cm^2 where the shadowing effect of the light ray was denoted for disinfection concern (Ozog et al., 2020). Rathnasinghe et al. reported a novel setup of a UVC decontamination device where log reduction up to 3.5 was achieved using 1.3 J/cm^2. However, this investigation did not include the decontamination of the FFR's strap (Rathnasinghe et al., 2020).

Through a review of multiple reported studies presented in Table 2.2, it is possible to estimate the approximate dosage levels needed to deactivate this targeted pathogen. Approximately a UVC dosage of 0.5 J/cm^2 is estimated to be the lower limit of the dosage required to reduce the pathogen burden by 3 logs. In addition, lower UVC doses in the range of (0 - 0.5 J/cm^2) presented a decline in the decontamination efficiency (Geldert et al., 2021). Therefore, the crossover area in the range of safe dosage must be calculated precisely in the case of public application devices which could pose a safety concern.

2.4.1.1 Quartz glass

Quartz glass is made from pure silicon tetrachloride (SiCl4) using a specific method called Flammpyrolyse-method. One of the key properties of this type of glass is the excellent range of light transmission. Quartz glass made of synthetic fused silica is widely used in UV-related optic fields (Schreiber et al., 2004). As shown in Figure 2.6, quartz glass allows more than 90% penetration of light rays across the spectrum. Specifically, UVC which possesses a wavelength in the range of 254nm able to pass through this quartz glass without significant losses.

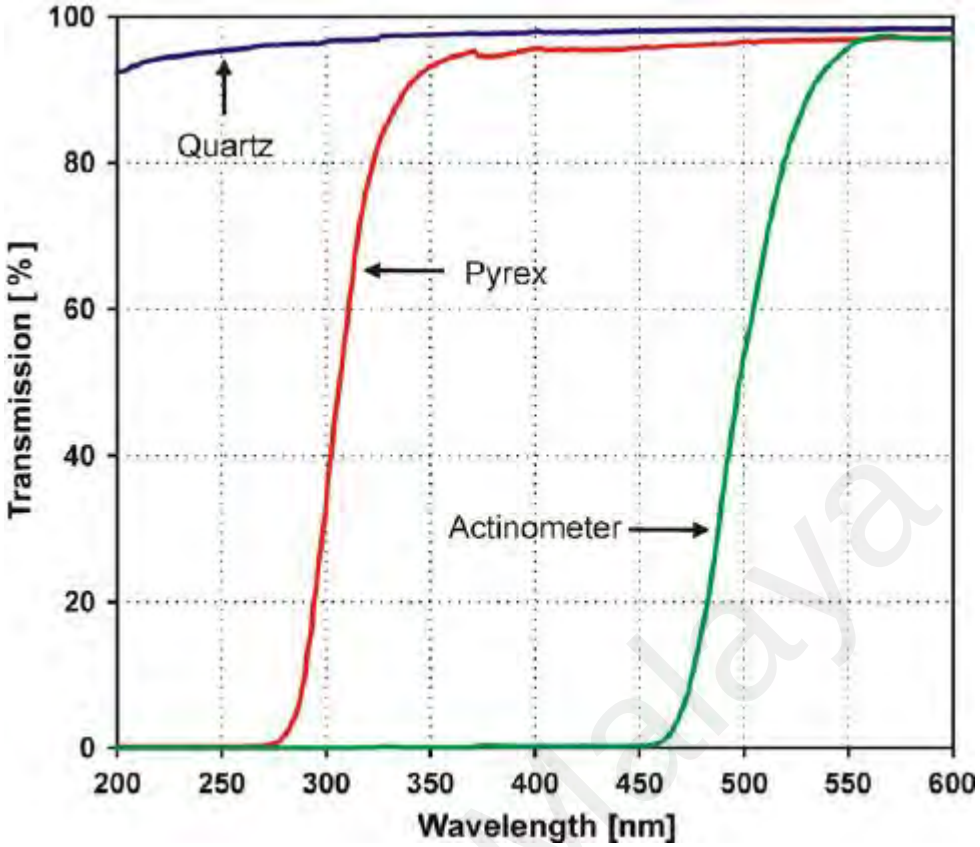

Figure 2.6: Optical transmittance of Pyrex and quartz spectrometric cells and 0.15M ferrioxalate actinometer for optical path length 1 cm (Lukes et al., 2008)

2.4.2 Hydrogen Peroxide

Hydrogen Peroxide (HP) which carries the molecular formula of H_2O_2 is a colorless liquid at room temperature which possesses a strong odor (Centers for Disease Control and Prevention [CDC], 2019). HP is a very strong oxidizing agent where spontaneous combustion is imminent if it comes into contact with organic substances. The wide application of HP includes medicinal application, hair bleach at the household application level, a bleach for textiles and paper, as a component of rocket fuels, and for producing foam rubber and organic chemicals at industry levels (National Center for Biotechnology Information [NCBI], 2022).

2.4.2.1 Hydrogen peroxide vapor (HPV)

The vaporous form of HP known as HPV is widely used as a disinfectant for various forms of surfaces. Investigations and research on HPV decontamination procedures

reveal promising results on the use of HPV as a disinfecting agent. Significant reduction in microbial load using HPV up to safety levels opens a path for the wide application of disinfection.

Research papers reviewed in Table 2.3 mostly describe HPV-based decontamination experiments using commercially available HPV-producing machines. The concentration of the HPV used and exposure time to the specimen are key factors that play a major role in the efficiency of an HPV-based decontamination system. Nevertheless, this decontamination system poses a critical safety concern where this treatment could leave some HP residue post-treatment which potentially compromises the safety of the user.

Table 2.3: HPV-based FFR decontamination system designs and outcomes

Study	Method	Concentration of HPV Used/ Achieved	Exposure Time (min)	Outcome
Pathogen Inactivation / Load Reduction				
(Oral et al., 2020)	Steris ARD1000®	410 ± 83 ppm	Gas: 180	- >4 log reduction in viable SARS-CoV-2 - Mask model: 3M 1860
(Smith et al., 2020)	Bioquell Z Vaporizer	30% (Peak 500 ppm)	Gassing: 20 Dwell: 60 Aeration: 210	- ≈5 log reduction in viable SARS-CoV-2 RNA - Mask model: 3M 1860
(Kumar et al., 2020)	VHP® ARD System	35% (Peak 750 ppm)	Conditioning: 3 Decontamination: 30 Aeration: 20	- (5.2 - 6.3) log reduction in viable SARS-CoV-2 virus - Mask model: 3M 1860 and 3M 8210
(Christie-Holmes et al., 2021)	V-PRO maX Low-Temperature Sterilization System by Steris	NA	Non-lumen cycle (28)	- 4 log reduction in viable SARS-CoV-2 titer and 5 in HCoV-229E - Mask model: 3M 8210
(Fischer et al., 2020)	Panasonic MCO-19AIC-PT	≈ 1000 ppm	Gas: 7	- ≥ 3 log reduction in viable SARS-CoV-2 virus - Mask model: AOSafety N9504C
(Ludwig-Begall et al., 2021)	V-PRO maX Low-Temperature Sterilization System by Steris	59%	Non-lumen cycle: 28	- No virus detection after 2 or 5 cycles (Porcine coronavirus and murine norovirus) - Mask model: KN95 FFR(Guangzhou Sunjoy Auto Sup-plies)
(Russo et al., 2021)	VHP® VICTORY unit	35% (400 - 800 ppm	Conditioning and Gassing: 90 Dwell: 180 Aeration: 900 - 1080	- No growth of 6-log Geobacillus stearothermophilus spores detected (1st, 7th day) - Mask model: 3M 1860s

Table 2.3, Continued

Study	Method	Concentration of HPV Used/ Achieved	Exposure Time (min)	Outcome
Pathogen Inactivation / Load Reduction				
(Moschella et al., 2021)	Bioquell® BQ-50	35%	NA	- No growth of 6-log Geobacillus stearothermophilus spores detected - Mask model: 3M 1860
(Dave et al., 2020)	A novel HPV-based system was constructed	3%	Gassing: 3 -5 Dwell: 60 Aeration: 15	- >6 log reduction in P22 bacteriophage - Mask model: 3M 1860
Performance / Structural Integrity				
(Oral et al., 2020)	Steris ARD1000®	410 ± 83 ppm	Gas: 180	- Mask fit and filtration efficiency preserved for one cycle - Mask model: 3M 1860
(Smith et al., 2020)	Bioquell Z Vaporizer	30% (Peak 500 ppm)	Gassing: 20 Dwell: 60 Aeration: 210	- Mask integrity is minimally affected - Average fit score: ≥ 100 - Mask model: 3M 1860
(Moschella et al., 2021)	Bioquell® BQ-50	35%	NA	- All processed masks passed fit testing - Mask model: 3M 1860
(Dave et al., 2020)	A novel HPV-based system was constructed	3%	Gassing: 3 - 5 Dwell: 60 Aeration: 15	- Minimum required filtration efficiency value of 95% preserved up to 20 cycles - Mask model: 3M 1860
(Kumar et al., 2020)	VHP® ARD System	35% (Peak 750 ppm)	Conditioning: 3 Decontamination: 30 Aeration: 20	- Structural and functional integrity preserved - Mask model: 3M 1860 and 3M 8210
(Christie-Holmes et al., 2021)	V-PRO maX Low-Temperature Sterilization System by Steris	NA	Non-lumen cycle (28)	- Filtration performance preserved - Mask model: 3M 8210

Table 2.3, Continued

Study	Method	Concentration of HPV Used/ Achieved	Exposure Time (min)	Outcome
Performance / Structural Integrity				
(Jatta et al., 2021)	V-PRO maX Low-Temperature Sterilization System by Steris	59%	Inject: 18 Aeration: 8	- Mask fit and filtration efficiency preserved for up to 10 cycles - Mask model: 3M 8211
(Fischer et al., 2020)	Panasonic MCO-19AIC-PT	≈ 1000 ppm	Gas: 7	- Filtration performance preserved after 1 treatment - Mask model: AOSafety N9504C
(Ludwig-Begall et al., 2021)	V-PRO maX Low-Temperature Sterilization System by Steris	59%	Non-lumen cycle: 28	- Remained physically unaffected for up to 5 cycles - Filtration efficiency of >95% up to five cycles - Breathability well within allowed range after 5 cycles -Mask model: KN95 FFR(Guangzhou Sunjoy Auto Supplies)

As reported, HPV-based FFR decontamination systems exhibit exceptional virucidal activity against SARS-CoV-2 (Christie-Holmes et al., 2021; Fischer et al., 2020; Kumar et al., 2020; Oral et al., 2020; Smith et al., 2020). Kumar et al. presented a remarkable 6-log reduction in pathogen load. In addition, the preservation of FFR's performance and integrity while completing the decontamination cycle was a notable feat (Kumar et al., 2020).

2.4.2.2 Aerosolized hydrogen peroxide (aHP)

aHP can be generated by emitting HP liquid through a nozzle. These resultant aHP particles can be 8 to 10 micrometers in size (Berger et al., 2022). Table 2.4 lists the previous FFR decontamination investigations using aHP. As shown in Table 2.4, aHP decontamination system was able to produce microbial efficiency beyond the required value.

Table 2.4: aHP-based FFR decontamination system designs and outcomes

Study	Method	Concentration of HP Used/ Achieved	Exposure Time (min)	Outcome
Pathogen Inactivation / Load Reduction				
(Cadnum et al., 2020)	AltapureAP-4	22%	Gassing: 1 Dwell: 5 Scrubbing: 15	- >5 log reduction in MRSA and bacteriophage MS2 (3 Cycle) - Mask model: Moldex 1517

2.4.2.3 Hydrogen peroxide traces

HP residue on an N95 mask surface post-treatment is harmful to users. Hence, a decontamination treatment such as aHP should not leave any residue that could pose a serious threat to the user. Multiple reports have been presented on ways and methods to calculate and measure the HP traces from a mask surface. A method describes that 10 mL of deionized water was used to extract the hydrogen peroxide residue from the mask by 2 min of shaking which eventually reacted with 0.4 mL of 7.5% wt titanium oxysulphate in 2mL of 25% wt sulfuric acid (Kumkrong et al., 2021). Hasani et al. reported a hydrogen peroxide tracing procedure using the MQuant Peroxide test kit. This procedure describes a small section of the treated N95 mask that was excised and left in a tube of 25 mL of distilled water for 1 hour. The distilled water was tested for hydrogen peroxide using the test strips (Hasani et al., 2021).

2.4.3 Microwave-Generated Steam (MGS)

Microwave technology is widely used as a household appliance in the form of an oven. The world's first-generation microwave ovens were created in 1954. Microwave is categorized under thermal sterilization where heat is utilized to denature or inactivate a pathogen (Soni et al., 2020). Table 2.5 depicts investigations that have been conducted to sterilize FFR using microwave technology specifically MGS. Rapid decontamination coupled with excellent virucidal activity promotes MGS as a good alternative for N95 decontamination.

Table 2.5: MGS-based FFR decontamination system designs and outcomes

Study	Method / Equipment	Exposure Time (s)	Outcomes
Pathogen Inactivation / Load Reduction and Performance / Structural Integrity			
(Fisher et al., 2011)	- N95 respirators placed inside Medela Quick CleanTM MICRO-STEAMTM BAGS - Steam bags were placed inside Sharp Model R-305KS (2450 MHz, 1100 W) microwave oven	90	- ≥ 3 log reduction in viable MS2 - Filtration efficiency was preserved after 1 cycle. - Mask model: 3M 1860, 8210
(Zulauf et al., 2020)	- 1150 W and 1100 W microwave ovens used. -1st set up: N95 respirator placed on mesh over mug containing water -2nd set up: N95 respirator placed on mesh over glass container containing water	180 (one cycle)	- ≥ 4 log reduction in viable MS2 with one cycle - Fit, seal, and filtration preserved for up to 20 cycles - Mask model: 3M 1860
(Pascoe et al., 2020)	-Inoculated membrane was placed over a folded N95 respirator which was suspended over a microwave steam sterilizer - Variables : (100ml, 200ml in steam sterilizer) (900W, 1800 W - 2.45 GHz microwave oven (NE-1853; Panasonic)	60, 90, 120	- ≥ 6 log reduction in viable S.aureus (1800W) with different treatment times and volumes of steam water. - Bacterial filtration efficiency preserved - Mask model: Kimberley-Clark N95 respirators
(Lore et al., 2012)	- N95 was suspended over holed boxes filled with 50ml of water - A 1250 W (2.45 GHz) microwave oven (Panasonic) was used	120	- ≥ 4 log reduction in viable Influenza A/H5N1with one cycle - Mask model: 3M 1860s, 1870

2.4.3.1 Microwave oven power estimation

The review of the previous study indicates that the power rating of a microwave oven and the treatment time of the treatment play a crucial role in the virucidal efficiency of the specific equipment. As per standard IEC 60705, the power of a microwave oven can be estimated to design precise experimental parameters (*Standard Test Method to Qualify Single-Use Foodservice Packaging for Use in Microwave Ovens*, 2007). The standard calculation used for the power estimation of a microwave oven is described as follows:

1. Measure the weight of an empty 2-L beaker. Add 1,000 g ± 5 g of distilled water having an initial temperature of 10°C + 1°C.
2. Measure the weight of the beaker to obtain the actual mass of water.
3. Measure the initial water temperature to the nearest 0.1°C.
4. Immediately place the beaker into the center of a microwave oven and operate the oven at full power until the water temperature is 20°C ± 2°C. Record the heating time to the nearest second, excluding the magnetron filament heat-up time.
5. Stir the water and measure the final water temperature to the nearest 0.1°C. NOTE: Stirring and temperature measuring devices are to have a low heat capacity
6. Calculate the microwave power output from the formula:

$$P = \left(\frac{4.187\ .\ \mathrm{Mw}(T_2 - T_1) + 0.55\ .\ \mathrm{Mc}\ (T_2 - T_0)}{t}\right) \qquad \text{(Equation 2.2)}$$

- P is the microwave power output, in watts, rounded off to nearest 50 W;
- Mw is the mass of the water, in grams;
- Mc is the mass of the container, in grams;
- T_o is the ambient temperature of the water, in degrees Celsius;
- T_1 is the ambient temperature of the water, in degrees Celsius;
- T_2 is the ambient temperature of the water, in degrees Celsius;
- t is the heating time, in seconds, excluding the magnetron filament heating-up time.

2.4.4 Other Methods

Apart from UVGI, HPV, aHP, and MGS decontamination systems, there are other procedures such as moist heat, dry heat, and ethanol being investigated by researchers worldwide. Despite having several drawbacks to the performance of the treated FFRs', these treatments still portray excellent potential if the treatments are well-designed and managed. Table 2.6 - 2.8 reports the list of articles that investigate FFR decontamination using moist heat dry heat, and ethanol respectively.

Table 2.6: Moist heat-based FFR decontamination system designs and outcomes

Study	Method	Temperature (˚C)	Exposure Time (min)	Relative Humidity (%)	Outcomes
Pathogen Inactivation / Load Reduction					
(Lore et al., 2012)	- Mask loaded into a sealed container and placed inside a heated oven. - Container filled with 1L tap water	65 ± 5	20	NA	- ≥ 4.62 log reduction in viable H5N1 influenza - Mask model: 3M 1860
(Rockey et al., 2020)	- Conducted using TestEquity 123H temperature/ humidity chamber	72, 82	30	1 - 89	- Increase in treatment temperature and humidity results in an increased log reduction of pathogen - Mask model: 3M 1860
Performance / Structural Integrity					
(Bopp et al., 2020)	- Moist heat autoclave	115 ˚C - 130 ˚C	2 - 60	NA	- Molded N95 respirators failed all tested fit testing - Slight degradation in filtration efficiency is notable - Mask model: 3M 1860
(Andereg g et al., 2020)	- Conducted using a convection oven (Despatch LAC1-38-8, 3.7 cu. Ft.)	70 ˚C - 85 ˚C	30	60% - 85%	- Passed fit testing - Filtration efficiency preserved - Mask model: 3M 1860

Table 2.7: Dry heat-based FFR decontamination system designs and outcomes

Study	Method	Temperature (˚C)	Exposure Time (min)	Outcomes
Pathogen Inactivation / Load Reduction				
(Daeschler et al., 2020)	BevLes Heated Holding Cabinet with humidity (Masks were enclosed within Steril-Peel Pouches	70	60	- Viable SARS-CoV-2 virus was inactivated beyond the detection limit - Mask model: 3M 1860s and 3M 8210
(Xiang et al., 2020)	Electric oven	60, 70	60 - 180	- 1 hour of exposure could successfully kill 7 types of bacteria as well as inactivate the H1N1 virus - Mask model: 3M 1860
Performance / Structural Integrity				
(Viscusi et al., 2008)	Fisher Isotemp 500 Series laboratory oven	80, 160	60	- S.D. of penetration (0.258 at 80 ˚C) -Mask did melt at 160 ˚C - Mask model: Not Specified
(Xiang et al., 2020)	Electric oven	60, 70	60 - 180	- No significant effect on the shape and filtration performance after exposure up to 3 hours - Mask model: 3M 1860

Table 2.8: Ethanol-based FFR decontamination system designs and outcomes

Study	Concentration (%)	Exposure Time	Outcome
Pathogen Inactivation / Load Reduction			
(Smith et al., 2020)	70	Air drying: ~8	- Viable SARS-CoV-2 RNA was not detected post-treatment - Mask model: 3M 1860
Performance / Structural Integrity			
(Liao et al., 2020)	75	Depends on the air-drying time	- Significant decrease in filtration efficiency (56.33±3.03%) - Mask model: 3M 8210

2.5 Advanced Oxidation Process (AOP)

The Advanced Oxidation Process (AOP) is a process that involves the production of hydroxyl radicals (OH•). The production of these radicals is the result of the combination of hydrogen peroxide (H2O2), ozone, photo-catalysis, or oxidants using ultraviolet (UV) radiation (Krishnan et al., 2017).

Hydroxyl radicals are known for their microbial activities. Reports indicate microbial activity of a various range of microorganisms is proved through the usage of hydroxyl radicals with a concentration of 0.8 mg/L and a spray density of 21 μL/m2 in 4 seconds (Vimbert et al., 2020).

Among the AOP techniques available, hydrogen peroxide photolysis is one of the most effective against contaminants. This process uses the principle of decomposing hydrogen peroxide into hydroxyl radicals by combining it with UV-C rays (Krystynik, 2021). The decomposition of hydrogen peroxide by photolysis is explained in Equation 2.2 (Ogata et al., 1981).

$$H_2O_2 + hv \rightarrow 2\ OH\bullet \qquad \text{(Equation 2.2)}$$

2.6 Fabrication Processes

2.6.1 Computer Numerical Control (CNC) Cutting

The CNC cutting process utilizes laser processing which is computer-controlled. This specific type of cutting was able to produce a high level of cutting quality which corresponds to higher accuracy in the fabricated parts (Li et al., 2023).

2.6.2 Slot Milling

Slot milling is a fabrication technique that uses a rotating tool with multiple cutting edges to create a slot in a workpiece. A few applications of this technique include the creation of pockets, keyways, and slots in a range of workpieces (Xometry, 2023).

2.7 Summary

Several factors contribute to the reusability of a decontaminated N95 respirator such as the level of virus inactivation achieved, the integrity of the mask, filtration performance, and leftover residue levels. UVGI, HPV, aHP, and MGS are among the studied decontamination investigations that portray excellent virucidal activity against SARS-CoV-2 and other wide ranges of pathogens. In addition, these studies prove that the integrity and performance of the respirator can be sustained after treatment if the system is managed well. Government policies on mask contingency plans may temporally ease the severity of mask shortage. Nevertheless, for a sustainable foreseeable future, FFR decontamination could play a major role. Furthermore, the usage of hydroxyl radicals which is produced through the advanced oxidation process in FFR decontamination procedures should be noted.

Currently, the investigations reviewed in this study regarding FFR decontamination procedures involve only a singular treatment conducted on contaminated FFR. Therefore, in this study, a novel idea of combining two different decontamination techniques in a single decontamination cycle will be approached. As these techniques exhibit excellent virucidal activities as a single decontamination treatment, combination or hybrid decontamination methods could potentially produce better decontamination results at a significantly shorter treatment cycle.

CHAPTER 3: METHODOLOGY

In this chapter, in-depth procedures that have been established in conducting this research are explained. The flow chart as illustrated in Figure 3.1 depicts a set of processes that have been followed in order.

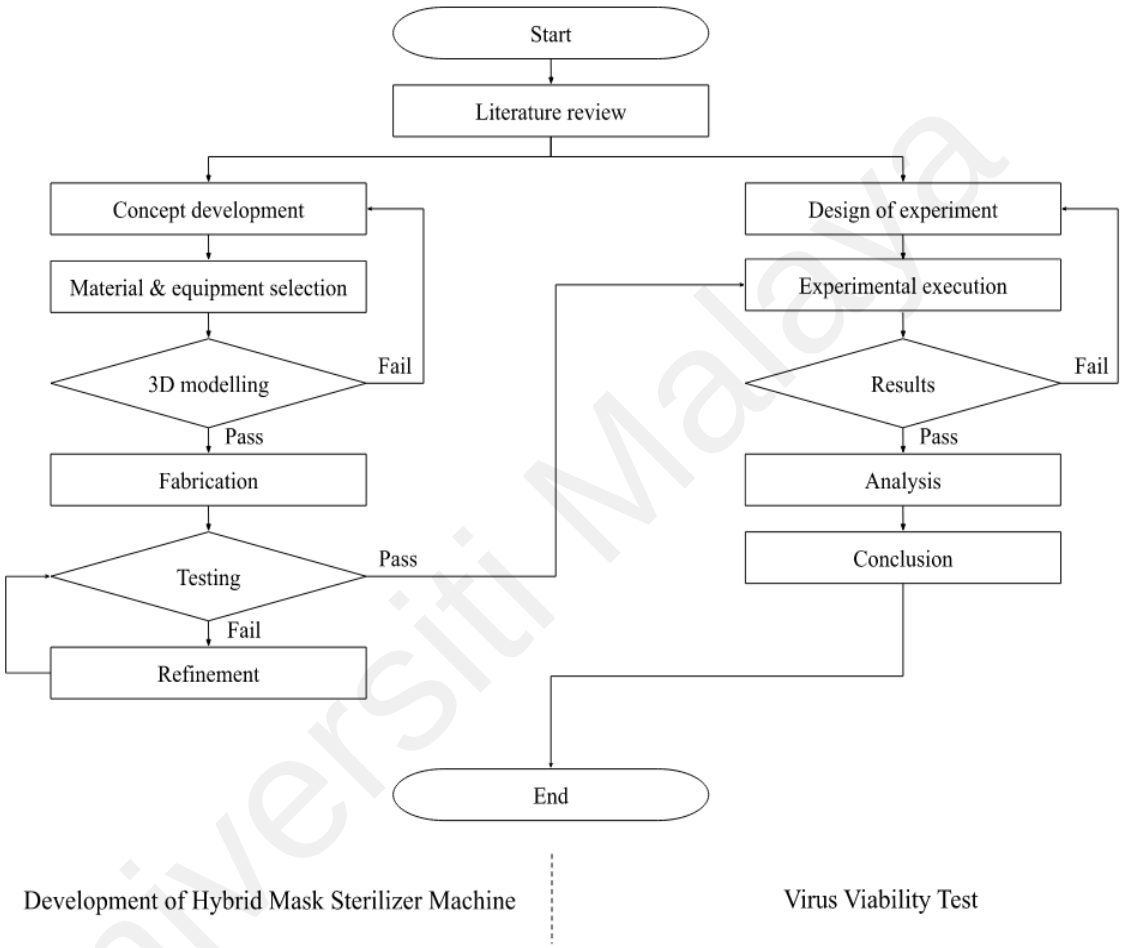

Figure 3.1: Methodology Flow Chart

3.1 Concept Development

Based on the extensive literature review, a practical concept of a hybrid mask sterilizer machine was developed. The created concept revolves around the portability of the machine, adaptability to the current Filtering Facepiece Respirator (FFR) models available in the market, the safety of the user, and efficient coordination of the selected two decontamination systems namely UVGI and Aerosolized Hydrogen Peroxide (aHP) to work in relation to the user input.

The concept of the UVGI system was developed with 5 UVC bulbs. These bulbs will be arranged in a manner where 3 will focus on the mask's exterior part and 2 will focus on the interior part of the mask. Bulbs will be connected to suitable ballast and power supply. Furthermore, the bulbs will be surrounded by reflective surfaces to increase the reflection of UV rays.

On the other hand, the aHP system was developed using several equipment such as an ultrasonic atomizer, DC air pump, and HP solution. Upon activation, the two ultrasonic atomizers are responsible for converting the HP solution into mist-like particles. Next, the DC pumps will move the vapor in and out of the specimen area as shown in Figure 3.2.

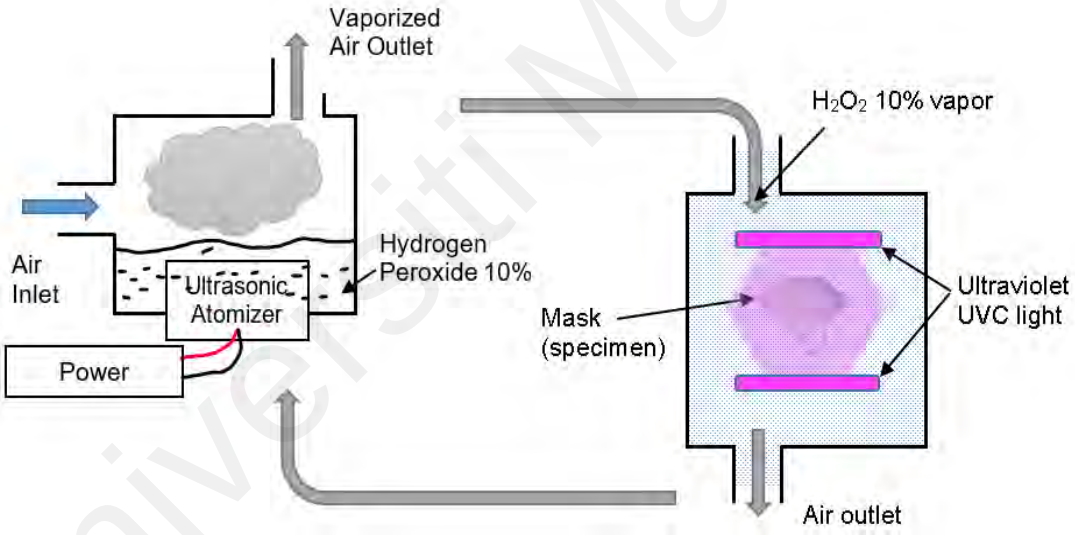

Figure 3.2: Concept of decontamination systems

Furthermore, as an additional safety feature, an enclosed acrylic case was planned to hold the FFR. This novel feature was introduced in the concept, in order to avoid cross-contamination of the whole machine, in the event of sterilizing contaminated face masks. Specifically, these cases were planned to have quartz surfaces on two of the ends to allow penetration of UV rays.

As for the Microwave-Generated Steam (MGS) decontamination system concept, it was decided to proceed with commercially available microwave ovens where contaminated FFRs are to be suspended on a small water reservoir.

3.2 Material and Equipment Selection

3.2.1 Stainless steel sheet metal

Most of the parts and the main structure of this machine were designed in stainless steel sheet metal. This is due to the distinct properties of stainless steel such as good weldability, excellent resistance against corrosion, and intergranular corrosion.

3.2.2 Aluminium block

Several parts were designed in aluminium to cater to the solid design of specific parts, as a cost-effective measure and ease in drilling which assists in machine assembly.

3.2.3 Acryl

Acryl offers excellent optical clarity and transparency which was essential to design two of the parts in the machine. Firstly, an enclosed case that holds the N95 FFR during the decontamination process. This case was designed in Grade A cast-type clear acrylic material which was 3mm in thickness as shown. In addition, the tube connection between hydrogen peroxide solution tanks and the decontamination specimen area was designed in acrylic tubing of 8mm in inner diameter in order to monitor the flow of the aHP in and out of the specimen area.

3.2.4 Quartz glass

Quartz glass or fused silica glass is widely used in worldwide applications such as optics, semiconductors, and so on. In this research, quartz glass is crucial in the implementation of the UVGI decontamination system in the machine where the top and bottom layers of the acrylic-enclosed case were designed to be quartz glass. This glass

plays a crucial role in allowing UVC rays from the source to penetrate through the glass and reach the N95 mask which is placed in an enclosed space. The properties of the quartz glass have been listed in Table 3.1.

Table 3.1: Properties of quartz glass

Product Type	**UVC Quartz Window Plate**
Dimension	150 x 150 x 3 mm
Size Tolerance	± 0.25 mm
Scratch Dig	40 - 20
Coating	No coating
Clear Aperture	Central 95%

3.2.5 UVC bulb

UVGI decontamination system design for this research requires a UVC-producing source. 5 UVC-producing bulbs were selected as the source. The selection of this bulb was based on irradiance value at a specific distance, adaptability for the small scale of the machine, and quality of UVC produced from the source (Phillips Lighting 2022).

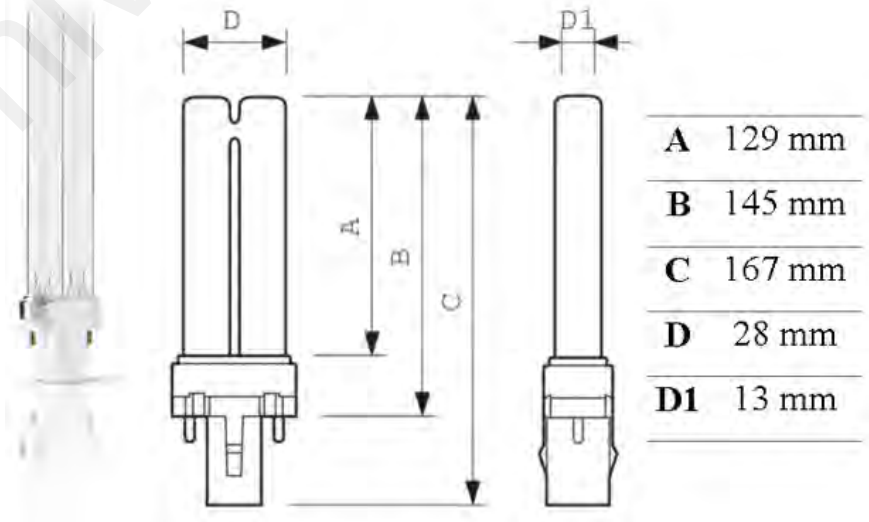

Figure 3.3: Phillips TUV PL-S 9W UVC bulb (Phillips Lighting 2022)

Table 3.2: Phillips TUV PL-S 9W UVC bulb specification

Brand	Phillips
Model	TUV PL-S 9W
Cap-Base	G23
Main application	Disinfection
Power (Nom)	8.6 W
Lamp current (Nom)	0.17 A
Voltage (Nom)	60 V
UV-C radiation at 100 hr	2.3 W
UV-C irradiance value at 10cm	2.5 mW/cm2

3.2.6 Ballast

Ballast functions to regulate current to the connected lamps or bulbs in a lighting system. The selection of ballast must be suitable to the applicable system. This is due to the type of ballast used can dictate the efficiency of the lighting operation. In addition, the output of the ballast must match the electrical requirement of the bulb such as current and voltage, so the quality and performance of the bulb can be fully utilized. The ballast selected for this machine is used to regulate the current to the selected UVC bulb.

Table 3.3: Osram QT-ECO 1X4W-16W ballast specification

Brand	Osram
Model	QT-ECO 1X4W-16W
Voltage (Nom)	220, 240 V
Mains frequency	50 Hz
Max output power	16 W
Efficiency at full-load	84 %

3.2.7 Ultrasonic atomizer

An ultrasonic atomizer is used to convert liquid in contact with the device into a uniform-sized mist. This equipment is crucial to the design of the aHP decontamination system of this mask hybrid sterilizer machine. This device was planned to be placed in one of the HP tanks that hold the HP solution. This atomizer is capable of humidifying 0.5 m^2 of area. Upon activation, the ultrasonic atomizer converts the liquid form of HP into a mist form of HP at a rate of ≥300ml/h which will be delivered into the specimen area during the decontamination cycle using a negative DC air pump (Section 3.2.8) at a rate of 17 L/min.

Figure 3.4: Ultrasonic atomizer

Table 3.4: Ultrasonic atomizer specifications

Brand	Not provided
Number of head	Single head
Voltage	24 V
Current	0.8 - 1 A
Adapter interface	5.5 x 2.1 mm
Diameter	≈ 3.6 cm
Height	≈ 25 mm

3.2.8 Negative DC air pump

A DC negative air pump was selected to pump the generated aHP. A small yet powerful enough DC pump was needed to pump the aHP into the specimen area without significant losses in airspeed and flow. One additional pump was designed in order to pump out any residue and excess aHP from the specimen area after the treatment cycle.

Figure 3.5: Negative pressure air pump

Table 3.5: Negative pressure air pump specifications

Voltage	6 - 24 V
Air pressure	80 kPa
Vacuum degree	> -50 kPa
No-load gas flow	> 17 L/min
Air inlet diameter	6.5 mm
Air outlet diameter	7 mm

3.2.9 Pneumatic air hose coupler

The inlet and outlet of the specimen area must be air-tight to avoid leakage of aHP during the treatment time. Therefore, the mask case which holds the specimen was designed with an inlet and outlet which was fitted with a pneumatic air hose coupler.

Figure 3.6: (a) Elbow pneumatic coupler; (b) Pneumatic quick coupler

Table 3.6: Pneumatic air hose coupler specification

(a) Elbow pneumatic coupler	
Model	KPL
Working pressure	0 - 0.9 MPa
Thread	3/8 "
Outer diameter	12 mm
(b) Pneumatic quick coupler	
Model	KPC
Working pressure	0 - 0.9 MPa
Thread	3/8 "
Outer diameter	12 mm

3.2.10 DC Fan

A total of 2 small-scale DC fans were selected for the development of the machine. These fans are positioned at the back of the machine to remove any excess heat trapped in the enclosed space of the machine and to improve air circulation inside the machine.

Figure 3.7: DC fan

Table 3.7: DC fan specifications

Rated voltage	24 V
Rated current	0.25 A
Power	3 W
Rotational speed	3200 rpm
Noise	28 dB(A)
Airflow	20- 28 CFM
Bearing type	Sleeve bearing
Life expectancy	10 000 hrs

3.2.11 Wireless relay module

A wireless relay module was introduced in the concept development of the machine so that the user will be able to control the parameter of the treatment as they desire. The remote-controlled approach to conduct the treatment strengthens the safety features available for the users. The selected module was a 4-channel relay module where a total of 4 parameters can be controlled in a toggle-programmed mode.

Figure 3.8: 4 CH wireless remote control input module

Table 3.8: 4 CH wireless remote control input module specifications

Rated current	Standby: <10mA,Working: <128mA
Rated voltage	24 V
Max load	10 A
Number of channel(s)	4 channels
Receiver frequency	433 MHz
Available modes	Momentary, toggle, latched
Encoding type	Learning code

3.2.12 Power supply

The design of the two decontamination systems and related equipment require sufficient direct current supply to remain operational during treatment. The selection of this power supply unit was based on the power requirement of all the equipment connected to the circuit of the machine such as 5 UVC bulbs, 2 ultrasonic atomizers, 2 DC air pumps, 2 DC fans, and a wireless relay module.

Figure 3.9: Switching power supply (AC to DC transformer)

Table 3.9: Switching power supply (AC to DC transformer) specification

Input voltage	AC 110 – 220 V
Output voltage	DC 24 V
Output current	5 A
Output power	120 W
Material	Electronic components and metal
Size (LxWxH)	± 160 x 100 x 40 mm

3.2.13 3D printed items

A total of 2 items which are a ballast cover and an LED indicator were 3D modeled and 3D printed due to the specific function and need for adaptability to the machine. The fabricated 3D items are illustrated in Figure 4.7. In addition, the 2D drawings of these designs are included in Appendix K-1 and K-2. Both of the parts were 3D printed using high-quality black polylactic acid (PLA) material.

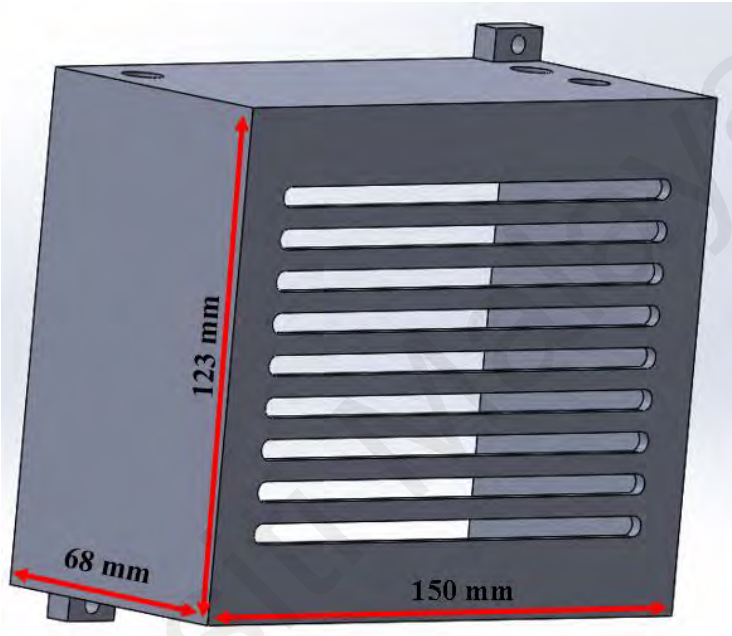

Figure 3.10: 3D design of ballast cover

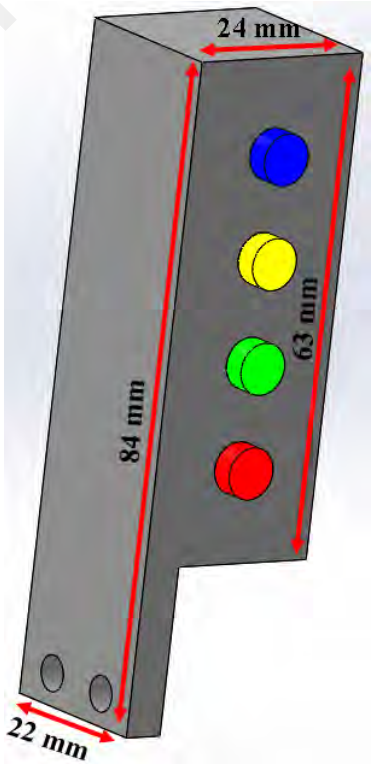

Figure 3.11: 3D design of LED indicator

3.3 Detail Design

The first objective of this research is to design and develop a mask sterilizing machine prototype equipped with a hybrid decontamination method by applying ultraviolet germicidal irradiation (UVGI) coupled with aerosolized hydrogen peroxide (aHP). Hence, before proceeding to the fabrication or development phase, an error-proof complete detailed 3D model was needed. SolidWorks ™ was the 3D modeling software used to design the mask sterilizing machine prototype for this research. Usage of this software enables simultaneous development of design in accordance with discussions. In addition, error-proofing could be completed while designing as this software highlights potential issues regarding individual parts and a complete assembly.

A total of 22 individual parts as shown in Appendix M were designed as per the decided concept development. Continuous improvement and review of the designed parts were done, in order to improve the adaptability of the whole assembly of parts and to cater to the requirements of the selected material and equipment. Continuous improvement of the designed part refers to the concept development and material and equipment selection phase denoted in Figure 3.1. In this step, the market was continuously explored to incorporate the latest, updated, and cost-effective options in the selection of equipment for the prototype. The new selection of equipment requires modification to the existing design. In short, the new revision of the design was based on the considerations listed below:

- Rectification of major assembly issues
- Possibility for a better cost-effective design
- Adaptability to the current specification of the chosen equipment
- Possibility of additional safety measures

A set of 2D drawings was established once the 3D modeled parts were approved for fabrication as shown in Appendix B - K.

3.4 Fabrication

As described in (3.2 Material and Equipment Selection), stainless steel was the major raw material needed for fabrication followed by aluminium. Procurement of the raw material needed for fabrication was completed beforehand to avoid any disruption in the fabrication process. Fabrication of these parts was completed using an outsourced service due to the need for their expertise. The designed parts were fabricated using a CNC laser cutting machine as described in section 2.6.1. 2 of the fabricated parts were polished to provide a reflective surface finish. The reflective surface was crucial to maximize the reflection of UV rays. The complete list of parts fabricated using outsourced service has been listed in Appendix M.

The mask case that holds the mask during the treatment was made using acryl. This acryl case was designed as 4 individual acryl parts combined to form an acryl box. Fabrication of these cases was done using a vertical milling machine as shown in Figure 3.12 which was described in section 2.6.2. A slot was milled in the acryl parts to position the quartz glass as designed during the concept development.

Figure 3.12: Milling a slot in an acryl sheet

3.5 Assembly

Fabricated parts were rechecked for defects before the parts were assembled to form the working prototype as indicated in Appendix L. Non - fabricated parts such as the selected equipment were coupled with the fabricated parts to create the working systems. Assembly of the prototype was performed based on a planned schedule as listed below:

1. Frame and the parts connected to it
2. Drawer and the parts connected to it
3. Electrical wiring
4. Equipment connection

3.6 Testing

The testing phase of the machine commenced once all the assembly processes were completed. In general, 3 major features were tested which were UVGI system activation, aHP system activation, and the response of the wireless relay module according to input. The testing results and issues found during the testing phase have been identified and listed in Section 4.3.2.

3.6.1 UVGI system activation

UVGI system comprises an electric supply and 5 UVC bulbs. Firstly, the system is activated to check for any faulty connection or equipment. As the next step, an uninterrupted cycle of 1-hour activation of the system was conducted. This was to test the prototype conditions against exposure to a longer period of treatment time. The selection of a specific 1-hour testing time is to test the capability of the machine to function well beyond the highest treatment time designed for this research which is 100 seconds (Table 3.10 and 3.13).

3.6.2 aHP system activation

aHP system activation comprises 3 main parts. Firstly, an ultrasonic atomizer transforms HP liquid into aHP. Next, the input and output pump functions to allow the flow of aHP into and out of the specimen area. An additional testing procedure was designed to ensure the flow of aHP into the specimen area. As illustrated in Figure 3.13, peroxide test strips were used to detect traces of hydrogen peroxide at predetermined locations.

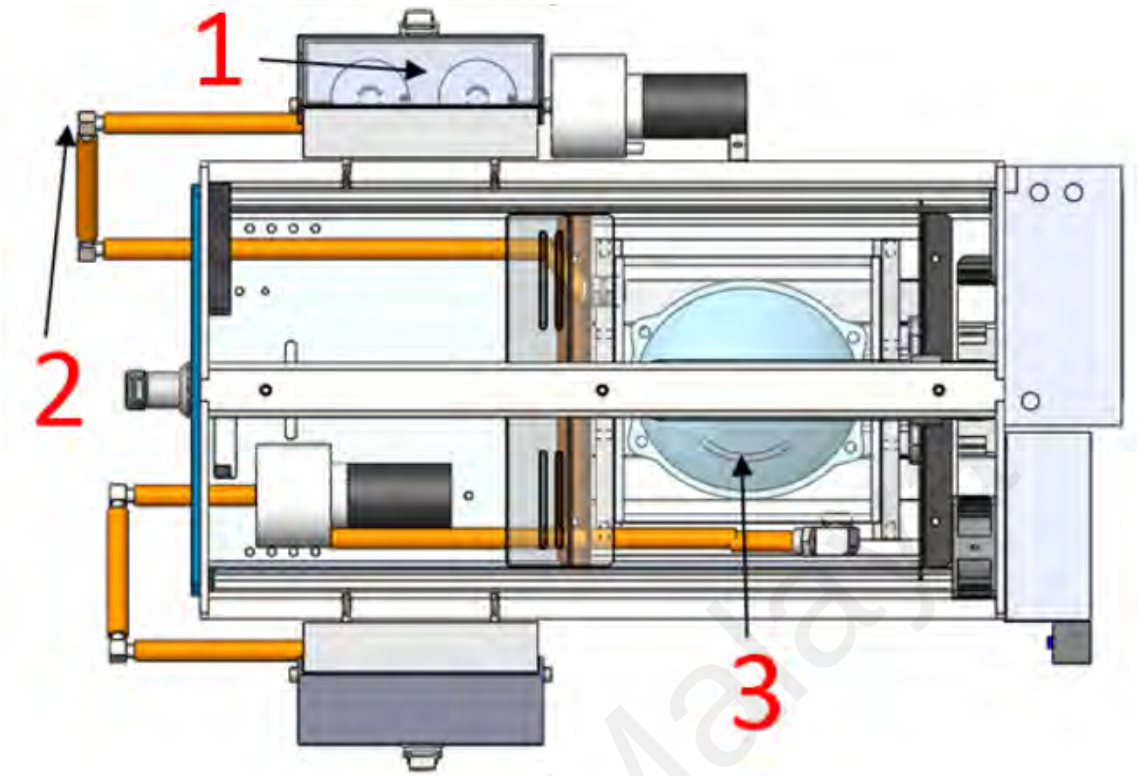

Figure 3.13: Detection of hydrogen peroxide traces at various points

3.6.3 Response of wireless relay module

The third test was conducted on the wireless relay module. All activation of systems was programmed using the wireless relay module in a toggle mode which is triggered by the remote control input.

3.7 Refinement

In addition, a refinement process was performed to address every issue found in the testing phase which is listed in Sub-section 4.4.5. The list of refinement processes is updated in Section 4.5.

3.8 Experimental Design

In order to achieve the second objective of this research, a virus viability test that comprises 5 different treatments with varying time parameters were designed which utilizes UVGI, aHP, and MGS decontamination techniques.

3.8.1 Virus Viability Test

The virus viability test or Tissue Culture Infective Dose (TCID50) test was conducted by the Tropical Infectious Diseases Research & Education Centre (TIDREC) in Universiti Malaya as illustrated in Figure 3.14. This test is conducted to determine the infectivity of a virus. The log reduction value (LRV) obtained from this test can be used to prove the decontamination efficiency of the mask sterilizer machine prototype against the virus.

Figure 3.14: Virus viability test conducted in TIDREC

To perform the virus viability test, each respirator piece (4x2 cm) was covered with 100 µl of FCoV suspension with a titre of 1x106 TCID50/ML. This was performed according to the test standard ISO18184-2019 (*ISO 18184:2019 Textiles—Determination of Antiviral Activity of Textile Products*). Next, the infected specimens were subject to treatments shown in Section 3.8.1.8. A control group, which was not exposed to any treatments, was included for comparison purposes.

To recover the virus from the infected respirators, rinsing was performed using 1 ml of DMEM containing 2% FBS. The recovered virus was then transferred to a microcentrifuge tube, and a 10x serial dilution was performed. The different dilutions of the virus were used to infect the CRFK cells seeded in a 96-well plate. The cells were incubated for 72 hours until cytopathic effects (CPE) developed. Fixation and staining of the infected cells were carried out using a mixture of paraformaldehyde and crystal violet. The virus titer was determined using the Spearman-Karber method and expressed as a tissue culture infectious dose 50% (TCID50/ml). The virucidal activity was assessed by calculating the difference in logarithmic titer (Δ log10 TCID50/ml) between the virus control and the test virus.

3.8.1.1 Feline Coronavirus (FCoV)

As a suitable surrogate virus for SARS-CoV-2, Feline Coronavirus (FCoV) was selected for this test.

3.8.1.2 Test respirator

The N95 respirator selected for this test was 3M 1860 as shown in Figure 3.15. The selection of this type of mask was based on the main purpose of this research which is to alleviate the shortage of masks encountered by health workers. 3M 1860 is the mask widely used in healthcare settings.

Figure 3.15: 3M™ Health Care Particulate Respirator and Surgical Mask 1860

3.8.1.3 Specimen preparation

A 2 cm by 4 cm rectangular piece was excised from the selected 3M 1860 mask. FCoV virus strain was inoculated into this rectangular piece which was placed on a smaller piece of quartz glass. This smaller piece will be placed in the quartz glass enclosure as demonstrated in Figure 3.16 for UVGI and aHP treatments.

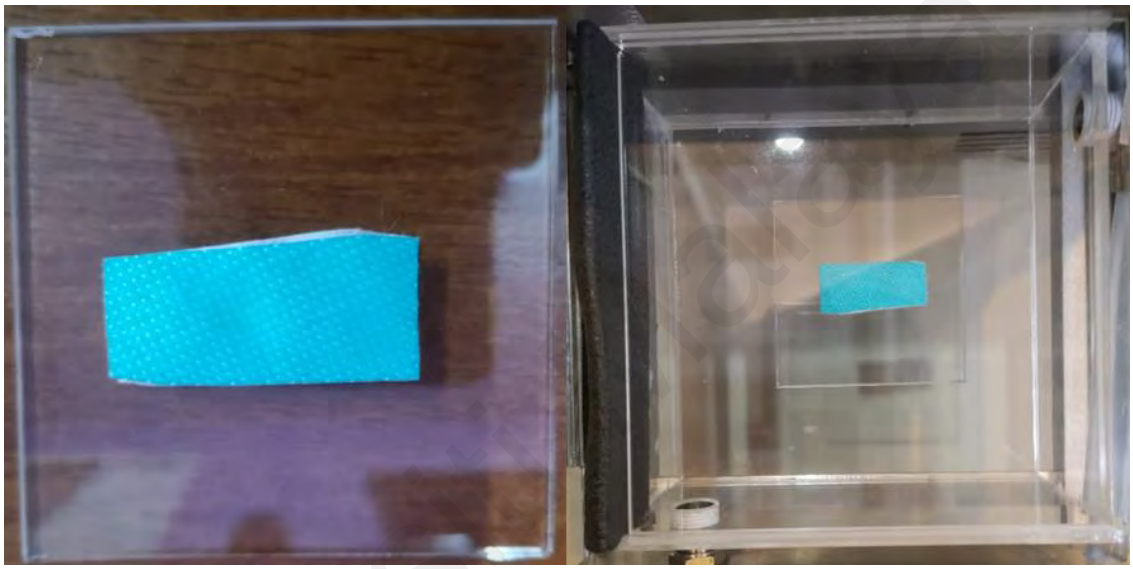

Figure 3.16: Inoculated mask piece on the quartz glass

3.8.1.4 UVGI system operation procedure

The UVC bulbs which are connected to the power supply can be activated via the programmed wireless relay remote. The system is activated and deactivated according to the treatment time which will be monitored using a stopwatch. Figure 3.17 illustrates the steps included in UVGI treatment.

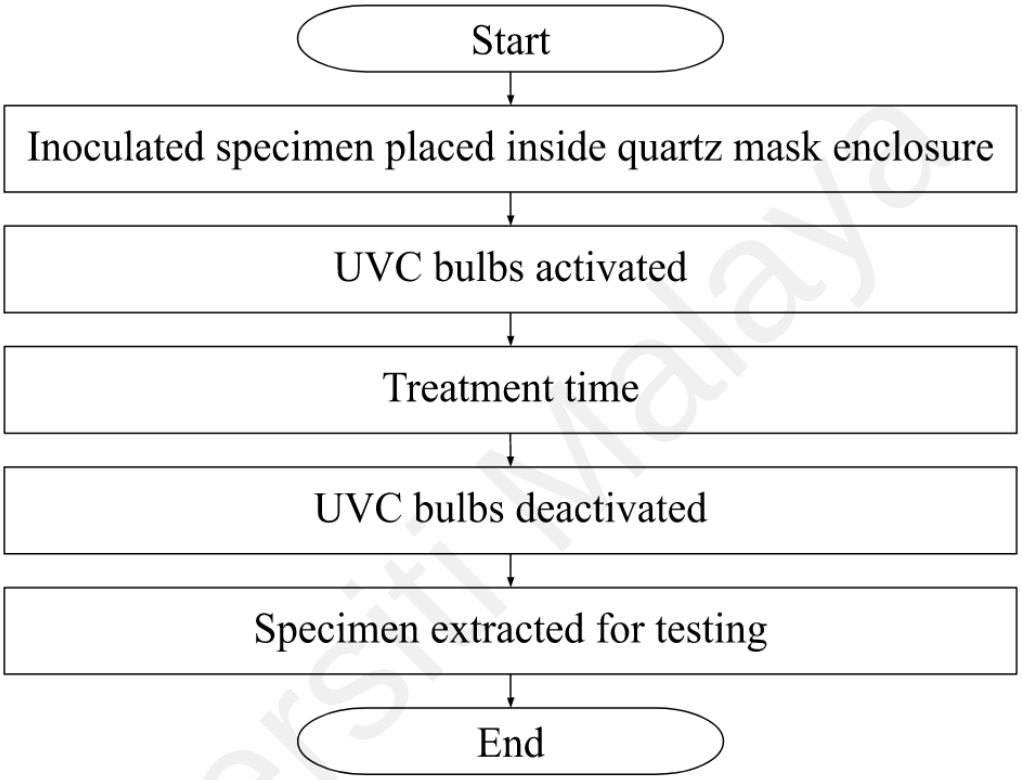

Figure 3.17: UVGI treatment flowchart

Estimation of UV dosage delivered to the specimen during a UVGI treatment is crucial to administer the required treatment time as described in Equation 2.1. The irradiance value that can be delivered by the UVC bulbs was obtained from the catalog of the product. The selected UVC bulb was capable of delivering irradiance in the range of 2.5 - 3.0 W/cm^2. The lower limit of 2.5 W/cm^2 irradiance value was selected for dosage calculation as the estimation was intended to achieve at least the specified amount of dosage. Collectively the three UVC bulbs positioned at the upper part of the machine were able to deliver irradiance of at least 7.5 W/cm^2. The dosage delivered can be calculated when this irradiance value is multiplied by the treatment time as specified in the parameter design.

3.8.1.5 aHP system operation procedure

There are 3 equipment associated with the activation and deactivation of the aHP decontamination system which are the ultrasonic atomizer, inlet DC pump, and outlet DC pump. Each of the equipment is controlled using a wireless relay remote. Figure 3.18 lists the steps involved in aHP system activation.

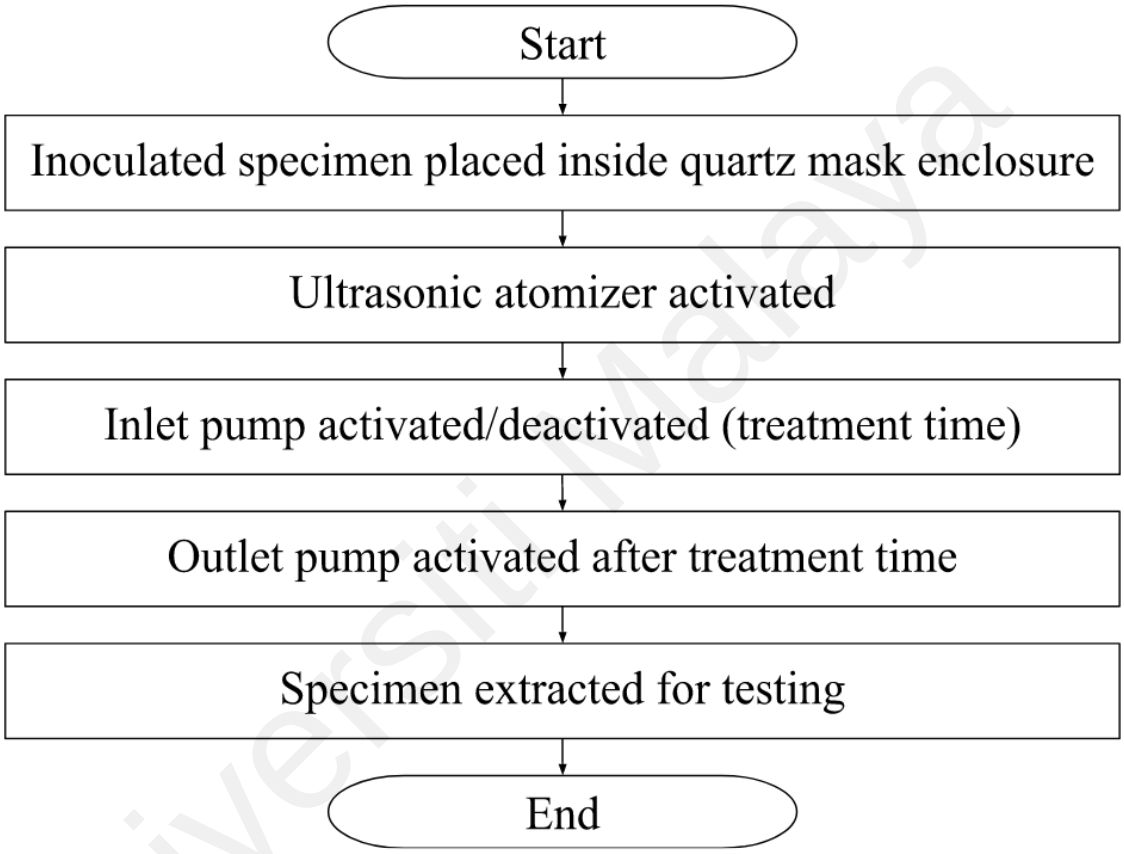

Figure 3.18: aHP treatment flowchart

3.8.1.6 MGS system operation procedure

MGS system uses a commercially available microwave model 23L grill microwave oven with healthy steam (Samsung). A different set-up was utilized for this treatment which was inspired by the investigation by (Zulauf et al., 2020) as illustrated in Figure 3.19. A pair of bag seal clips was used to clip the inoculated mask piece which was suspended over a glass bowl containing water. Figure 3.20 shows the steps involved in MGS system activation.

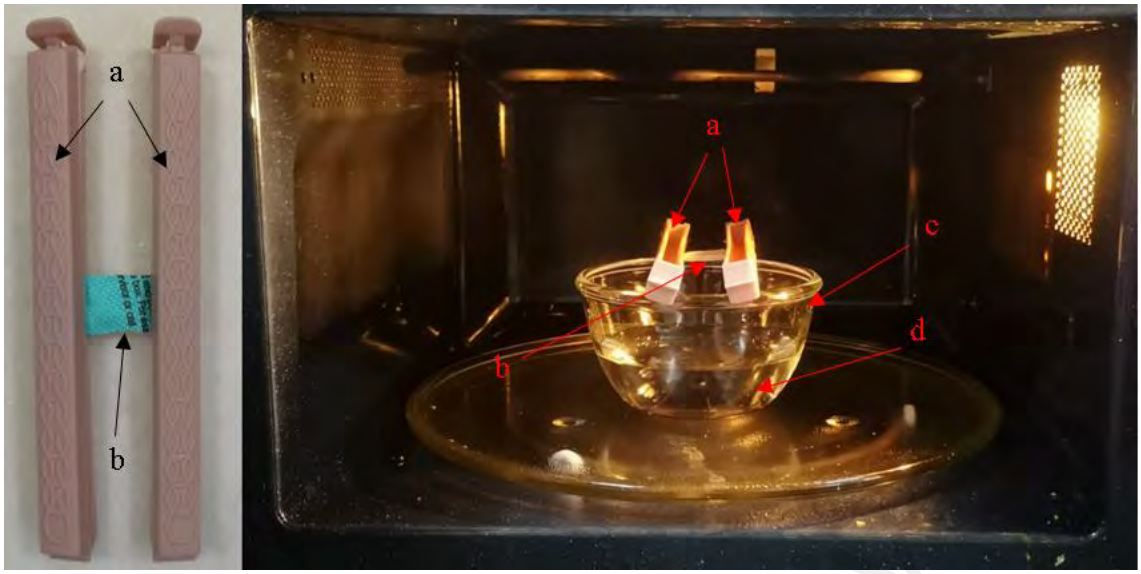

Figure 3.19: Experimental setup for MGS deactivation system (a) Sealer clips; (b) Excised N95; (c) Glass bowl; (d) Water

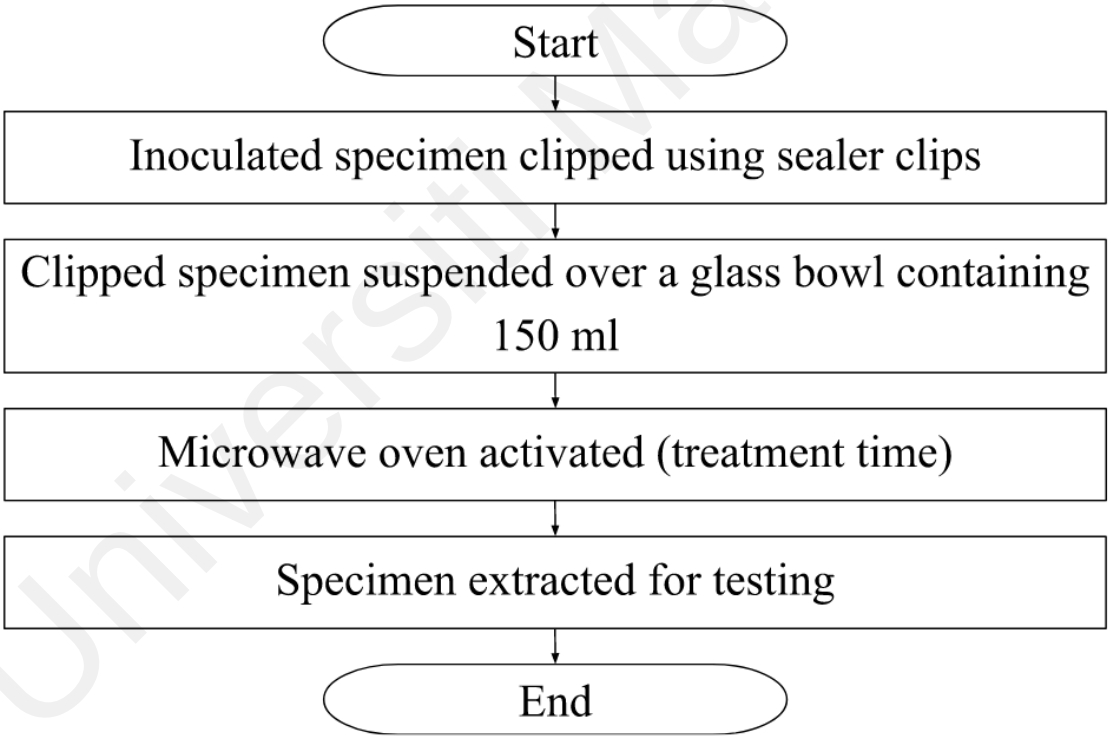

Figure 3.20: MGS treatment flowchart

3.8.1.7 Hybrid system operation procedure

Two hybrid decontamination treatments were designed for this research. Firstly, UVGI + aHP hybrid treatment utilizes the constructed machine prototype which is equipped with both the selected treatments. The order of this specific treatment is an aHP cycle (Figure 3.18) followed by a UVGI cycle (Figure 3.17). The second hybrid

decontamination method of UVGI + MGS utilizes UVGI treatment equipped in the machine prototype and MGS from a microwave oven. The order of this specific treatment is the MGS cycle (Figure 3.20) followed by the UVGI cycle (Figure 3.17).

3.8.1.8 Experiment parameter

The experiment parameter design for the virus viability test was divided into two main treatment designs which are standalone treatment and hybrid treatment. Standalone treatment design comprises 3 treatments which include UVGI-only tests, aHP-only tests, and MGS-only tests as shown in Table 3.10 - 3.12 respectively. Hybrid test design includes two experiments which are UVGI + aHP (Hybrid) tests, and UVGI + MGS (Hybrid) tests depicted in Tables 3.13 and 3.14. The main criterion behind the selection of the treatment time is the number of log reductions achieved using a specific treatment. The target log reduction value was set at 4 log reduction for this experiment. Therefore, based on the existing literature shown in Table 2.2 - 2.5, the treatment time parameter was estimated. Each test sample was tested 3 times to produce one log reduction data for higher accuracy of the data.

Table 3.10: Virus viability test parameter (UVGI-Only)

Sample	Exposure time (s)
UV Control	0
UV 1	3
UV 2	6
UV 3	9
UV 4	17
UV 5	34
UV 6	67
UV 7	100

Table 3.11: Virus viability test parameter (aHP-Only)

Sample	Exposure time (s)
aHP Control	0
aHP 1	120

Table 3.12: Virus viability test parameter (MGS-Only)

Sample	Exposure time (s)
MGS Control	0
MGS 1	15
MGS 2	30
MGS 3	45
MGS 4	60

Table 3.13: Virus viability test parameter (UVGI + aHP)

Sample	UVGI	aHP
	Exposure time (s)	Exposure time (s)
HYB(aHP) Control	0	0
HYB(aHP) 1	3	120
HYB(aHP) 2	6	120
HYB(aHP) 3	9	120
HYB(aHP) 4	17	120
HYB(aHP) 5	34	120
HYB(aHP) 6	67	120
HYB(aHP) 7	100	120

Table 3.14: Virus viability test parameter (UVGI + MGS)

Sample	UVGI	MGS
	Exposure time (s)	Exposure time (s)
HYB(MGS) Control	0	0
HYB(MGS) 1	3	30
HYB(MGS) 2	6	30
HYB(MGS) 3	9	30
HYB(MGS) 4	17	30
HYB(MGS) 5	34	30

CHAPTER 4: RESULTS AND DISCUSSION

Chapter 4 describes the design results of the prototype machine, fabrication process, assembly of the machine, testing, and refinement process. In addition, the virus viability test results are presented in detail. This chapter also includes a detailed analysis of the virus viability results of tested decontamination treatments.

4.1 Detail Design

22 parts were designed in total for the development of the mask sterilizer machine prototype excluding non - fabricated parts. These non-fabricated parts refer to equipment and fixtures that have been selected for the implementation of decontamination systems in the machine. Most of the 3D models of the non-fabricated parts were obtained directly from manufacturers to avoid any issues in adapting the part to the overall assembly.

As stated in Chapter 3, a series of discussions and continuous improvement to the design was conducted to provide a design that is error-free and covers the latest updates in terms of equipment availability. Hence, 2 major designs were produced which are the preliminary design and revision 1 (attached in Appendix A and Appendix B). The preliminary design was developed at a timeframe close to concept development which indicates the design was at a very early development stage. Revision 1 was the design produced as the finalized version of the design which was approved for fabrication based on revision consideration noted in Section 3.3.

4.1.1 Design Improvement

The revised design of the preliminary design resulted in a total of 3 major changes. These major changes are due to considerations listed in Section 3.3.

4.1.1.1 Position of input DC air pump

The position of the input DC air pump was changed as a solution to mitigate the issue regarding the formation of hydrogen peroxide mist. This issue was found while checking the function of the DC pump during the early procurement phase. The new position was found to be effective in retaining the hydrogen peroxide in mist form during the procurement phase. This is confirmed by observation.

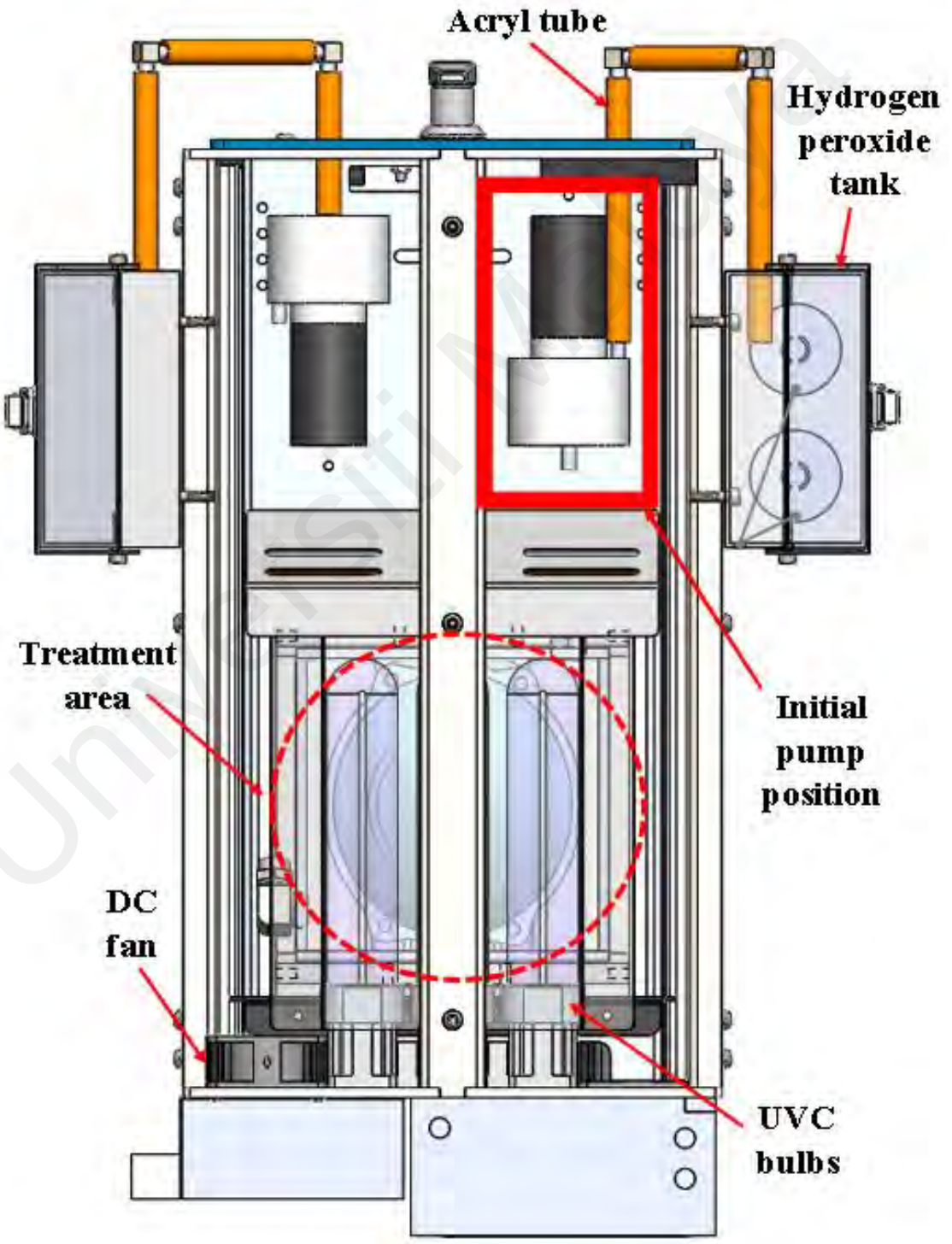

Figure 4.1: Initial position of the input DC air pump (Preliminary)

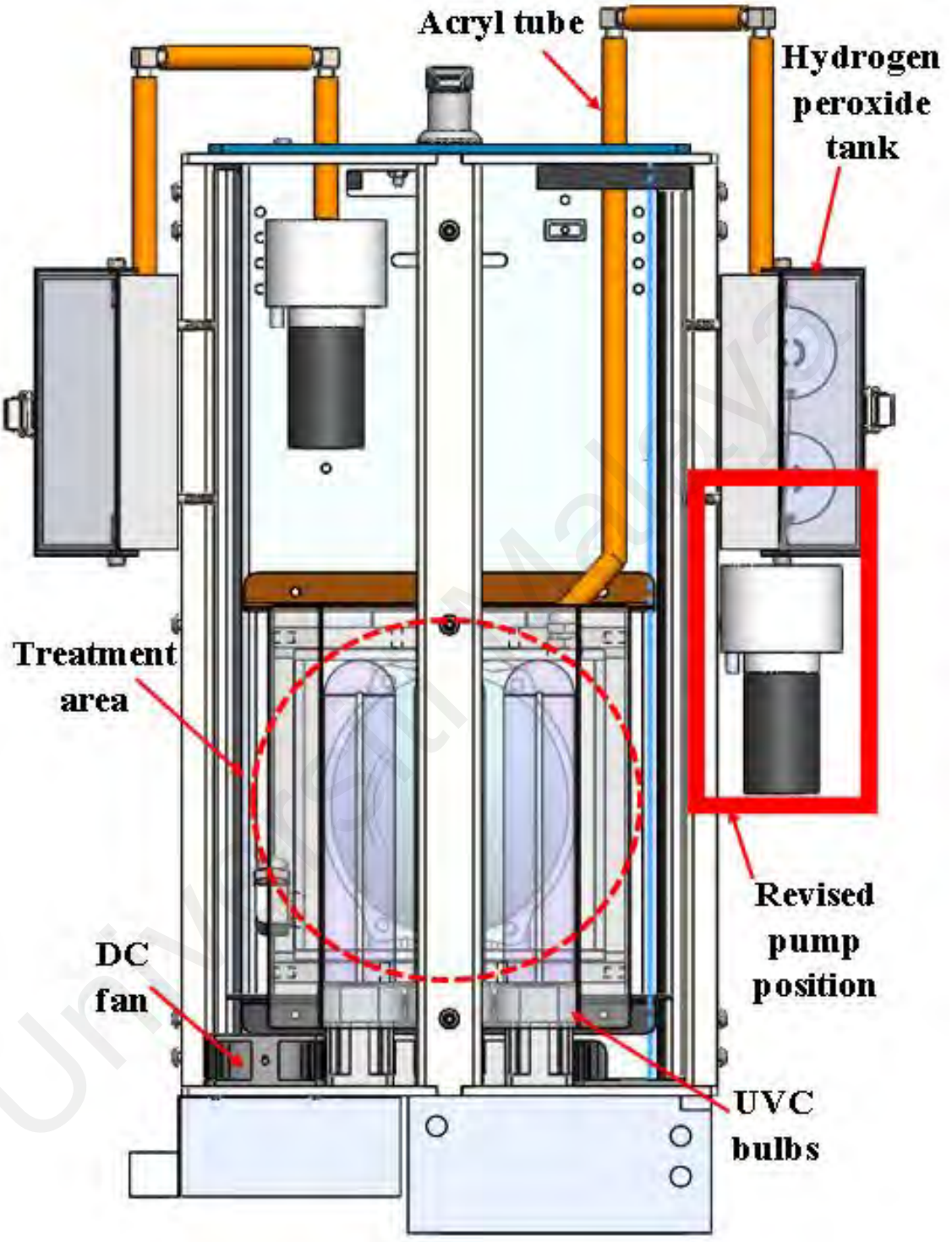

Figure 4.2: Revised position of input DC air pump (Revision 1)

4.1.1.2 Design of hydrogen peroxide tanks

The initial bigger design of the HP tanks was reduced in size. As per the 2nd consideration listed in section 3.3, these changes are due to the possibility of a better cost-effective design. The smaller new design was a cost-effective measure while preserving the minimum volume needed to hold the HP liquid needed for the decontamination operation. The volume of the tank is reduced from 1000 cm^3 to 891.48 cm^3. Based on early testing of the ultrasonic atomizer device during the procurement phase, the new volume is capable of holding HP liquid sufficiently for more than 4 cycles of 120 seconds (The longest treatment time of aHP cycle). As illustrated in Figure 4.3, the tank cover was a design improvement that could eliminate any possibility of leakage where the cover of the tank was designed to provide an enclosure with more area covered.

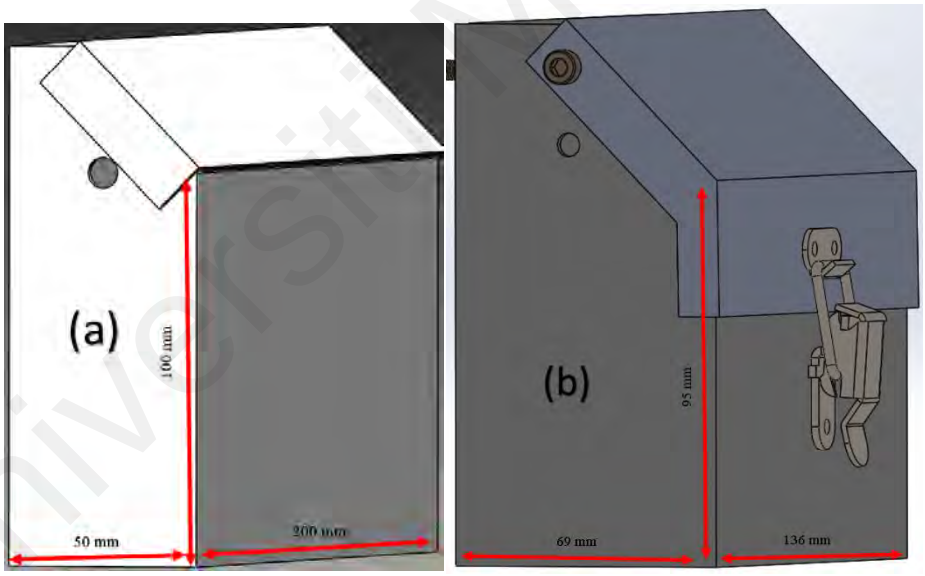

Figure 4.3: Hydrogen peroxide tank: a) Preliminary; b) Revision 1

4.1.1.3 Replacement of quartz rods with quartz case

As an added safety feature, quartz rods were replaced with a quartz case. As per the 4th consideration listed in Section 3.3, these changes in design are due to the possibility of additional safety measures. Initially, the mask subjected to treatment was to be placed on a set of quarts rods without restriction. Nevertheless, further discussion has resulted in adding this quartz case as its replacement. An enclosed quartz case will be able to avoid any cross-contamination inside the machine in the event of treating a contaminated mask. In addition, aHP exposure was able to be contained with ease using an enclosed case.

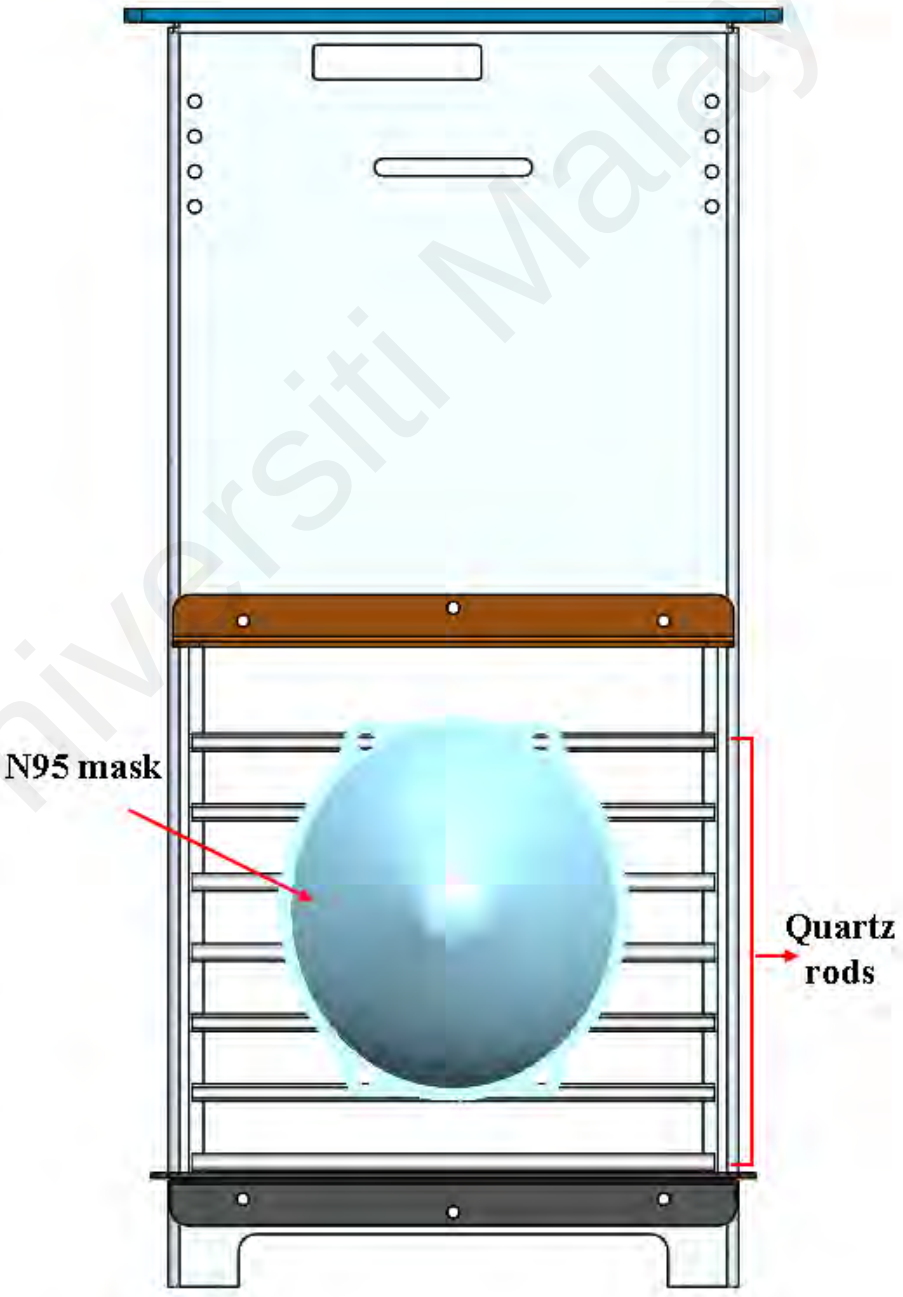

Figure 4.4: Mask placed on quartz rods (Preliminary)

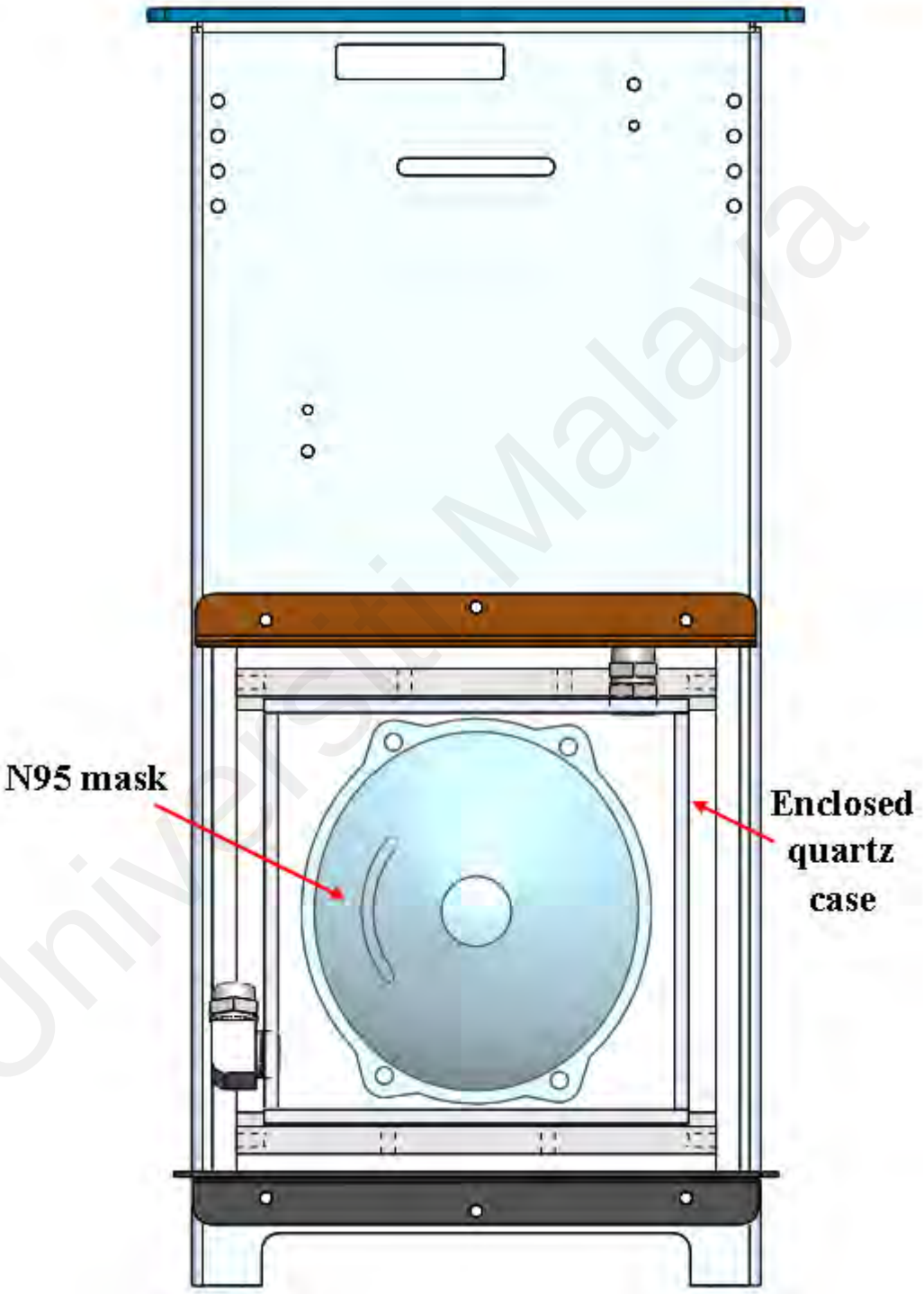

Figure 4.5: Mask inside an enclosed quartz case (Revision 1)

4.2 Fabrication

22 parts in total were fabricated for the assembly of the whole machine prototype. Procedures involved in this fabrication process include CNC laser cutting, bending, milling, drilling, and polishing. Appendix M depicts the list of fabricated materials and non-fabricated equipment used in this research. In addition, each part drawing has been included in Appendix C - K.

As described in section 3.4, most of the fabricated parts were procured through outsourcing due to the need for specific expertise. All the received parts were checked for fabrication errors and the error rectification process was performed. Several errors were identified which include:

- Non-uniform hole thread
- Non-tight closing of HP tanks

Figure 4.6 illustrates all the fabricated parts received from the hired outsource and Figure 4.7 shows the 3D printed parts after undergoing error checking and error rectification processes.

Figure 4.6: Fabricated parts before assembly: a) Frame; b) Drawer assembly, c) Reflector (Above Bulb); d) Reflector (Below Bulb); e) Reflector (Top); f) Reflector (Bottom); g) Lock plate; h) HP tank; i) Jig mounting

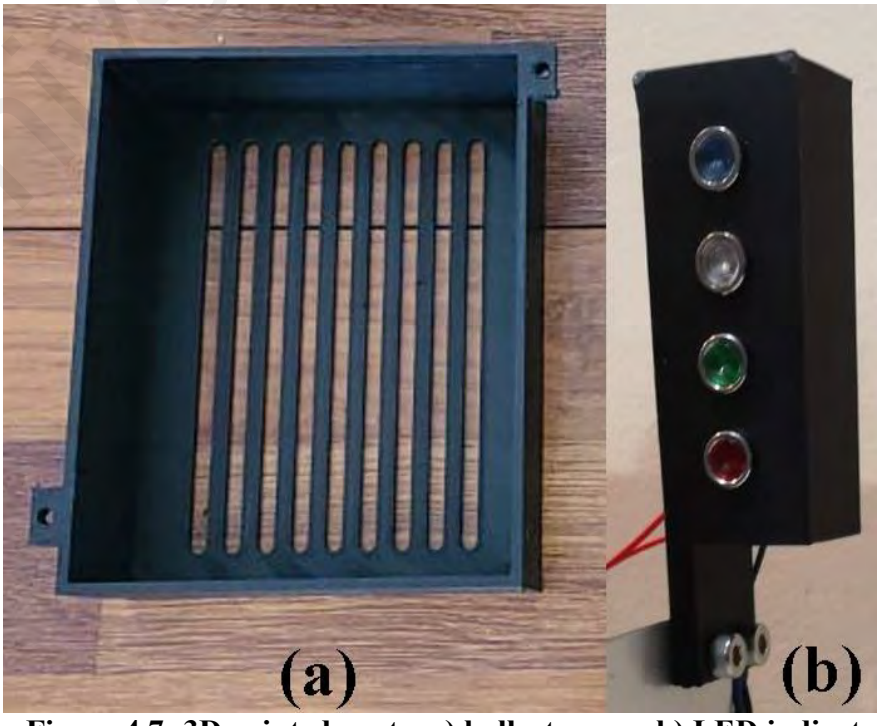

Figure 4.7: 3D printed parts: a) ballast cover; b) LED indicator

4.3 Assembly

Assembly of the working mask sterilizer machine prototype (Appendix L) was conducted in several stages. The preplanned assembly schedule as shown in Section 3.5 was followed to troubleshoot any issues regarding a smaller section of the machine before connecting it as a whole unit.

4.3.1 Frame assembly

The mainframe or structure of this machine was assembled with several related parts such as a reflector (above bulb), reflector (below bulb), reflector (top), reflector (bottom), lock plate, slide rails, and 3D printed ballast cover as shown in Figure 4.8.

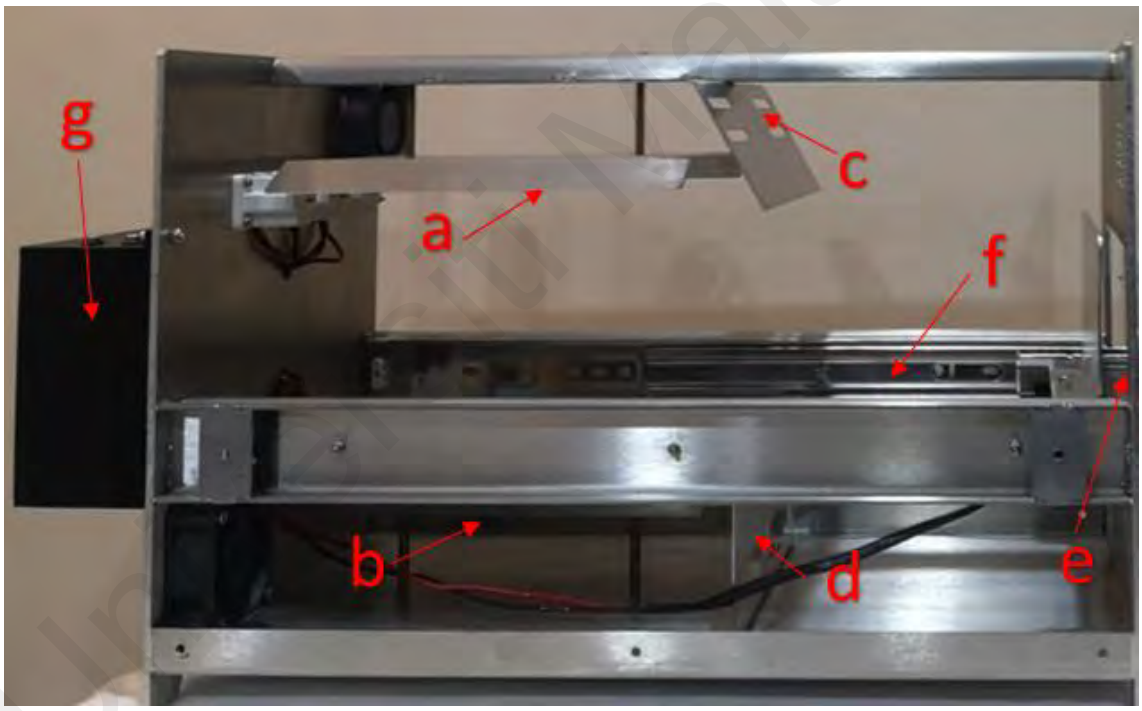

Figure 4.8: Frame assembly: a) Reflector (Above Bulb); b) Reflector (Below Bulb); c) Reflector (Top); d) Reflector (Bottom); e) Lock plate; f) Slide rails; g) Ballast cover

4.3.2 Drawer assembly

The drawer part which acts as a base to hold the quartz case and the mask was connected to parts that include the slide rail, lock latch, jig mounting, jig mounting 2, and other drawer parts.

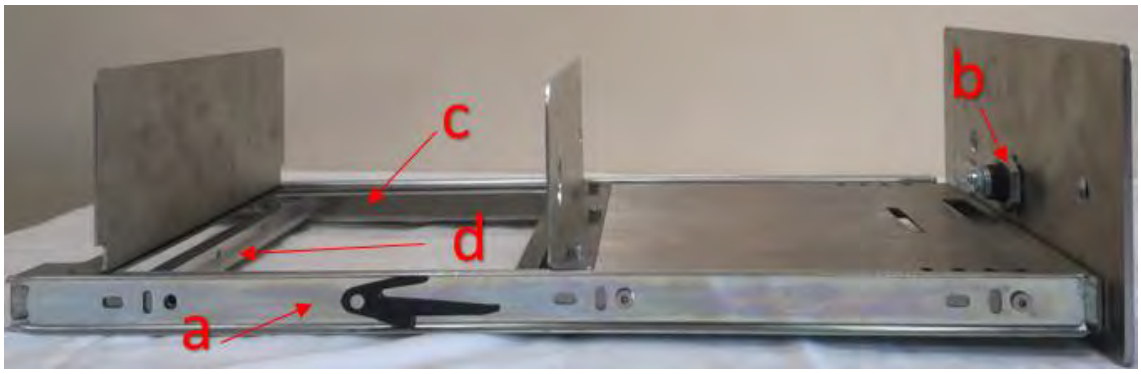

Figure 4.9: Drawer assembly: a) Slide rails; b) Lock latch; c) Jig mounting; d) Jig mounting 2

4.3.3 Electrical wiring

The electric supply unit for this machine was positioned at the back of the machine. Meanwhile, selected equipment were positioned at the front of the machine. Hence, the electrical wire was connected from the back to the front of the machine through newly drilled holes.

4.3.4 Equipment connection

Lastly, once all the wiring ends have been set up, the intended equipment is connected. The connected equipment include 5 UV bulbs, 2 ultrasonic atomizers, 2 DC fans, 2 air pumps, and a wireless relay module.

4.4 Testing

The testing phase of the machine commenced once all the assembly processes were completed. In general, 3 major features were tested which were UVGI system activation, aHP system activation, and the response of the wireless relay module according to input.

4.4.1 UVGI system activation

UVGI system comprises an electric supply and 5 UVC bulbs. There were no issues encountered during the activation of the UVGI system as demonstrated in Figure 4.10 which indicates that all the equipment and electrical connection was not faulty. As the next step, an uninterrupted cycle of 1-hour activation of the system was conducted. This was to test the prototype conditions against exposure to a longer period of treatment time and no effect was noted.

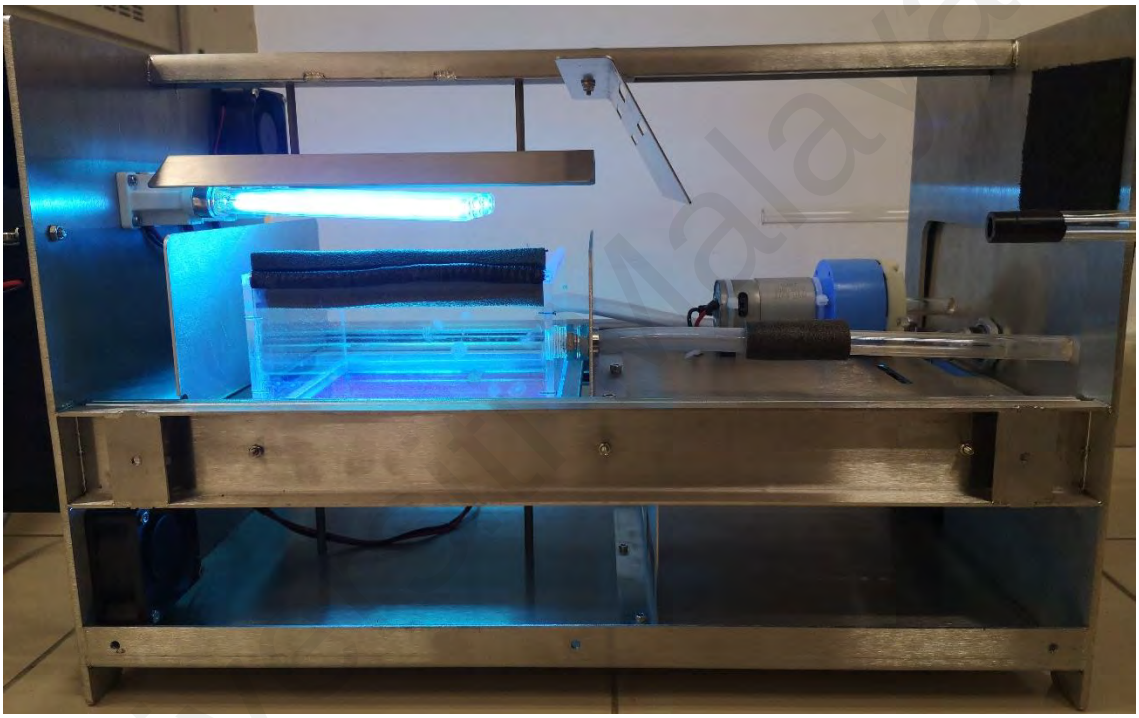

Figure 4.10: UVGI system activation

4.4.2 aHP system activation

aHP system activation comprises 3 main parts. Firstly, an ultrasonic atomizer transforms HP liquid into aHP as illustrated in Figure 4.11. Next, the input and output pump functions to allow the flow of aHP into and out of the specimen area. The ultrasonic atomizers were found to be sensitive to the height of the liquid it was submerged in. Therefore, a few levels of water were tested with an ultrasonic atomizer to identify the optimum level of HP liquid to be in the tank during the operation. In addition, both pumps were functioning without any issues upon activation.

Figure 4.11: Ultrasonic atomizer in operation

An additional testing procedure was designed to ensure the flow of aHP into the specimen area. As illustrated in Figure 4.12, peroxide test strips were used to detect traces of hydrogen peroxide at predetermined locations. Tests at 3 locations returned positive for peroxide traces which indicates that the flow of HP was delivered as per system design.

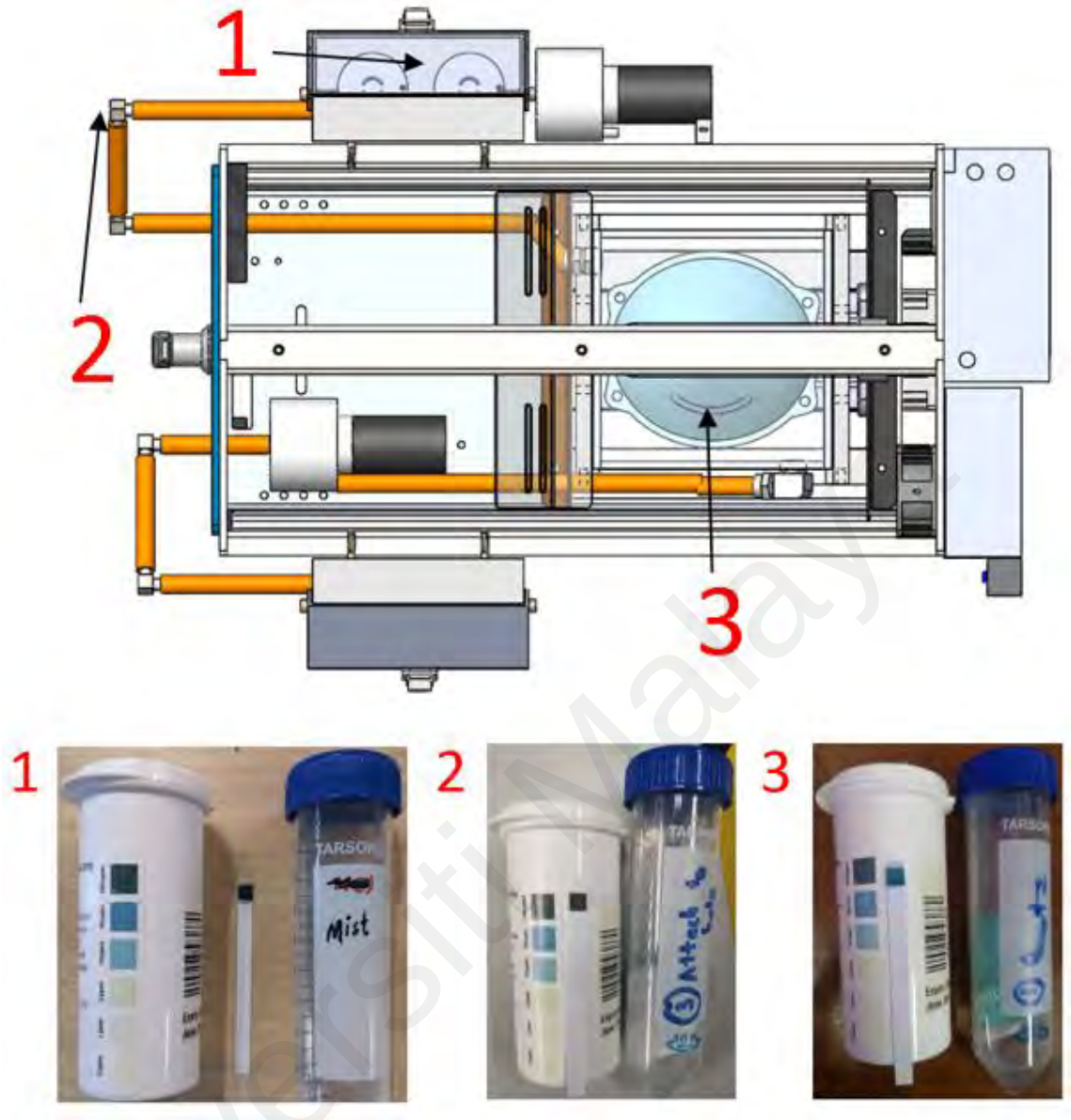

Figure 4.12: Detection of hydrogen peroxide traces at various points

4.4.3 Response of wireless relay module

The third test was conducted on the wireless relay module. All activation of systems was programmed using the wireless relay module in a toggle mode which is triggered by the remote control input. Activation of systems was working as programmed (Blue: UVC bulb, Yellow: Ultrasonic Atomizer, Green: Input pump, Red: Output pump). Figure 4.13 shows an LED indicator associated with the activation and inactivation of a system. According to the remote input, the system and the associated LED were working.

Figure 4.13: LED indicator during activation of all system

4.4.4 Testing results

The testing of the hybrid mask sterilizer machine according to the proposed testing procedures proved that this machine is a stable machine that functions perfectly according to the user inputs. In addition, excellent 1-hour long-run results of the machine indicated that this machine could be operational in a safe manner for a time frame well beyond the estimated usage times.

4.4.5 Issues

The testing phase revealed two issues with the prototype that are crucial to be addressed. The issues are rectified using a customized refinement process for each issue which is explained in detail in Section 4.5. Issues found during the testing phase are listed below:

1. aHP condensed to liquid form rather than staying in mist form.
2. Mist aHP escapes through the small gaps between the HP tank and cover.

4.5 Refinement

Several adjustments were made to alleviate issues found during the testing phase. Firstly, the pump was shifted as shown in Figure 4.14. This solution was due to aHP being condensed to liquid form when passing through the DC pump. Therefore, rather than sucking and pumping the aHP mist, the dc pump was positioned to pump out the air to carry the aHP mist along thru the tubing.

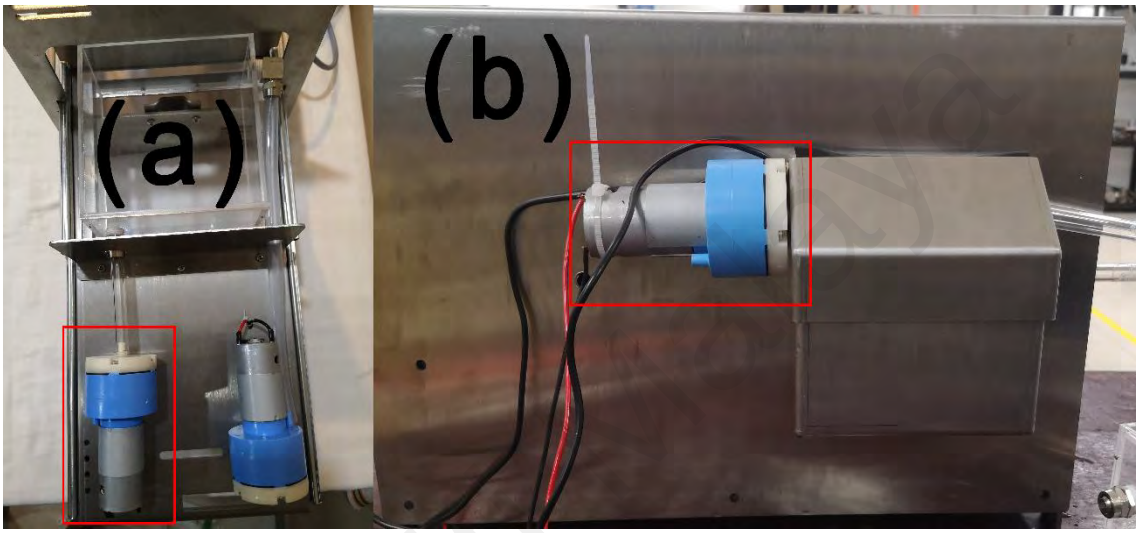

Figure 4.14: Repositioning input DC pump (a) Initial pump position; (b) Revised pump position

Next, it was found that the cover of the HP tank does not offer a tight closing as expected. As a result, the generated aHP was leaking from the small spaces of the closing. Therefore, foam tape was used to cover the spaces and to provide much tighter closing as displayed in Figure 4.15. As expected, the tape functions perfectly to fill the gaps, and the testing procedure was conducted again.

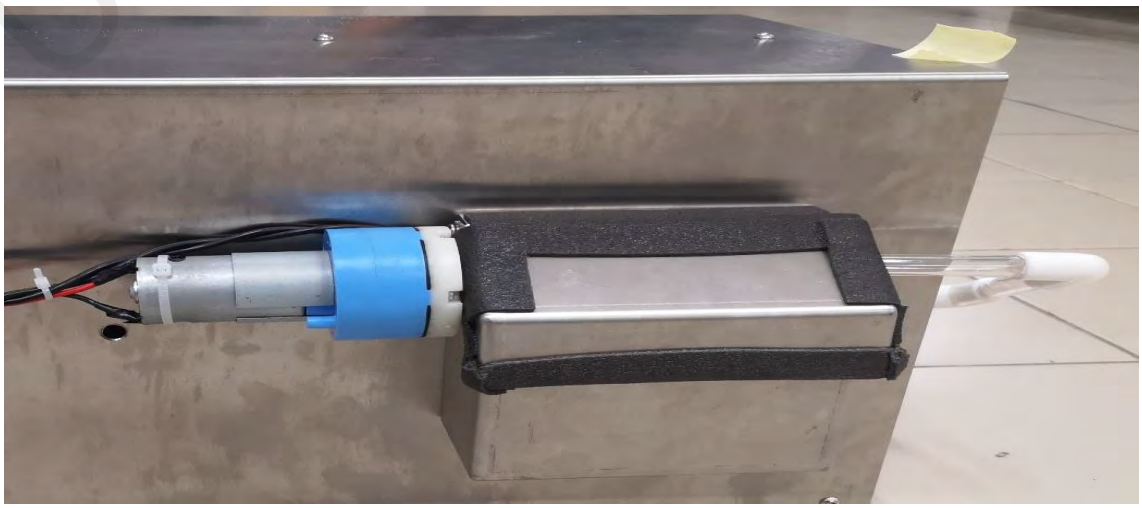

Figure 4.15: Hydrogen peroxide tank covered with foam tape

4.6 Virus Viability Test

As described in section 3.8.1.8, 5 tests were designed to test the efficiency of the selected decontamination procedures against the FCoV virus. In general, the 5 tests include 3 standalone treatments and 2 hybrid treatments. The efficiency of the treatments was measured using Log Reduction Value (LRV) / log10. In relation, the greater the value of LRV, the greater the efficiency of the specific decontamination technique against the tested organism. Moreover, the detection limit or the highest possible detectable LRV value for this test is set at 4. The full procedure of this test has been explained in section 3.8.1.

4.6.1 Ultraviolet Germicidal Irradiation (UVGI) Only

Table 4.1 lists the results of the virus viability test using UVGI treatment. As described in Table 4.1, a total of 2 data were omitted due to irregularity and ambiguity. The maximum value of 4 log reduction was achieved at the exposure time of 100 seconds. With a combined irradiance value of 7.5×10^{-3} W/cm^2, 100 seconds of exposure could generate a UV dosage of at least 0.75 J/cm^2. It is also notable that the minimum required log reduction value of 3 for safe decontamination was achieved at 9 seconds or a dosage of 0.0675 J/cm^2 as shown in Figure 4.16.

Findings of the UVGI-only tests reveal that the results were consistent with existing literature that describes decontamination investigation involving SARS-CoV-2 (Geldert et al., 2021; Golovkine et al., 2021; Ozog et al., 2020; Rathnasinghe et al., 2020), Escherichia virus MS2 (Kayani et al., 2021) and H1N1 influenza (Mills et al., 2018). Notably, the current study produced a 3-log reduction at a slightly lower dosage of 0.0675 J/cm^2 in comparison with the existing investigation (Golovkine et al., 2021; Kayani et al., 2021; Ozog et al., 2020).

Table 4.1: Virus viability test results (UVGI Only)

Sample	Exposure time (s)	Dosage (J/cm^2)	Log Reduction Value (LRV) / log10
UV Control	0	0	0
UV 1	3	0.0225	1
UV 2	6	0.045	*4 (Data omitted due to irregularity)
UV 3	9	0.0675	3
UV 4	17	0.1275	3
UV 5	34	0.255	*2 (Data omitted due to irregularity)
UV 6	67	0.5025	3
UV 7	100	0.75	4

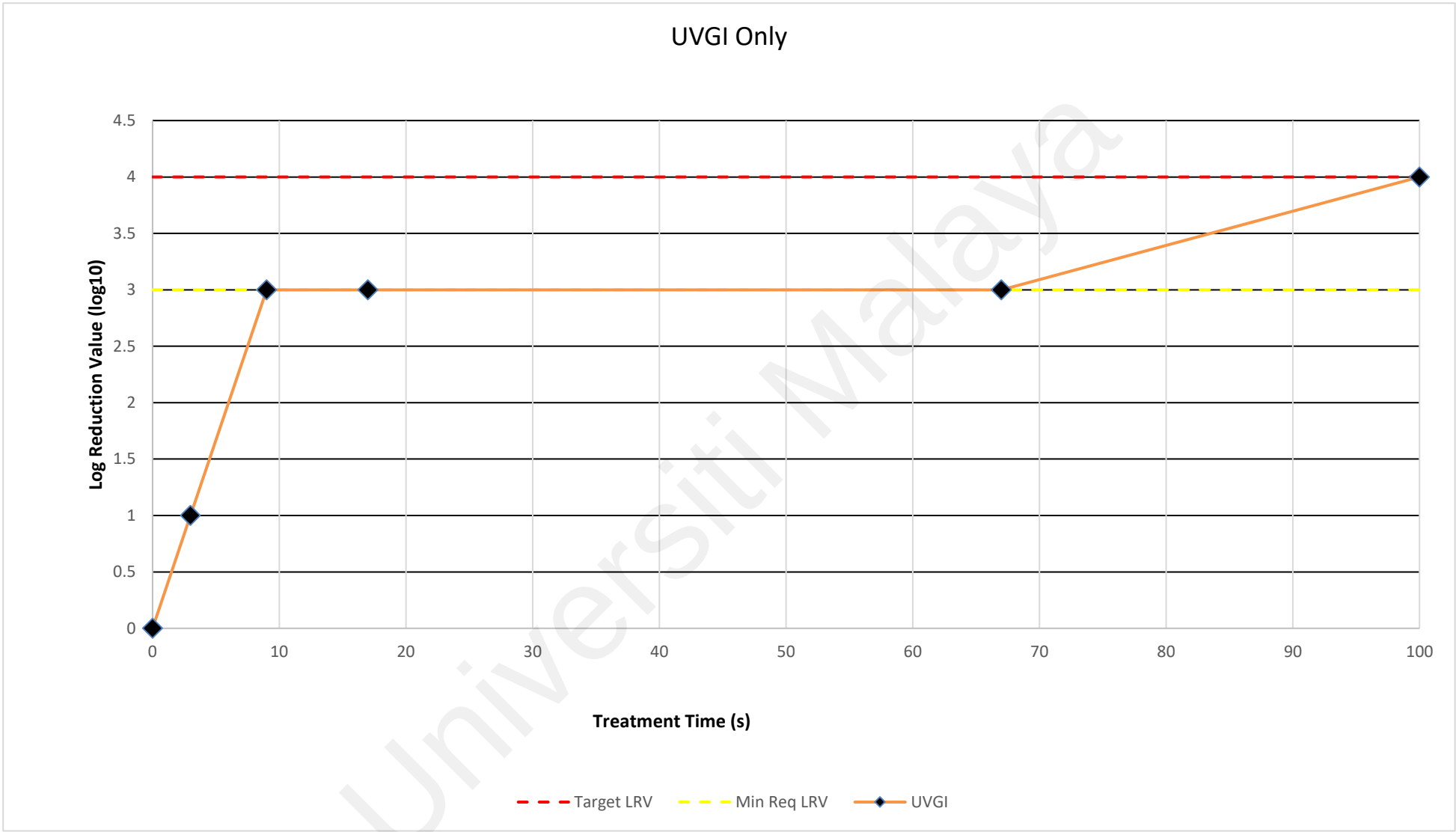

Figure 4.16: Graph of Log Reduction Value against Treatment Time (UVGI-Only)

4.6.2 Aerosolized Hydrogen Peroxide (aHP) Only

Table 4.2 and Figure 4.17 exhibits the results of aHP decontamination treatment results. aHP testing produced an unsatisfactory outcome where there was no log reduction produced for the specified time point. Upon further review of the results, the omission of the dwell phase in the decontamination cycle could be a potential reason for this result. Comparing most of the decontamination investigations that have been conducted using HPV or aHP, a specified time in the range of 5 to 180 minutes was allocated for the dwell phase in a decontamination cycle. Nevertheless, the dwell phase was omitted in this investigation, as it focuses on a rapid decontamination procedure. In addition, this omission was necessary to make the efficiency of the aHP decontamination cycle comparable to the treatment times of UVGI and MGS.

Table 4.2: Virus viability test results (aHP Only)

Sample	Exposure time (s)	Log Reduction Value (LRV) / log10
aHP Control	0	0
aHP 1	120	0

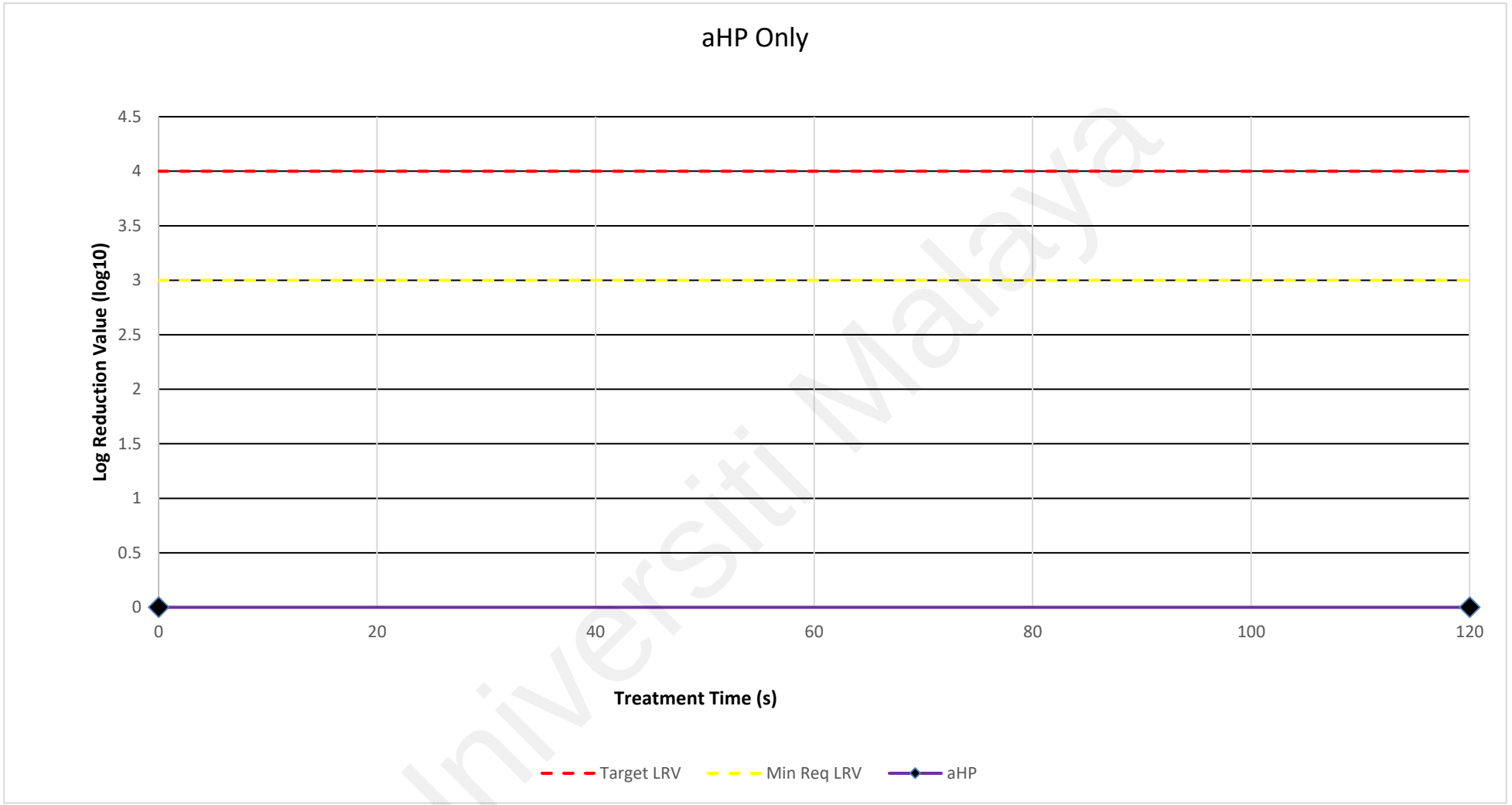

Figure 4.17: Graph of Log Reduction Value against Treatment Time (aHP Only)

4.6.3 Microwave-Generated Steam (MGS) Only

The decontamination cycle using the MGS procedure yielded the target or maximum log reduction of 4 at a treatment time of 45 seconds as shown in Table 4.3 and Figure 4.18. The virucidal efficiency of the MGS system was excellent in terms of log reduction per treatment time. In addition, as the treatment focuses on using steam to disinfect the specimen, the presence of moisture on the exposed layer of the mask can be found post-decontamination. In comparison to the investigation by Zulauf et al which utilized an almost similar setup, the results of this specific treatment were in agreement and slightly better in terms of producing higher log reduction at a lower treatment time (Zulauf et al., 2020).

Table 4.3: Virus viability test results (MGS Only)

Sample	Exposure time (s)	Log Reduction Value (LRV) / log10
MGS Control	0	0
MGS 1	15	0
MGS 2	30	2
MGS 3	45	4
MGS 4	60	4

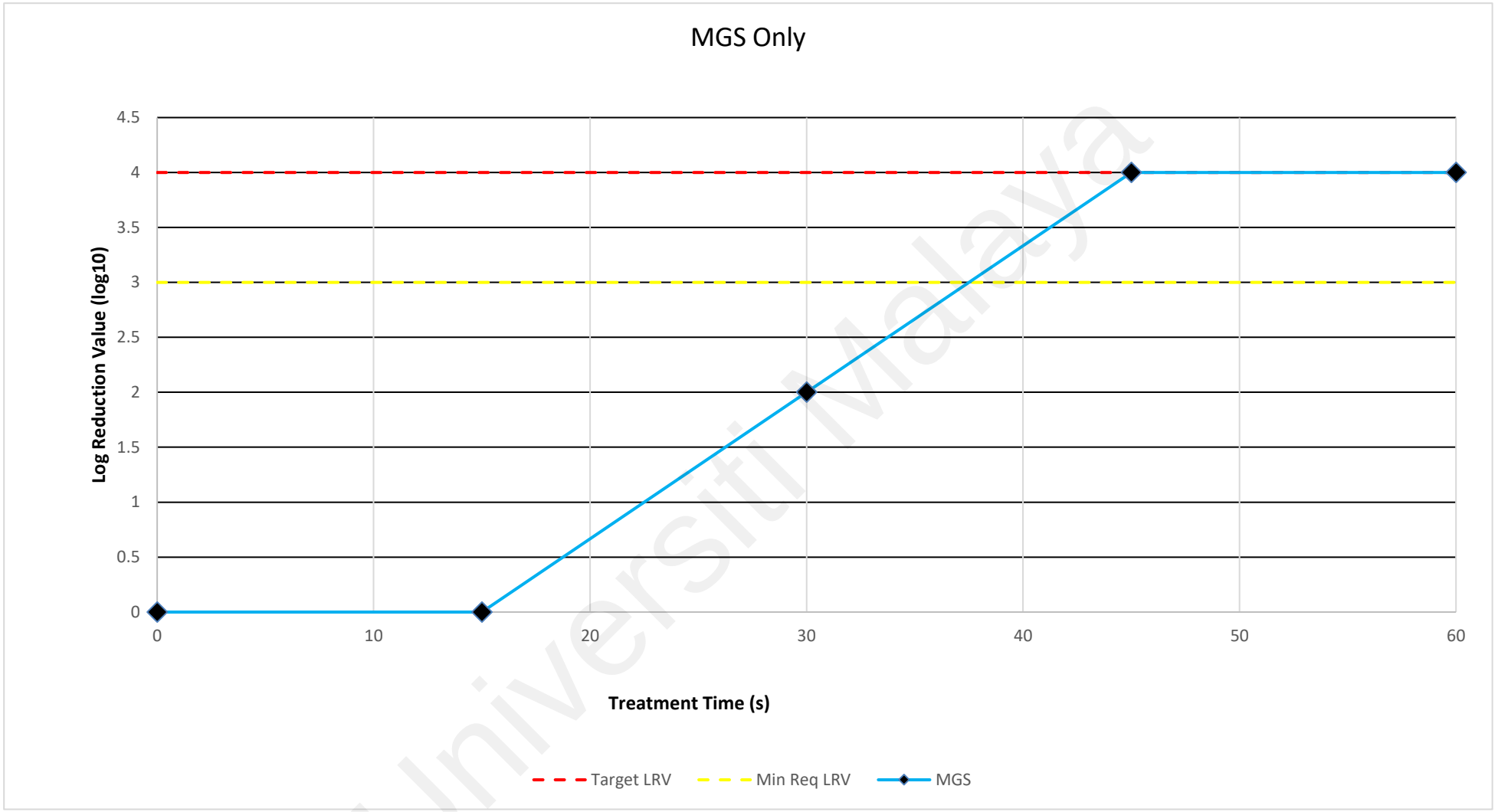

Figure 4.18: Graph of Log Reduction Value against Treatment Time (MGS Only)

4.6.4 Hybrid - Ultraviolet Germicidal Irradiation (UVGI) + Aerosolized Hydrogen Peroxide (aHP)

As the previous aHP-only test indicate, the aHP decontamination system was not effective against the tested specimen for the hybrid test. However, this new hybrid test resulted in a new breakthrough where even the UVGI system was not able to produce any log reduction when combined with the new aHP system as indicated in Table 4.4 and Figure 4.19. In comparison, UVGI alone was able to produce up to 4 log reduction with an exposure time of 100 seconds in previous tests.

Table 4.4: Virus viability test results (UVGI + aHP)

Sample	UVGI		aHP	Total exposure time (s)	Log Reduction Value (LRV) / log10
	Exposure time (s)	Dosage (J/cm^2)	Exposure time (s)		
HYB(aHP) Control	0	0	0	0	0
HYB(aHP) 1	3	0.0225	120	123	0
HYB(aHP) 2	6	0.045	120	126	0
HYB(aHP) 3	9	0.0675	120	129	0
HYB(aHP) 4	17	0.1275	120	137	0
HYB(aHP) 5	34	0.255	120	154	0
HYB(aHP) 6	67	0.5025	120	187	0
HYB(aHP) 7	100	0.75	120	220	0

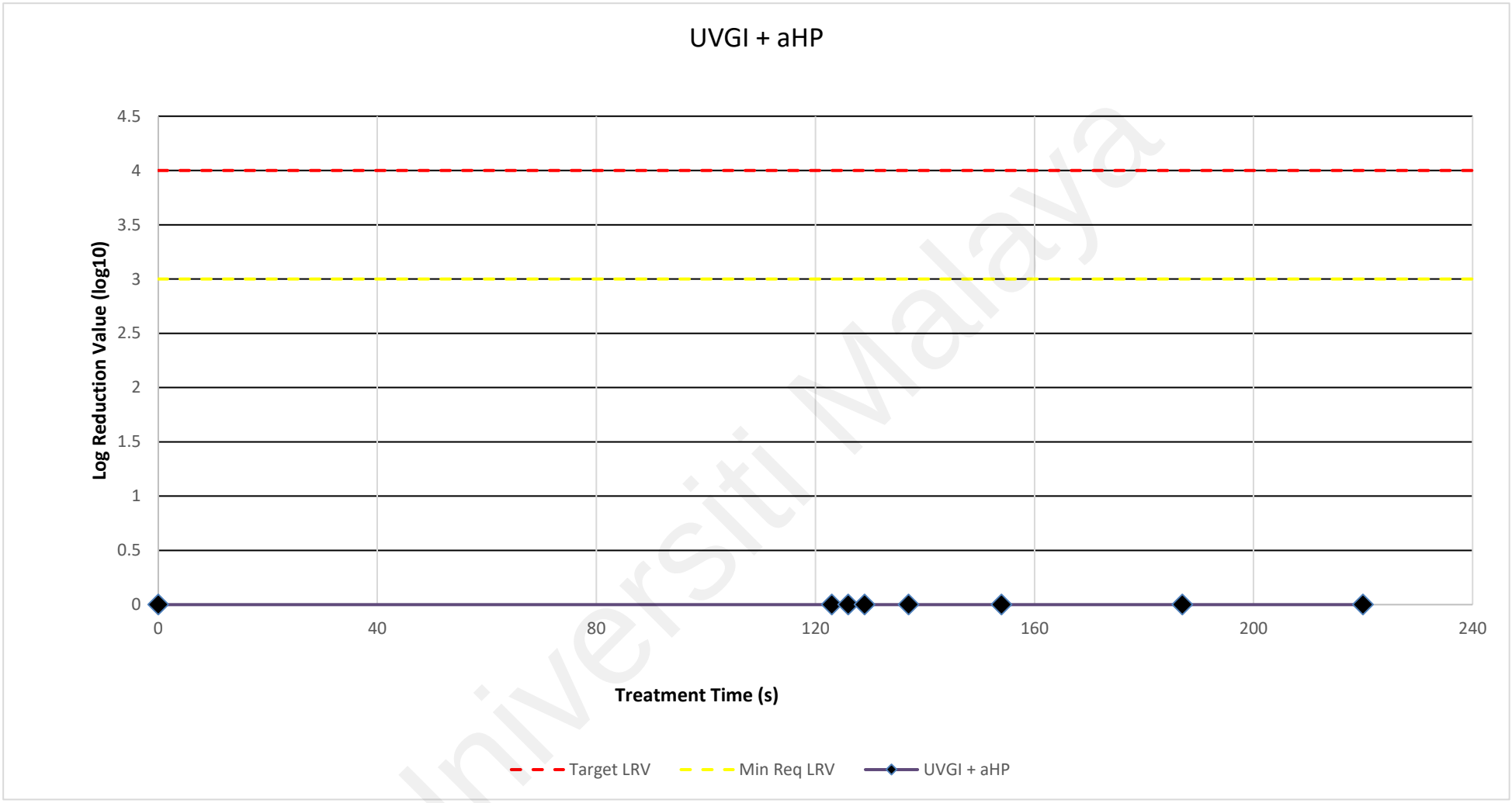

Figure 4.19: Graph of Log Reduction Value against Treatment Time (UVGI + aHP)

In addition, upon completing a full aHP decontamination cycle, it was found that there was a moisture layer present on the mask specimen. Hence, there was an immense possibility of moisture affecting the efficiency of the UVGI system that followed. A single test experiment (Table 4.5) was designed using a relatively higher dosage of UVGI treatment to identify the issues present in this test. As expected, at a relatively higher dosage of UVGI, the hybrid test produced a 2-log reduction. Assuming the aHP did not contribute any log reduction, the UV rays possibly evaporated the water layer initially. After the moisture layer has been removed, the UV rays perform virucidal activity on the virus placed on the mask. This could potentially be one of the scenarios on why the hybrid test behaved in this manner.

Table 4.5: Virus viability test results (UVGI + aHP) - Additional Test

Sample	UVGI		aHP	Total exposure time (s)	Log Reduction Value (LRV) / log10
	Exposure time (s)	Dosage (J/cm^2)	Exposure time (s)		
HYB(aHP) Add	267	2.0025	120	387	2

4.6.5 Hybrid - Ultraviolet Germicidal Irradiation (UVGI) + Microwave-Generated Steam (MGS)

Table 4.6 and Figure 4.20 indicate the virus viability test conducted for hybrid decontamination treatment of (UVGI +MGS). UVGI and MGS were able to produce excellent virucidal efficiency as individual treatments as discussed in previously conducted tests. As expected, in the hybrid experiment design these treatments were able to produce good log reduction where the target log reduction of 4 was achieved at a

combined treatment time of 39 seconds while the minimum required log reduction of 3 was achieved at 33 seconds. The steady trend of increasing log reduction value with increasing treatment times enhances the reliability of the received data.

Table 4.6: Virus viability test results (UVGI + MGS)

Sample	UVGI		MGS	Total exposure time (s)	Log Reduction Value (LRV) / log10
	Exposure time (s)	Dosage (J/cm^2)	Exposure time (s)		
HYB(MGS) Control	0	0	0	0	0
HYB(MGS) 1	3	0.0225	30	33	2
HYB(MGS) 2	6	0.045	30	36	3
HYB(MGS) 3	9	0.0675	30	39	4
HYB(MGS) 4	17	0.1275	30	47	4
HYB(MGS) 5	34	0.255	30	64	4

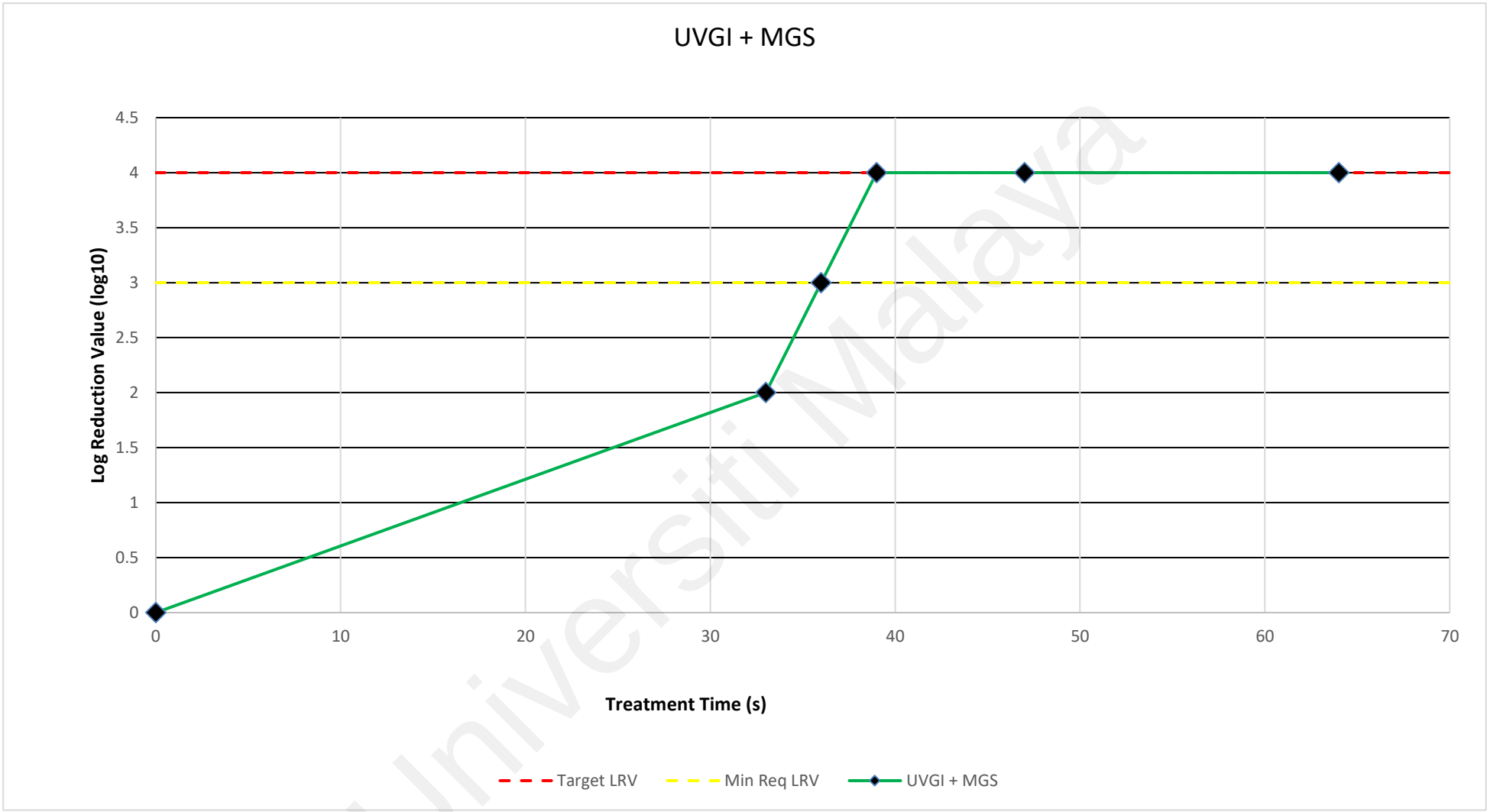

Figure 4.20: Graph of Log Reduction Value against Treatment Time (UVGI + MGS)

4.6.6 Comparison Between Single And Hybrid Decontamination Systems

Figure 4.21 shows the log reduction values achieved using single (UVGI, MGS) and hybrid (UVGI+MGS) decontamination procedures. In reference to the log reduction data of the hybrid test, UVGI treatment was able to achieve 3 log reduction at a faster rate. Nevertheless, the hybrid decontamination method achieved the target log reduction value of 4 at a lower treatment time compared to UVGI and MGS alone. In addition, in terms of achieving 4-log reduction, the MGS-only test was able to surpass the efficiency of the UVGI-only decontamination procedure. In short, the hybrid decontamination procedure was able to achieve the target log reduction faster than single treatments of UVGI and MGS. Completion of the detailed analysis of the virus viability tests indicates that the 2nd objective of this research was fulfilled successfully.

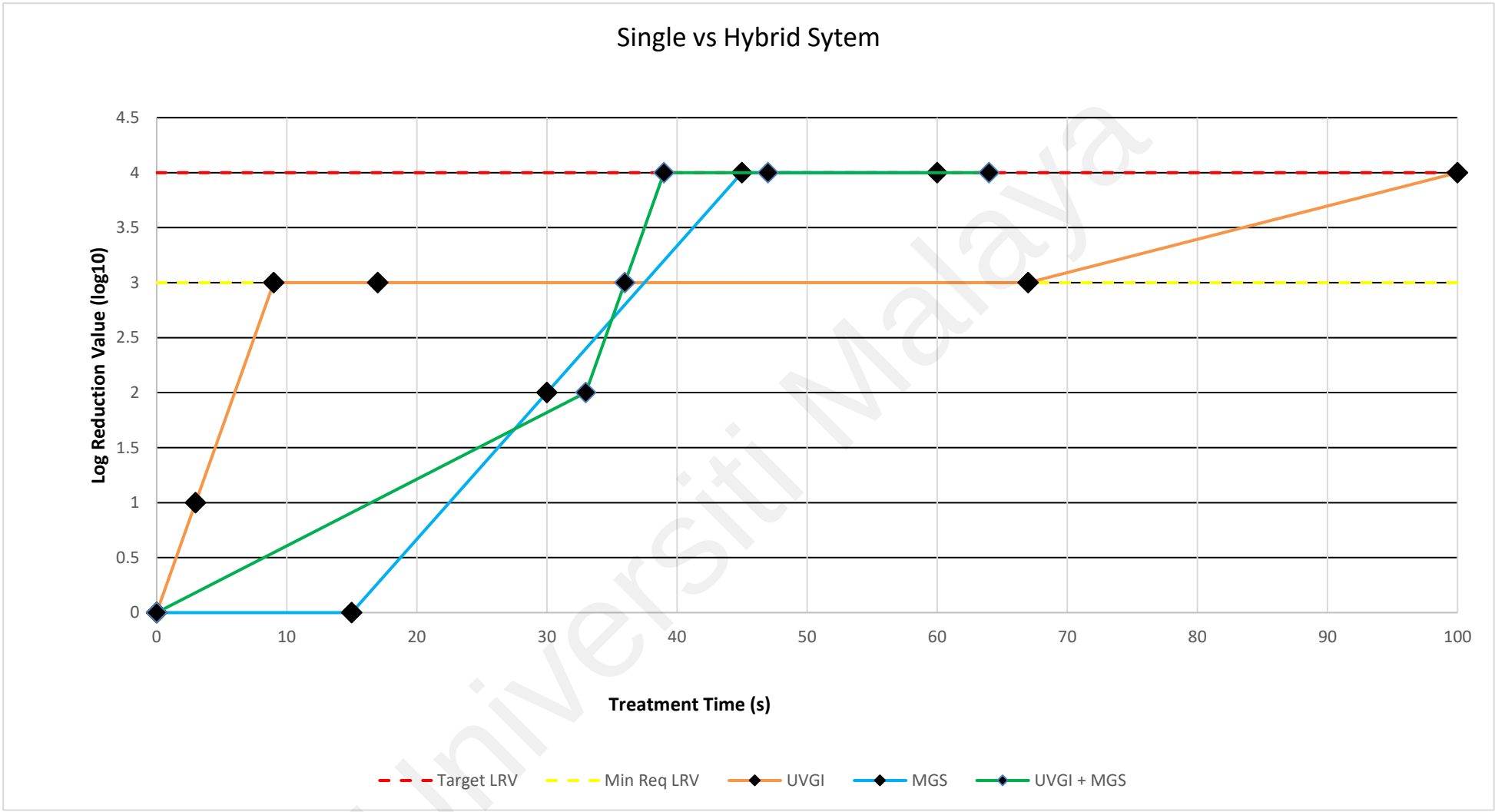

Figure 4.21: Graph of Log Reduction Value against Treatment Time (Single vs Hybrid)

4.6.7 Significance of Hybrid Decontamination System

The utmost priority in the background of approaching the hybrid decontamination procedure in this study was the treatment time required in decontaminating a face mask for reuse purposes. As the existing works of literature and the test results from the current study suggest, hybrid decontamination systems using UVGI and MGS were able to perform better collectively compared to single treatments in terms of treatment time. At a bigger scale and multiple cycles, the number of masks decontaminated safely can be increased using the hybrid decontamination system.

Notably, each type of treatment has its effect on the integrity of the mask whenever exposed to a longer or higher dosage treatment (Lindsley et al., 2015; Lore et al., 2012; Smith et al., 2020; Zulauf et al., 2020). Therefore, a secondary treatment such as MGS which has a minimal effect on to mask surface would be able to work efficiently when coupled with UVGI treatment without affecting the integrity of the treated mask.

CHAPTER 5: CONCLUSION

This chapter provides a conclusive verdict based on the experimental data and analysis. In addition, limitations present in the current study and recommendations for future work are discussed.

5.1 Conclusion

A concept was developed to equip two decontamination systems (UVGI and aHP) in the same portable machine. A total of two 3D models of the hybrid mask decontamination machine were developed. 22 parts in total were fabricated using stainless steel 304 and aluminium 5083 which were incorporated with other equipment to form a working hybrid mask sterilizer prototype. A novel feature made of quartz glass to form a mask enclosure was added as a safety measure for this machine. Testing procedures performed on the machine revealed that the equipped decontamination systems were working without an issue. In addition, the UVGI system was able to perform for a long uninterrupted cycle of 1 hour and aHP system was able to deliver the aHP flow throughout the treatment area as designed. Refinement procedures were conducted in order to address the issues and further enhance the efficiency of the equipped decontamination systems.

The hybrid decontamination system (UVGI + MGS) was able to produce 4 log reduction of the selected SARS-CoV-2 surrogate virus, Feline Coronavirus (FCoV) at a shorter treatment time compared to singular treatment of UVGI and MGS. Comparing the 3 singular treatments, UVGI achieved the minimum required LRV of 3 faster than MGS and aHP. Nevertheless, MGS was able to achieve the target LRV of 4 at a faster treatment time than UVGI and aHP. Notably, aHP treatment was not effective against the virus at all the tested parameters.

The hybrid mask decontamination procedure of (UVGI + MGS) has proven to be an effective technique to decontaminate N95 respirators (3M 1860) safely for reuse purposes. Nevertheless, implementation of this procedure for public use requires further testing on several criteria such as filtration performance, fit testing, and model of the mask which are explained in **5.2 Future Scope**.

5.2 Limitations

There are limitations to be addressed as a reference for future investigations that will be based on the current investigation which include:

1) The excised mask was investigated rather than the whole mask. The virus viability test in this current study utilized a portion of the N95 respirator during the UV decontamination procedure due to the restrictions present in the virus viability test. Nevertheless, in an actual application of a whole mask decontamination, a whole mask could receive a higher dosage in the same set-up as most of the mask will be nearer to the UV source. In short, the UVGI set-up utilized in this study can be a benchmark for the minimum log reduction value that can be guaranteed to be achieved using a specified dosage.

2) Only the exterior part of the mask exterior was investigated. The virus viability test utilized in this study only investigated the efficiency of a specific treatment against the virus that inoculated on the exterior part of the N95 mask. For a real-world application, decontamination treatment should focus on both surfaces, as we should not eliminate the possibility of the user as the host of the virus.

3) Dosage estimation. As described in 3.6.1.4 UVGI system operation procedure, dosage calculation for the UV design parameter was based on the minimum dosage value that can be achieved in this set-up. Therefore, there is a possibility that the actual dosage

value might be slightly higher than the estimation. Notably, existing literature reported dosage value utilized in the experiment using a keyword of 'at least achieved'. Therefore, the estimation procedure utilized in this study is consistent with the existing literature.

5.3 Future Scope

The future scope of this research can be directed toward the investigation of the integrity of the mask. According to (3M, 2021), apart from decontamination of virus load, there are 3 more key criteria that classify a decontaminated mask as safe to reuse material. These 3 additional criteria include filtration performance, fit testing, and safety of the user. As this research has addressed the main criteria, future investigations could explore these additional criteria using the dosage and techniques proposed in the current study as a reference.

In addition, a modification to the decontamination set-up using a more powerful set of equipment could potentially deliver better decontamination results at a shorter treatment time. UVC bulbs with a higher irradiance value, an increase in the number of UVC bulbs, and utilizing a microwave oven with a higher power rating are among the potential solutions to achieve a shorter treatment time for the desired decontamination results.

REFERENCES

3M. (2018). *3M™ Particulate Respirator, 8210, N95 Technical Specifications*. Retrieved 16 July 2021 from https://multimedia.3m.com/mws/media/1425070O/3m-particulate-respirator-8210-n95-technical-specifications.pdf

3M. (2021). Decontamination of 3M Filtering Facepiece Respirators, such as N95 Respirators, in the United States - Considerations.

Anderegg, L., Meisenhelder, C., Ngooi, C. O., Liao, L., Xiao, W., Chu, S., . . . Doyle, J. M. (2020). A scalable method of applying heat and humidity for decontamination of N95 respirators during the COVID-19 crisis. *PLoS One*, *15*(7), e0234851. https://doi.org/10.1371/journal.pone.0234851

Bedell, K., Buchaklian, A. H., & Perlman, S. (2016). Efficacy of an Automated Multiple Emitter Whole-Room Ultraviolet-C Disinfection System Against Coronaviruses MHV and MERS-CoV. *Infect Control Hosp Epidemiol*, *37*(5), 598-599. https://doi.org/10.1017/ice.2015.348

Berger, D., Gundermann, G., Sinha, A., Moroi, M., Goyal, N., & Tsai, A. (2022). Review of aerosolized hydrogen peroxide, vaporized hydrogen peroxide, and hydrogen peroxide gas plasma in the decontamination of filtering facepiece respirators. *Am J Infect Control*, *50*(2), 203-213. https://doi.org/10.1016/j.ajic.2021.06.012

Bopp, N., Bouyer, D., Gibbs, C., Nichols, J., Ntiforo, C., & Grimaldo, M. (2020). Multicycle Autoclave Decontamination of N95 Filtering Facepiece Respirators. *Applied Biosafety*, *25*, 153567602092417. https://doi.org/10.1177/1535676020924171

Cadnum, J. L., Li, D. F., Redmond, S. N., John, A. R., Pearlmutter, B., & Donskey, C. J. (2020). Effectiveness of Ultraviolet-C Light and a High-Level Disinfection Cabinet for Decontamination of N95 Respirators. *Pathog Immun*, *5*(1), 52-67. https://doi.org/10.20411/pai.v5i1.372

Centers for Disease Control and Prevention [CDC], C. (2019, 21/06/2019). *Hydrogen Peroxide*. Retrieved 24/04/2022 from https://www.cdc.gov/niosh/topics/hydrogen-peroxide/default.html

Centers for Disease Control and Prevention [CDC], C. (2020a, 06/04/2022). *Implementing Filtering Facepiece Respirator (FFR) Reuse, Including Reuse after Decontamination, When There Are Known Shortages of N95 Respirators*. Retrieved 21/04/2022 from https://www.cdc.gov/coronavirus/2019-ncov/hcp/ppe-strategy/decontamination-reuse-respirators.html

Centers for Disease Control and Prevention [CDC], C. (2020b, 23/11/2020). *Strategies for Optimizing the Supply of Facemasks*. Retrieved 21/04/2022 from https://www.cdc.gov/coronavirus/2019-ncov/hcp/ppe-strategy/face-masks.html#crisis-capacity

Centers for Disease Control and Prevention [CDC], C. (2021, 09/04/2021). *Upper-Room Ultraviolet Germicidal Irradiation (UVGI)*. Retrieved 21/04/2022 from https://www.cdc.gov/coronavirus/2019-ncov/community/ventilation/uvgi.html

Chen, P. Z., Ngan, A., Manson, N., Maynes, J. T., Borschel, G. H., Rotstein, O. D., & Gu, F. X. (2020). Transmission of aerosols through pristine and reprocessed N95 respirators. *medRxiv*, 2020.2005.2014.20094821. https://doi.org/10.1101/2020.05.14.20094821

Chen, Y., Liu, Q., & Guo, D. (2020). Emerging coronaviruses: Genome structure, replication, and pathogenesis. *J Med Virol*, *92*(4), 418-423. https://doi.org/10.1002/jmv.25681

Chin, A. W. H., Chu, J. T. S., Perera, M. R. A., Hui, K. P. Y., Yen, H. L., Chan, M. C. W., . . . Poon, L. L. M. (2020). Stability of SARS-CoV-2 in different environmental conditions. *Lancet Microbe*, *1*(1), e10. https://doi.org/10.1016/s2666-5247(20)30003-3

Christie-Holmes, N., Tyli, R., Budylowski, P., Guvenc, F., Weiner, A., Poon, B., . . . Scott, J. A. (2021). Vapourized hydrogen peroxide decontamination in a hospital setting inactivates SARS-CoV-2 and HCoV-229E without compromising filtration efficiency of unexpired N95 respirators. *Am J Infect Control*, *49*(10), 1227-1231. https://doi.org/10.1016/j.ajic.2021.07.012

Daeschler, S. C., Manson, N., Joachim, K., Chin, A. W. H., Chan, K., Chen, P. Z., . . . Borschel, G. H. (2020). Effect of moist heat reprocessing of N95 respirators on SARS-CoV-2 inactivation and respirator function. *Cmaj*, *192*(41), E1189-e1197. https://doi.org/10.1503/cmaj.201203

Dave, N., Pascavis, K. S., Patterson, J., Wallace, D., Chowdhury, A., Abbaszadegan, M., . . . Naufel, M. (2020). Characterization of a novel, low-cost, scalable vaporized hydrogen peroxide system for sterilization of N95 respirators and other COVID-19 related personal protective equipment. *medRxiv*, 2020.2006.2024.20139436. https://doi.org/10.1101/2020.06.24.20139436

Degesys, N. F., Wang, R. C., Kwan, E., Fahimi, J., Noble, J. A., & Raven, M. C. (2020). Correlation Between N95 Extended Use and Reuse and Fit Failure in an Emergency Department. *JAMA*, *324*(1), 94-96. https://doi.org/10.1001/jama.2020.9843

Derr, T. H., James, M. A., Kuny, C. V., Patel, D., Kandel, P. P., Field, C., . . . Szpara, M. (2020). Aerosolized Hydrogen Peroxide Decontamination of N95 Respirators, with Fit-Testing and Virologic Confirmation of Suitability for Re-Use During the COVID-19 Pandemic. *medRxiv*, 2020.2004.2017.20068577. https://doi.org/10.1101/2020.04.17.20068577

Duan, S. M., Zhao, X. S., Wen, R. F., Huang, J. J., Pi, G. H., Zhang, S. X., . . . Dong, X. P. (2003). Stability of SARS coronavirus in human specimens and environment and its sensitivity to heating and UV irradiation. *Biomed Environ Sci*, *16*(3), 246-255.

Fischer, R. J., Morris, D. H., van Doremalen, N., Sarchette, S., Matson, M. J., Bushmaker, T., . . . Munster, V. J. (2020). Assessment of N95 respirator decontamination and re-use for SARS-CoV-2. *medRxiv*, 2020.2004.2011.20062018. https://doi.org/10.1101/2020.04.11.20062018

Fisher, E. M., & Shaffer, R. E. (2011). A method to determine the available UV-C dose for the decontamination of filtering facepiece respirators. *J Appl Microbiol*, *110*(1), 287-295. https://doi.org/10.1111/j.1365-2672.2010.04881.x

Fisher, E. M., Williams, J. L., & Shaffer, R. E. (2011). Evaluation of microwave steam bags for the decontamination of filtering facepiece respirators. *PLoS One*, *6*(4), e18585-e18585. https://doi.org/10.1371/journal.pone.0018585

Geldert, A., Su, A., Roberts, A. W., Golovkine, G., Grist, S. M., Stanley, S. A., & Herr, A. E. (2021). Nonuniform UV-C dose across N95 facepieces can cause 2.9-log variation in SARS-CoV-2 inactivation. *medRxiv*, 2021.2003.2005.21253022. https://doi.org/10.1101/2021.03.05.21253022

Golovkine, G. R., Roberts, A. W., Cooper, C., Riano, S., DiCiccio, A. M., Worthington, D. L., . . . Stanley, S. A. (2021). Practical considerations for Ultraviolet-C radiation mediated decontamination of N95 respirator against SARS-CoV-2 virus. *PLoS One*, *16*(10), e0258336. https://doi.org/10.1371/journal.pone.0258336

Goyal, S. M., Chander, Y., Yezli, S., & Otter, J. A. (2014). Evaluating the virucidal efficacy of hydrogen peroxide vapour. *J Hosp Infect*, *86*(4), 255-259. https://doi.org/10.1016/j.jhin.2014.02.003

Gray, A. (2020). *Exploring the Shortage of Affordable Masks in Developing Countries*. BORGEN Magazine. Retrieved 6 September 2021 from https://www.borgenmagazine.com/affordable-masks/

Hasani, M., Campbell, T., Wu, F., & Warriner, K. (2021). Decontamination of N95 and surgical masks using a treatment based on a continuous gas phase-Advanced Oxidation Process. *PLoS One*, *16*(3), e0248487. https://doi.org/10.1371/journal.pone.0248487

He, W., Guo, Y., Gao, H., Liu, J., Yue, Y., & Wang, J. (2020). Evaluation of Regeneration Processes for Filtering Facepiece Respirators in Terms of the Bacteria Inactivation Efficiency and Influences on Filtration Performance. *ACS nano*, *14*(10), 13161-13171. https://doi.org/10.1021/acsnano.0c04782

Henneberry, B. (n.d). *How to Make N95 Masks*. Retrieved 16 July 2021 from https://www.thomasnet.com/articles/plant-facility-equipment/how-to-make-n95-masks/#_How_are_N95

Huber, T., Goldman, O., Epstein, A., Stella, G., & Sakmar, T. (2020). *Principles and practice of SARS-CoV-2 decontamination of N95 masks with UV-C*. https://doi.org/10.1101/2020.06.08.20125062

ISO 18184:2019 Textiles—Determination of Antiviral Activity of Textile Products. Retrieved 24 November 2023 from https://www.iso.org/standard/71292.html

Jaimes, J. A., & Whittaker, G. R. (2018). Feline coronavirus: Insights into viral pathogenesis based on the spike protein structure and function. *Virology*, *517*, 108-121. https://doi.org/10.1016/j.virol.2017.12.027

Jatta, M., Kiefer, C., Patolia, H., Pan, J., Harb, C., Marr, L. C., & Baffoe-Bonnie, A. (2021). N95 reprocessing by low temperature sterilization with 59% vaporized hydrogen peroxide during the 2020 COVID-19 pandemic. *American Journal of Infection Control*, *49*(1), 8-14. https://doi.org/https://doi.org/10.1016/j.ajic.2020.06.194

Ji, D., Fan, L., Li, X., & Ramakrishna, S. (2020). Addressing the worldwide shortages of face masks. *BMC Mater*, *2*(1), 9. https://doi.org/10.1186/s42833-020-00015-w

Kayani, B. J., Weaver, D. T., Gopalakrishnan, V., King, E. S., Dolson, E., Krishnan, N., . . . Charnas, I. (2021). UV-C tower for point-of-care decontamination of filtering facepiece respirators. *Am J Infect Control*, *49*(4), 424-429. https://doi.org/10.1016/j.ajic.2020.11.010

Krishnan, S., Rawindran, H., Sinnathambi, C., & Lim, J. (2017). Comparison of various advanced oxidation processes used in remediation of industrial wastewater laden with recalcitrant pollutants. *IOP Conference Series: Materials Science and Engineering*, *206*, 012089. https://doi.org/10.1088/1757-899X/206/1/012089

Krystynik, P. (2021). Advanced Oxidation Processes (AOPs) – Utilization of Hydroxyl Radical and Singlet Oxygen. In R. Ahmad (Ed.), *Reactive Oxygen Species*. IntechOpen. https://doi.org/10.5772/intechopen.98189

Kumar, A., Kasloff, S. B., Leung, A., Cutts, T., Strong, J. E., Hills, K., . . . Krishnan, J. (2020). N95 Mask Decontamination using Standard Hospital Sterilization Technologies. *medRxiv*, 2020.2004.2005.20049346. https://doi.org/10.1101/2020.04.05.20049346

Kumkrong, P., Scoles, L., Brunet, Y., & Baker, S. (2021). Determination of hydrogen peroxide on N95 masks after sanitization using a colorimetric method. *MethodsX*, *8*, 101485. https://doi.org/https://doi.org/10.1016/j.mex.2021.101485

Li, L., Wu, Z., Zhang, Z., & Zhang, Y. (2023). An Optimization Method for CNC Laser Combination Cutting of Irregular Plate Remainders. *Coatings*, *13*(5), 914. https://www.mdpi.com/2079-6412/13/5/914

Liao, L., Xiao, W., Zhao, M., Yu, X., Wang, H., Wang, Q., . . . Cui, Y. (2020). Can N95 Respirators Be Reused after Disinfection? How Many Times? *ACS nano*, *14*(5), 6348-6356. https://doi.org/10.1021/acsnano.0c03597

Lieu, A., Mah, J., Zanichelli, V., Exantus, R. C., & Longtin, Y. (2020). Impact of extended use and decontamination with vaporized hydrogen peroxide on N95 respirator fit. *Am J Infect Control*, *48*(12), 1457-1461. https://doi.org/10.1016/j.ajic.2020.08.010

Lin, T. H., Tang, F. C., Hung, P. C., Hua, Z. C., & Lai, C. Y. (2018). Relative survival of Bacillus subtilis spores loaded on filtering facepiece respirators after five

decontamination methods. *Indoor Air*, *28*(5), 754-762. https://doi.org/10.1111/ina.12475

Lindsley, W. G., Martin, S. B., Jr., Thewlis, R. E., Sarkisian, K., Nwoko, J. O., Mead, K. R., & Noti, J. D. (2015). Effects of Ultraviolet Germicidal Irradiation (UVGI) on N95 Respirator Filtration Performance and Structural Integrity. *J Occup Environ Hyg*, *12*(8), 509-517. https://doi.org/10.1080/15459624.2015.1018518

Lore, M. B., Heimbuch, B. K., Brown, T. L., Wander, J. D., & Hinrichs, S. H. (2012). Effectiveness of three decontamination treatments against influenza virus applied to filtering facepiece respirators. *Ann Occup Hyg*, *56*(1), 92-101. https://doi.org/10.1093/annhyg/mer054

Ludwig-Begall, L. F., Wielick, C., Jolois, O., Dams, L., Razafimahefa, R. M., Nauwynck, H., . . . Haubruge, E. (2021). "Don, doff, discard" to "don, doff, decontaminate"—FFR and mask integrity and inactivation of a SARS-CoV-2 surrogate and a norovirus following multiple vaporised hydrogen peroxide-, ultraviolet germicidal irradiation-, and dry heat decontaminations. *PLoS One*, *16*(5), e0251872. https://doi.org/10.1371/journal.pone.0251872

Lukes, P., Clupek, M., Babicky, V., & Sunka, P. (2008). Ultraviolet radiation from the pulsed corona discharge in water. *PLASMA SOURCES SCIENCE AND TECHNOLOGY Plasma Sources Sci. Technol*, *17*, 24012-24011. https://doi.org/10.1088/0963-0252/17/2/024012

Mills, D., Harnish, D. A., Lawrence, C., Sandoval-Powers, M., & Heimbuch, B. K. (2018). Ultraviolet germicidal irradiation of influenza-contaminated N95 filtering facepiece respirators. *Am J Infect Control*, *46*(7), e49-e55. https://doi.org/10.1016/j.ajic.2018.02.018

Moschella, P., Liao, W., Litwin, A., Foulk, J., Anthony, J., Player, M., . . . Cole, C. (2021). Repeated vaporised hydrogen peroxide disinfection of 3M 1860 N95 mask respirators does not degrade quantitative fit performance. *Br J Anaesth*, *126*(3), e125-e127. https://doi.org/10.1016/j.bja.2020.12.021

National Center for Biotechnology Information [NCBI], N. (2022). *Hydrogen peroxide*. PubChem Compound Summary for CID 784. Retrieved 24/04/2022 from https://pubchem.ncbi.nlm.nih.gov/compound/Hydrogen-peroxide

National Institute for Occupational Safety and Health [NIOSH], N. (2021a, 15/09/2021). *NIOSH-Approved Particulate Filtering Facepiece Respirators*. Retrieved 21/04/2022 from https://www.cdc.gov/niosh/npptl/topics/respirators/disp_part/default.html

National Institute for Occupational Safety and Health [NIOSH], N. (2021b, 02/08/2021). *Respirators*. Retrieved 21/04/2022 from https://www.cdc.gov/niosh/topics/respirators/default.html

Nie, C., Trimpert, J., Moon, S., Haag, R., Gilmore, K., Kaufer, B. B., & Seeberger, P. H. (2021). In vitro efficacy of Artemisia extracts against SARS-CoV-2. *Virol J*, *18*(1), 182. https://doi.org/10.1186/s12985-021-01651-8

O'Kelly, E., Arora, A., Pirog, S., Ward, J., & Clarkson, P. J. (2021). Comparing the fit of N95, KN95, surgical, and cloth face masks and assessing the accuracy of fit checking. *PLoS One*, *16*(1), e0245688. https://doi.org/10.1371/journal.pone.0245688

Ogata, Y., Tomizawa, K., & Takagi, K. (1981). Photo-oxidation of formic, acetic, and propionic acids with aqueous hydrogen peroxide. *Canadian Journal of Chemistry*, *59*(1), 14-18. https://doi.org/10.1139/v81-003

Ontiveros, C. C., Sweeney, C. L., Smith, C., MacIsaac, S., Bennett, J. L., Munoz, S., . . . Gagnon, G. A. (2021). Assessing the impact of multiple ultraviolet disinfection cycles on N95 filtering facepiece respirator integrity. *Sci Rep*, *11*(1), 12279. https://doi.org/10.1038/s41598-021-91706-1

Oral, E., Wannomae, K. K., Connolly, R., Gardecki, J., Leung, H. M., Muratoglu, O., . . . Emmal, B. (2020). Vapor H2O2 sterilization as a decontamination method for the reuse of N95 respirators in the COVID-19 emergency. *medRxiv*, 2020.2004.2011.20062026. https://doi.org/10.1101/2020.04.11.20062026

Ou, Q., Pei, C., Chan Kim, S., Abell, E., & Pui, D. Y. H. (2020). Evaluation of decontamination methods for commercial and alternative respirator and mask materials - view from filtration aspect. *J Aerosol Sci*, *150*, 105609. https://doi.org/10.1016/j.jaerosci.2020.105609

Ozog, D. M., Sexton, J. Z., Narla, S., Pretto-Kernahan, C. D., Mirabelli, C., Lim, H. W., . . . Mi, Q. S. (2020). The effect of ultraviolet C radiation against different N95 respirators inoculated with SARS-CoV-2. *Int J Infect Dis*, *100*, 224-229. https://doi.org/10.1016/j.ijid.2020.08.077

Parshley, L. (2020). *The mask shortage is forcing health workers to disregard basic coronavirus infection control*. Vox Media. Retrieved 6 September 2021 from https://www.vox.com/2020/4/3/21206726/coronavirus-masks-n95-hospitals-health-care-doctors-ppe-shortage

Pascoe, M. J., Robertson, A., Crayford, A., Durand, E., Steer, J., Castelli, A., . . . Maillard, J. Y. (2020). Dry heat and microwave-generated steam protocols for the rapid decontamination of respiratory personal protective equipment in response to COVID-19-related shortages. *Journal of Hospital Infection*, *106*(1), 10-19. https://doi.org/https://doi.org/10.1016/j.jhin.2020.07.008

Phillips Lighting , P. (2022). TUV PL-S (TUV PL-S 9W/2P 1CT/6X10BOX). In.

Rashid, T. U., Sharmeen, S., & Biswas, S. (2022). Effectiveness of N95 Masks against SARS-CoV-2: Performance Efficiency, Concerns, and Future Directions. *ACS Chemical Health & Safety*, *29*(2), 135-164. https://doi.org/10.1021/acs.chas.1c00016

Rathnasinghe, R., Karlicek, R. F., Schotsaert, M., Koffas, M. A., Arduini, B., Jangra, S., . . . Balchandani, P. (2020). Scalable, effective, and rapid decontamination of SARS-CoV-2 contaminated N95 respirators using germicidal ultra-violet C (UVC) irradiation device. *medRxiv*. https://doi.org/10.1101/2020.10.05.20206953

Reed, N. G. (2010). The history of ultraviolet germicidal irradiation for air disinfection. *Public health reports (Washington, D.C. : 1974)*, *125*(1), 15-27. https://doi.org/10.1177/003335491012500105

Rockey, N., Arts, P. J., Li, L., Harrison, K. R., Langenfeld, K., Fitzsimmons, W. J., . . . Wigginton, K. R. (2020). Humidity and Deposition Solution Play a Critical Role in Virus Inactivation by Heat Treatment of N95 Respirators. *mSphere*, *5*(5). https://doi.org/10.1128/mSphere.00588-20

Russo, R., Levine, C., Grady, C., Peixoto, B., McCormick-Ell, J., Block, T., . . . Alland, D. (2021). Decontaminating N95 respirators during the COVID-19 pandemic: simple and practical approaches to increase decontamination capacity, speed, safety and ease of use. *J Hosp Infect*, *109*, 52-57. https://doi.org/10.1016/j.jhin.2020.12.006

Samsung. *23L Grill Microwave Oven with Healthy Steam*. Samsung Malaysia Electronics (SME) Sdn. Bhd. https://www.samsung.com/my/microwave-ovens/grill/microwave-oven-grill-mg23k3513gk/

Schreiber, A., Kuehn, B., Arnold, E., Schilling, F. J., & Witzke, H. D. (2004). *Radiation Resistance of Quartz Glass for VUV Discharge Lamps*. https://doi.org/10.13140/RG.2.1.1516.3605

Science Centre, H. (n.d). *Surrogate Virus*. Retrieved 06/05/2022 from https://www.hartmann-science-center.com/en/hygiene-knowledge/glossary/glossary-19/surrogate-virus?

Scientific Animations Inc, S. (2020). *3D medical animation corona virus*. Retrieved 16 July 2021 from https://commons.wikimedia.org/wiki/File:3D_medical_animation_corona_virus.jpg

Sharun, K., Sircar, S., Malik, Y. S., Singh, R. K., & Dhama, K. (2020). How close is SARS-CoV-2 to canine and feline coronaviruses? *J Small Anim Pract*, *61*(8), 523-526. https://doi.org/10.1111/jsap.13207

Shereen, M. A., Khan, S., Kazmi, A., Bashir, N., & Siddique, R. (2020). COVID-19 infection: Emergence, transmission, and characteristics of human coronaviruses. *Journal of Advanced Research*, *24*, 91-98. https://doi.org/https://doi.org/10.1016/j.jare.2020.03.005

Simmons, S. E., Carrion, R., Alfson, K. J., Staples, H. M., Jinadatha, C., Jarvis, W. R., . . . Stibich, M. A. (2021). Deactivation of SARS-CoV-2 with pulsed-xenon ultraviolet light: Implications for environmental COVID-19 control. *Infect Control Hosp Epidemiol*, *42*(2), 127-130. https://doi.org/10.1017/ice.2020.399

Smith, J. S., Hanseler, H., Welle, J., Rattray, R., Campbell, M., Brotherton, T., . . . Stucky, N. L. (2020). Effect of various decontamination procedures on disposable N95 mask integrity and SARS-CoV-2 infectivity. *J Clin Transl Sci*, *5*(1), e10. https://doi.org/10.1017/cts.2020.494

Soni, A., Smith, J., Thompson, A., & Brightwell, G. (2020). Microwave-induced thermal sterilization- A review on history, technical progress, advantages and challenges as compared to the conventional methods. *Trends in Food Science & Technology*, *97*, 433-442. https://doi.org/https://doi.org/10.1016/j.tifs.2020.01.030

Standard Test Method to Qualify Single-Use Foodservice Packaging for Use in Microwave Ovens. (2007). F. P. Institute.

Turtil, S. (2016). *Sterility Review of 510(k) Submissions: Common Microbiology Issues Found in 510(k) Submissions*. U.S. Food & Drug Administration. Retrieved 16 July 2021 from https://www.fda.gov/media/141277/download

U.S. Food and Drug Administration [FDA], F. (2021a). *N95 Respirators, Surgical Masks, Face Masks, and Barrier Face Coverings*. Retrieved 21/04/2022 from https://www.fda.gov/medical-devices/personal-protective-equipment-infection-control/n95-respirators-surgical-masks-face-masks-and-barrier-face-coverings

U.S. Food and Drug Administration [FDA], F. (2021b, 02/01/2021). *UV Lights and Lamps: Ultraviolet-C Radiation, Disinfection, and Coronavirus*. Retrieved 21/04/2022 from https://www.fda.gov/medical-devices/coronavirus-covid-19-and-medical-devices/uv-lights-and-lamps-ultraviolet-c-radiation-disinfection-and-coronavirus

Vimbert, R. M., Loyo, M. A., Sánchez, J. D. C., Raurich, J. G., & Asensio, P. M. (2020). Evidence of OH· radicals disinfecting indoor air and surfaces in a harmless for humans method. *International Journal of Engineering Research and*, *6*, 26-38.

Viscusi, D., King, W. P., & Shaffer, R. (2008). Effect of Decontamination on the Filtration Efficiency of Two Filtering Facepiece Respirator Models.

Vo, E., Rengasamy, S., & Shaffer, R. (2009). Development of a test system to evaluate procedures for decontamination of respirators containing viral droplets. *Appl Environ Microbiol*, *75*(23), 7303-7309. https://doi.org/10.1128/aem.00799-09

Weaver, D. T., McElvany, B. D., Gopalakrishnan, V., Card, K. J., Crozier, D., Dhawan, A., . . . Scott, J. G. (2021). UV decontamination of personal protective equipment with idle laboratory biosafety cabinets during the COVID-19 pandemic. *PLoS One*, *16*(7), e0241734. https://doi.org/10.1371/journal.pone.0241734

World Health Organization [WHO], W. (2020a). *Coronavirus disease 2019 (COVID-19): situation report, 94*. https://apps.who.int/iris/handle/10665/331865

World Health Organization [WHO], W. (2020b). *Shortage of personal protective equipment endangering health workers worldwide*. Retrieved July 16, 2021 from https://www.who.int/news/item/03-03-2020-shortage-of-personal-protective-equipment-endangering-health-workers-worldwide

Wu, H.-L., Huang, J., Zhang, C. J. P., He, Z., & Ming, W.-K. (2020). Facemask shortage and the novel coronavirus disease (COVID-19) outbreak: Reflections on public health measures. *EClinicalMedicine*, *21*, 100329-100329. https://doi.org/10.1016/j.eclinm.2020.100329

Xiang, Y., Song, Q., & Gu, W. (2020). Decontamination of surgical face masks and N95 respirators by dry heat pasteurization for one hour at 70°C. *American Journal of Infection Control*, *48*(8), 880-882. https://doi.org/10.1016/j.ajic.2020.05.026

Xometry, T. (2023). *Slot Milling: How It Works, Types, Advantages, and Disadvantages*. Team Xometry. https://www.xometry.com/resources/machining/slot-milling/

Zhang, Y., Geng, X., Tan, Y., Li, Q., Xu, C., Xu, J., . . . Wang, H. (2020). New understanding of the damage of SARS-CoV-2 infection outside the respiratory system. *Biomed Pharmacother*, *127*, 110195. https://doi.org/10.1016/j.biopha.2020.110195

Zulauf, K. E., Green, A. B., Nguyen Ba, A. N., Jagdish, T., Reif, D., Seeley, R., . . . Kirby, J. E. (2020). Microwave-Generated Steam Decontamination of N95 Respirators Utilizing Universally Accessible Materials. *mBio*, *11*(3). https://doi.org/10.1128/mBio.00997-20